

Functional Autoregressive Processes in Reproducing Kernel Hilbert Spaces

Daren Wang

Zifeng Zhao

University of Chicago

University of Notre Dame

Rebecca Willett

Chun Yip Yau

University of Chicago

Chinese University of Hong Kong

Abstract

We study the estimation and prediction of functional autoregressive (FAR) processes, a statistical tool for modeling functional time series data. Due to the infinite-dimensional nature of FAR processes, the existing literature addresses its inference via dimension reduction and theoretical results therein require the (unrealistic) assumption of fully observed functional time series. We propose an alternative inference framework based on Reproducing Kernel Hilbert Spaces (RKHS). Specifically, a nuclear norm regularization method is proposed for estimating the transition operators of the FAR process directly from discrete samples of the functional time series. We derive a representer theorem for the FAR process, which enables infinite-dimensional inference without dimension reduction. Sharp theoretical guarantees are established under the (more realistic) assumption that we only have finite discrete samples of the FAR process. Extensive numerical experiments and a real data application of energy consumption prediction are further conducted to illustrate the promising performance of the proposed approach compared to the state-of-the-art methods in the literature.

Keywords: Reproducing Kernel Hilbert Space; Functional time series; Representer theorem; Nuclear norm regularization.

1 Introduction

Functional Data Analysis (FDA) has emerged as an important area of modern statistics as it provides effective tools for analyzing complex data. As described in the excellent monographs by [Ramsay and Silverman \(2005\)](#), [Ferraty and Vieu \(2006\)](#) and [Horváth and Kokoszka \(2012\)](#), FDA considers the analysis and theory of data that can be viewed in the form of functions, offering a natural and parsimonious solution to a variety of problems that are difficult to cast into classical statistical frameworks designed for scalar and vector valued data.

An important type of functional data is functional time series ([Hörmann and Kokoszka, 2010](#); [Aue et al., 2015](#)), where the functional observations are collected in a sequential manner. A typical scheme is a continuous-time record that can be partitioned into natural consecutive time intervals, such as hours, days or years, where similar behavior is expected across intervals. Common examples of functional time series include the intraday return curves or volatility curves of a stock market index and the daily or annual patterns of meteorological and environmental data such as temperature or precipitation.

Formally speaking, a functional time series takes the form $\{X_t(s), s \in [a, b]\}_{t \in \mathbb{Z}}$, where each observation $X_t(s)$ is a (random) function defined for s taking values in some compact interval $[a, b]$. By rescaling if needed, throughout the paper, without loss of generality, we assume $[a, b] = [0, 1]$. Due to the intrinsic high dimensionality of functional observations, classical univariate and multivariate time series methods, such as (vector) autoregressive models, may fail to track the dynamics of functional time series and thus are unable to provide accurate prediction. See more discussions in, for example, [Bosq \(2000\)](#), [Hyndman and Ullah \(2007\)](#) and [Shang \(2013\)](#). Thus, a key task for functional time series analysis is the design and estimation of a reliable statistical model tailored for the functional nature of the data, which serves as the foundation for understanding the behavior of the data and providing accurate prediction.

The most widely-used functional time series model proven to work well in practice is the functional autoregressive (FAR) process in \mathcal{L}^2 ([Bosq, 2000](#)), where \mathcal{L}^2 denotes the Hilbert space of square-integrable functions on $[0, 1]$ equipped with the inner product $\langle f, g \rangle_{\mathcal{L}^2} =$

$\int_0^1 f(r)g(r)dr$. Generally speaking, a functional time series $\{X_t\}$ follows an FAR process (in \mathcal{L}^2) of order D if

$$X_t(\cdot) = \mu(\cdot) + \sum_{d=1}^D \Psi_d(X_{t-d})(\cdot) + \epsilon_t(\cdot), \quad (1)$$

where $\mu(\cdot) \in \mathcal{L}^2$ is a deterministic function, $\epsilon_t(\cdot) \in \mathcal{L}^2$ are *i.i.d.* zero-mean noise functions, and $\{\Psi_d\}_{d=1}^D$ are bounded linear operators mapping $\mathcal{L}^2 \rightarrow \mathcal{L}^2$. Conditions for the existence of a stationary and causal solution of (1) in \mathcal{L}^2 and other theoretical properties of FAR in \mathcal{L}^2 are studied extensively in Bosq (2000). Besides FAR, other types of models and prediction approaches, such as nonlinear kernel-distance based methods, for functional times series are considered in Bosq (1998), Besse et al. (2000), Antoniadis et al. (2006), Kokoszka et al. (2017) and Bueno-Larraz and Klepsch (2019), among others. In this paper, we focus on the FAR process.

Due to the infinite-dimensional nature of the functional space \mathcal{L}^2 , existing literature addresses the inference of FAR mainly via dimension reduction, where a projection onto a finite basis is conducted to facilitate the estimation of $\{\Psi_d\}_{d=1}^D$ and the prediction of future realizations. Most literature reduces the dimension via functional principal component analysis (FPCA), where the finite basis is chosen as the leading p functional principal components (FPC) of an estimated covariance operator of the underlying FAR process (e.g. the sample covariance operator based on the observations $\{X_t\}_{t=1}^T$). See Besse and Cardot (1996), Bosq (2000), Besse et al. (2000), Hyndman and Shang (2009), Didericksen et al. (2012) and Aue et al. (2015) for influential works on FPCA-based approaches. Notable methods based on other basis such as wavelets or predictive factors include Antoniadis and Sapatinas (2003) and Kargin and Onatski (2008).

Theoretical justification for dimension reduction based methods can be found in, for example, Bosq (2000) and Kargin and Onatski (2008), where results such as the consistency of $\{\hat{\Psi}_d\}_{d=1}^D$ are provided. For these results to hold, a typical condition is that the number of basis elements p grows with the sample size T at a rate that implicitly depends on the intricate interrelation of eigenvalues and spectral gaps of the true covariance operator of the underlying FAR process, making the convergence rate derived therein rather opaque and

case-specific. As a result, there seems to be no clear guidance on the selection of p in practice, with most literature using a heuristic threshold (e.g. 80%) on the cumulative variance of FPCs, see for example [Didericksen et al. \(2012\)](#). An exception is [Aue et al. \(2015\)](#), where a novel functional prediction error criterion is developed for the selection of p .

A notable limitation of the current FAR literature is that existing estimation methods and theoretical results require fully observed functional time series $\{X_t(s), s \in [0, 1]\}_{t=1}^T$. However, this is an unrealistic assumption as, in reality, the FAR process is measured discretely and observations instead take the form $\{X_t(s_i), 1 \leq i \leq n\}_{t=1}^T$, where $\{s_i\}_{i=1}^n$ denotes n discrete grid points in $[0, 1]$. In practice, the aforementioned methods typically rely on an extra smoothing step to convert discrete measurements $\{X_t(s_i), 1 \leq i \leq n\}_{t=1}^T$ into (estimated) fully functional data $\{\tilde{X}_t(s), s \in [0, 1]\}_{t=1}^T$, and the statistical analysis is performed on $\{\tilde{X}_t(s), s \in [0, 1]\}_{t=1}^T$. Intuitively, the smoothing step may have substantial impact on the inference of FAR (as is illustrated via simulation studies in [Section 4.3](#)). However, to establish theoretical guarantees, existing literature commonly ignores the smoothing error and assumes the analysis is conducted on the true functional time series $\{X_t(s), s \in [0, 1]\}_{t=1}^T$, possibly due to technical difficulties. One ramification is that the derived convergence rate therein typically only involves T but not n .

In this paper, we study the inference of FAR processes through the lens of Reproducing Kernel Hilbert Spaces (RKHS, [Wahba \(1990\)](#)) and propose new estimation and prediction procedures for FAR without dimension reduction. Specifically, we consider a refined FAR process in RKHS (see detailed definition in [Section 2.2](#)),

$$X_t(\cdot) = \mu(\cdot) + \sum_{d=1}^D \int_0^1 A_d(\cdot, s) X_{t-d}(s) ds + \epsilon_t(\cdot), \quad (2)$$

where the bounded linear operators $\{\Psi_d\}_{d=1}^D$ take the explicit form of integral operators with bivariate kernels $\{A_d(r, s) : [0, 1] \times [0, 1] \rightarrow \mathbb{R}\}_{d=1}^D$. Note that statistically speaking, (2) is essentially equivalent to (1), as consistent estimation of $\{\Psi_d\}_{d=1}^D$ requires them to be Hilbert-Schmidt operators (e.g. [Bosq, 2000](#); [Kargin and Onatski, 2008](#)), which indeed implies $\{\Psi_d\}_{d=1}^D$ can be written as integral operators with square-integrable kernels ([Heil, 2018](#)).

By viewing $\{A_d(r, s)\}_{d=1}^D$ as compact linear operators in RKHS, we first derive its re-

producing property, which facilitates its consistent estimation directly based on discrete measurements without smoothing. We then propose a nuclear norm regularization method for the estimation of $\{A_d(r, s)\}_{d=1}^D$ and further derive the representer theorem, which enables the (infinite-dimensional) inference without dimension reduction. For efficient implementation, we reformulate the regularization of functional operators into the well-studied trace norm minimization in the machine learning literature, which can be readily solved via the accelerated gradient method (Ji and Ye, 2009). The consistency and explicit convergence rate (incorporating both T and n) of the proposed procedure are provided. To our best knowledge, this is the first rigorous theoretical guarantee for estimation and prediction of FAR processes based on discrete observations of functional time series.

The rest of the paper is organized as follows. Section 2 gives a brief review of RKHS and defines the FAR process in RKHS. Section 3 proposes the penalized nuclear norm estimator for FAR and studies its theoretical properties. The promising performance of the proposed method over existing procedures is demonstrated via extensive numerical experiments in Section 4 and a real data application of energy consumption prediction in Section 5. Section 6 concludes with a discussion. Some notations used throughout the paper are defined as follows. Denote $\|f\|_{\mathcal{L}^2}^2 = \langle f, f \rangle_{\mathcal{L}^2}$ and $\|f\|_{\infty} := \sup_{s \in [0,1]} |f(s)|$. For a matrix W , denote $\|W\|_F$ as its Frobenius norm and $\|W\|_*$ as its trace norm. We omit $[0, 1]$ in the integral whenever the domain of functions is clear.

2 Functional Autoregressive Processes in RKHS

2.1 RKHS and compact linear operators

In this subsection, we briefly review the Reproducing Kernel Hilbert Spaces (RKHS) and introduce the class of compact linear operator, which is later used for defining the FAR process in RKHS.

Let $\mathbb{K} : [0, 1] \times [0, 1] \rightarrow \mathbb{R}^+$ be a reproducing kernel and $\mathcal{H} \subset \mathcal{L}^2$ be the corresponding reproducing kernel Hilbert space. Denote $\langle \cdot, \cdot \rangle_{\mathcal{H}}$ as the inner product for \mathcal{H} and define

$\|f\|_{\mathcal{H}}^2 = \langle f, f \rangle_{\mathcal{H}}$ as the RKHS norm. The eigen-expansion of \mathbb{K} has the form

$$\mathbb{K}(r, s) = \sum_{k=1}^{\infty} \mu_k \phi_k(r) \phi_k(s), \quad (3)$$

where $\{\phi_k\}_{k=1}^{\infty}$ is an orthonormal basis of \mathcal{L}^2 such that $\|\phi_k\|_{\mathcal{L}^2}^2 = 1$ and $\|\phi_k\|_{\mathcal{H}}^2 = 1/\mu_k$. Thus for $f = \sum_{k=1}^{\infty} a_k \phi_k$ and $g = \sum_{k=1}^{\infty} b_k \phi_k$, we have $\langle f, g \rangle_{\mathcal{H}} = \sum_{k=1}^{\infty} a_k b_k / \mu_k$. In particular, $f(r) = \langle f, \mathbb{K}(\cdot, r) \rangle_{\mathcal{H}}$ for $f \in \mathcal{H}$, which is known as the reproducing property of RKHS. In Assumption 1, we impose some mild regularity conditions on the \mathcal{H} that we study in this paper.

Assumption 1.

a. *There exists an absolute constant $C_{\mathcal{H}}$ such that for any $f, g \in \mathcal{H}$, it holds that*

$$\|fg\|_{\mathcal{H}} \leq C_{\mathcal{H}} \|f\|_{\mathcal{H}} \|g\|_{\mathcal{H}}. \quad (4)$$

b. *There exists a constant $C_{\mathbb{K}}$ such that $\sup_{0 \leq r \leq 1} \mathbb{K}(r, r) \leq C_{\mathbb{K}}$.*

Assumption 1a is a mild regularity condition on \mathcal{H} and is mainly made for technical simplicity in the proof. A wide class of RKHS satisfies Assumption 1a. For a concrete example, consider the commonly used Sobolev space $\mathcal{H} = W^{\alpha,2}$ on $[0, 1]$ where $W^{\alpha,2} := \{f : \|f\|_{W^{\alpha,2}}^2 = \|f\|_{\mathcal{L}^2}^2 + \sum_{k=1}^{\alpha} \|f^{(k)}\|_{\mathcal{L}^2}^2 < \infty\}$. From the definition of $W^{\alpha,2}$, it is straightforward to show that there exists a constant C_{α} such that $\|fg\|_{W^{\alpha,2}} \leq C_{\alpha} \|f\|_{W^{\alpha,2}} \|g\|_{W^{\alpha,2}}$. For illustration, letting $\alpha = 1$, we have $\|(fg)'\|_{\mathcal{L}^2}^2 \leq 2 \int (f'(s)g(s))^2 + (f(s)g'(s))^2 ds \leq 2\|f'\|_{\mathcal{L}^2}^2 \|g\|_{\infty}^2 + 2\|f\|_{\infty}^2 \|g'\|_{\mathcal{L}^2}^2 \leq 4\|f\|_{W^{1,2}}^2 \|g\|_{W^{1,2}}^2$, therefore it suffices to take $C_{\mathcal{H}} = \sqrt{5}$ in (4) for $W^{1,2}$. We refer to Brezis (2011) for a comprehensive introduction to Sobolev spaces. Throughout the paper, we assume $C_{\mathcal{H}} = 1$ for notational simplicity as the theoretical analysis holds for any constant $C_{\mathcal{H}}$.

Assumption 1b is a widely-used assumption on the kernel function \mathbb{K} and is satisfied by most commonly used kernels. Note that Assumption 1b implies that for any $s \in [0, 1]$ and any $f \in \mathcal{H}$,

$$f(s) = \langle f, \mathbb{K}_s(\cdot) \rangle_{\mathcal{H}} \leq \|f\|_{\mathcal{H}} \|\mathbb{K}_s(\cdot)\|_{\mathcal{H}} \leq \|f\|_{\mathcal{H}} \sqrt{C_{\mathbb{K}}}.$$

As a result, $\|f\|_{\mathcal{L}^2} \leq \|f\|_{\infty} \leq \sqrt{C_{\mathbb{K}}} \|f\|_{\mathcal{H}}$. Note that for any positive constant β , the two

kernel functions \mathbb{K} and $\beta\mathbb{K}$ generate the same function space. Thus with rescaling if necessary, we assume without loss of generality that $C_{\mathbb{K}} = 1$ throughout the paper.

We now introduce the compact linear operator mapping $\mathcal{H} \rightarrow \mathcal{H}$, which is used to regulate the transition kernels $\{A_d(r, s) : [0, 1] \times [0, 1] \rightarrow \mathbb{R}\}_{d=1}^D$ of the FAR process in \mathcal{H} (see (2) in Section 1). Denote $A(r, s)$ as a function from $[0, 1] \times [0, 1] \rightarrow \mathbb{R}$ such that $A(\cdot, s) \in \mathcal{H}$ for any $s \in [0, 1]$ and $A(r, \cdot) \in \mathcal{H}$ for any $r \in [0, 1]$. Thus, $A(r, s)$ induces a linear operator on \mathcal{H} via

$$A[v](r) := \langle A(r, \cdot), v(\cdot) \rangle_{\mathcal{H}}, \quad r \in [0, 1], \quad \text{for any } v \in \mathcal{H}. \quad (5)$$

If we further have $A[v] \in \mathcal{H}$ for all $v \in \mathcal{H}$, the bivariate function $A(r, s)$ can be viewed as a linear operator A mapping $\mathcal{H} \rightarrow \mathcal{H}$ in the light of (5). To utilize the smoothness of the RKHS, we focus on the class of linear operators $A : \mathcal{H} \rightarrow \mathcal{H}$ that are compact, as defined in the following definition.

Definition 1. *A linear operator $A : \mathcal{H} \rightarrow \mathcal{H}$ is said to be compact if the image of any bounded set in \mathcal{H} is (relatively) compact.*

The space of compact operators on a Hilbert space is the closure of the space of finite rank operators. It is well known that in the classical functional analysis (see e.g. Brezis (2011)), the compact operators share many desirable properties with matrices such as the existence of the singular value decomposition, which facilitates its theoretical analysis.

Denote \mathcal{C} as the space of compact linear operators on \mathcal{H} and denote $\Phi_k = \sqrt{\mu_k} \phi_k$. For a compact linear operator $A \in \mathcal{C}$, define $a_{ij} := A[\Phi_i, \Phi_j] := \langle A[\Phi_j], \Phi_i \rangle_{\mathcal{H}}$. We have $A[f, g] := \langle A[g], f \rangle_{\mathcal{H}} = \sum_{i,j=1}^{\infty} a_{ij} \langle \Phi_i, f \rangle_{\mathcal{H}} \cdot \langle \Phi_j, g \rangle_{\mathcal{H}}$, which implies the useful decomposition

$$A(r, s) = A[\mathbb{K}(\cdot, r), \mathbb{K}(\cdot, s)] = \sum_{i,j=1}^{\infty} a_{ij} \Phi_i(r) \Phi_j(s), \quad (6)$$

which is essentially the reproducing property of A and is used to derive the Representer theorem later in Proposition 2. Note that by (6), any compact linear operator $A \in \mathcal{C}$ can be viewed as a bivariate function $A(r, s)$ such that $A[f](r) = \langle A(r, \cdot), f(\cdot) \rangle_{\mathcal{H}}, r \in [0, 1]$, for any $f \in \mathcal{H}$.

We now define norms of the operator $A : \mathcal{H} \rightarrow \mathcal{H}$ that are later used to regulate its smoothness. Denote $\|A\|_{\mathcal{H},*}$ as the nuclear norm of A such that $\|A\|_{\mathcal{H},*} = \sum_{i=1}^{\infty} \sqrt{\lambda_i}$, where

λ_i is the i -th eigenvalue of $A^\top A$ and A^\top is the adjoint operator of A such that $\langle A[u], v \rangle_{\mathcal{H}} = \langle u, A^\top[v] \rangle_{\mathcal{H}}$. In addition, define $\text{rank}(A) = \sum_{i=1}^{\infty} \mathbb{1}_{\{\lambda_i \neq 0\}}$. An operator A is said to be a bounded operator if its operator norm $\|A\|_{\mathcal{H},\text{op}}$ is finite, where

$$\|A\|_{\mathcal{H},\text{op}} := \sup_{\|u\|_{\mathcal{H}} \leq 1, \|v\|_{\mathcal{H}} \leq 1} \langle A[u], v \rangle_{\mathcal{H}} = \sup_{\sum_{i=1}^{\infty} u_i^2 \leq 1, \sum_{j=1}^{\infty} v_j^2 \leq 1} \sum_{i,j=1}^{\infty} a_{ij} u_i v_j. \quad (7)$$

2.2 FAR processes in an RKHS

In this subsection, based on the compact linear operators discussed in the previous section, we define the FAR process in an RKHS and further study its probabilistic properties.

Definition 2. For an RKHS \mathcal{H} , a functional time series $\{X_t\}_{t=1}^T \subset \mathcal{H}$ is said to follow a functional autoregressive process of order D in \mathcal{H} , hereafter $\text{FAR}(D)$, if

$$X_t(r) = \sum_{d=1}^D \int A_d^*(r, s) X_{t-d}(s) ds + \epsilon_t(r), \text{ for } r \in [0, 1], \quad (8)$$

where $\{\epsilon_t\}_{t=1}^T \subset \mathcal{H}$ is a collection of i.i.d. functional noise and the transition operators $\{A_d^*\}_{d=1}^D \subset \mathcal{C}$ are compact linear operators on \mathcal{H} .

Note that compared to (2), for ease of presentation, Definition 2 does not include the deterministic function $\mu(\cdot)$, as $\mu(\cdot)$ can be easily removed by centering X_t via $X_t - E(X_t)$ for stationary $\{X_t\}_{t=1}^T$.

Definition 2 requires that the functional time series $\{X_t\}_{t=1}^T$ resides in \mathcal{H} . This is an intuitive and necessary condition which allows us to estimate the transition operators $\{A_d^*\}_{d=1}^D$ from discrete measurements of $\{X_t\}_{t=1}^T$. As discussed in the introduction, most existing FAR literature assumes that $\{X_t\}_{t=1}^T$ are \mathcal{L}^2 functions with no additional regularity assumptions. We remark that in this latter setting, it is theoretically impossible to recover the transition operators $\{A_d^*\}_{d=1}^D$ from discrete measurements of $\{X_t\}_{t=1}^T$. In fact, in this case we cannot even consistently estimate one function X_t without extra regularity assumptions, as suggested by existing information theoretical lower bounds discussed in Mendelson (2002) and Raskutti et al. (2012).

In Assumption 2, we introduce regularity conditions on the transition operators $\{A_d^*\}_{d=1}^D$

and the i.i.d. functional noise $\{\epsilon_t\}_{t=1}^T$ of the FAR(D) process.

Assumption 2.

- a.** The transition operators $\{A_d^*\}_{d=1}^D \subset \mathcal{C}$ is a collection of compact linear operators with finite nuclear norm such that $\max_{1 \leq d \leq D} \|A_d^*\|_{\mathcal{H},*} < C$ for some constant C .
- b.** The functional noise is zero-mean with $E\epsilon_t(s) = 0$ for all $s \in [0, 1]$. In addition, there exist positive constants C_ϵ and κ_ϵ such that

$$P(\|\epsilon_t\|_{\mathcal{H}} \leq C_\epsilon) = 1, \quad (9)$$

$$E \left(\int v(s) \epsilon_t(s) ds \right)^2 \geq \kappa_\epsilon \|v\|_{\mathcal{L}^2}^2 \text{ for all } v \in \mathcal{H}. \quad (10)$$

Assumption 2a essentially requires that the transition operator $A_d^*(r, s)$ is a smooth function on $[0, 1]^2$ and implies that for any $s \in [0, 1]$, both $A_d^*(\cdot, s)$ and $A_d^*(s, \cdot)$ are functions in \mathcal{H} (see Lemma 2). This ensures that the reproducing property holds for both arguments of $A_d^*(r, s)$ and therefore allows us to estimate A_d^* from discrete measurements of $\{X_t\}_{t=1}^T$. Assumption 2a is similar to the commonly used assumption in functional principle component analysis (FPCA) literature that the covariance operator (and therefore the transition operators) of the FAR process can be well approximated by a finite number of eigenfunctions.

Assumption 2b is a commonly used condition in functional analysis literature. Since $E\epsilon_t(s) = 0$, condition (10) simply implies that the covariance operator $\Sigma_\epsilon(s, r) := E(\epsilon_t(s)\epsilon_t(r))$ of the noise function is positive definite. Condition (9) can be relaxed to a sub-Gaussian condition where $P(\|\epsilon_t\|_{\mathcal{H}} > \tau) \leq \exp(-c\tau^2)$. In this case, all of our theoretical results still hold and the convergence rate will only be slower by a log factor of T .

Assumption 3 imposes regularity conditions directly on the FAR(D) process $\{X_t\}_{t=1}^T$.

Assumption 3. The functional time series $\{X_t\}_{t=1}^T$ is stationary and there exist positive constants C_X and κ_X such that $P(\|X_t\|_{\mathcal{H}} \leq C_X) = 1$ and

$$E \left(\int \sum_{d=1}^D v_d(s) X_{t-d}(s) ds \right)^2 \geq \kappa_X \sum_{d=1}^D \|v_d\|_{\mathcal{L}^2}^2 \text{ for all } \{v_d\}_{d=1}^D \subset \mathcal{H}. \quad (11)$$

Assumption 3 is a high-level assumption made for explicitness. Note that when $D = 1$, condition (11) reduces to $\iint v(s) \Sigma_X(r, s) v(r) ds dr \geq \kappa_X \|v\|_{\mathcal{L}^2}^2$ for all $v \in \mathcal{H}$, where $\Sigma_X(r, s) :=$

$E(X_t(r)X_t(s))$. Therefore condition (11) can be thought of as the restricted eigenvalue condition for FAR(D), which is a frequently used condition in the high-dimensional time series literature, see for example Basu and Michailidis (2015).

Proposition 1 shows that Assumption 3 holds for a large family of FAR processes in RKHS.

Proposition 1. *Given Assumption 1 and Assumption 2b, for the FAR(D) process in Definition 2, if the transition operators $\{A_d^*\}_{d=1}^D$ satisfy*

$$\sup_{|z| \leq 1, z \in \mathbb{C}} \left\| \sum_{d=1}^D z^d A_d^* \right\|_{\mathcal{H}, op} = \gamma_A < 1, \quad (12)$$

then there exists a unique stationary solution $\{X_t\}_{t=-\infty}^{\infty}$ to (8) and there exists C_X depending only on C_ϵ and γ_A such that $P(\|X_t\|_{\mathcal{H}} \leq C_X) = 1$. In addition, if $\max_{1 \leq d \leq D} \text{rank}(A_d^) < \infty$, then (11) holds with κ_X depending only on κ_ϵ and γ_A .*

The stationarity result in Proposition 1 is similar to that in Theorem 5.1 of Bosq (2000), which gives the stationarity condition of an FAR process in \mathcal{L}^2 . For $D = 1$, condition (12) in Proposition 1 reduces to $\|A_1^*\|_{\mathcal{H}, op} < 1$, which is intuitive and resembles the stationarity condition for the classical AR(1) process (Brockwell and Davis (1991)). For a general D , condition (12) resembles the stability condition of the VAR(D) process (Lütkepohl (2005)).

3 Estimation Methodology and Main Results

In this section, we propose a penalized nuclear norm estimator for the transition operators of the FAR process in RKHS (Definition 2) and further study its consistency.

Section 3.1 proposes the RKHS-based penalized estimation procedure for the transition operators $\{A_d^*\}_{d=1}^D$ with discrete realizations of $\{X_t\}_{t=1}^T$. Section 3.2 establishes the consistency and the sharp convergence rate for the proposed estimator. Section 3.3 formulates the penalized estimation as a trace norm minimization problem and discusses its numerical implementation.

3.1 Penalized estimation and Representer theorem

As discussed before, in almost all real applications, instead of fully observed functional time series $\{X_t(s), s \in [0, 1]\}_{t=1}^T$, the available data are typically discrete measurements $\{X_t(s_i)\}_{1 \leq t \leq T, 1 \leq i \leq n}$, where $\{s_i\}_{i=1}^n$ denotes the collection of sampling points. Following the standard RKHS literature, we assume $\{s_i\}_{i=1}^n$ to be a collection of random designs uniformly sampled from the domain $[0, 1]$. Given $\{X_t(s_i)\}_{1 \leq t \leq T, 1 \leq i \leq n}$, our interest is the D unknown transition operators $\{A_d^*\}_{d=1}^D$, as the estimation of $\{A_d^*\}_{d=1}^D$ facilitates important inference tasks such as prediction.

We remark that for mathematical brevity, in this paper we only consider the case that $\{s_i\}_{i=1}^n$ are uniformly sampled from the domain $[0, 1]$. As a common feature in the RKHS literature (see e.g., [Koltchinskii and Yuan \(2010\)](#), [Raskutti et al. \(2012\)](#) and reference therein), all the results presented in the paper continue to hold under the more general setting where the random designs $\{s_i\}_{i=1}^n$ are i.i.d sampled from a common continuous distribution on $[0, 1]$ with density p such that $\inf_{r \in [0, 1]} p(r) > 0$, if we redefine \mathcal{L}^2 with the inner product $\langle f, g \rangle_{\mathcal{L}^2} := \int_0^1 f(s)g(s)p(s)ds$ and adjust the definition of \mathcal{H} accordingly.

Utilizing the finiteness of the nuclear norm of $\{A_d^*\}_{d=1}^D$ imposed in Assumption 2, we construct its estimator $\{\hat{A}_d\}_{d=1}^D$ via a constrained nuclear norm optimization such that

$$\{\hat{A}_d\}_{d=1}^D = \arg \min_{\{A_d\}_{d=1}^D \in \mathcal{C}_\tau} \frac{1}{Tn} \sum_{t=D+1}^T \sum_{i=1}^n \left(X_t(s_i) - \sum_{d=1}^D \frac{1}{n} \sum_{j=1}^n A_d(s_i, s_j) X_{t-d}(s_j) \right)^2 \quad (13)$$

where $\tau = (\tau_1, \dots, \tau_D)$ is the tuning parameter and $\mathcal{C}_\tau := \{(A_1, \dots, A_D) : A_d \in \mathcal{C} \text{ and } \|A_d\|_{\mathcal{H},*} \leq \tau_d, d = 1, \dots, D\}$ is the constraint space. We name $\{\hat{A}_d\}_{d=1}^D$ in (13) the penalized/constrained nuclear norm estimator for transition operators of FAR. (We use the term constrained and penalized nuclear norm estimator exchangeably due to the equivalence between constrained and penalized optimization. See Section 3.3 for more detail.)

To motivate the formulation of (13), consider the (ideal yet infeasible) scenario in which $\{X_t\}_{t=1}^T$ are fully observed in the entire domain $[0, 1]$, thus we can solve

$$\{\tilde{A}_d\}_{d=1}^D = \arg \min_{\{A_d\}_{d=1}^D \in \mathcal{C}_\tau} \frac{1}{T} \sum_{t=D+1}^T \int \left(X_t(r) - \sum_{d=1}^D \int A_d(r, s) X_{t-d}(s) ds \right)^2 dr.$$

However, since only discrete measurements $\{X_t(s_i)\}_{1 \leq t \leq T, 1 \leq i \leq n}$ are observed, we instead solve (13) where we use the integral approximation $\int A_d(s_i, r)X_{t-d}(r)dr \approx \frac{1}{n} \sum_{j=1}^n A_d(s_i, s_j)X_{t-d}(s_j)$.

Observe that (13) is an optimization problem in an infinite dimensional Hilbert space due to the nature of functional time series. As discussed in Section 1, existing literature (e.g. Bosq, 2000; Didericksen et al., 2012; Aue et al., 2015) uses dimension reduction to bypass such difficulty. Instead, we derive the Representer theorem for the penalized estimator in RKHS, which reduces the infinite dimensional optimization problem in (13) to finite dimension without dimension reduction.

Proposition 2 (Representer theorem). *There exists a minimizer $\{\hat{A}_d\}_{d=1}^D$ of the constrained nuclear norm optimization (13) such that for any $(r, s) \in [0, 1] \times [0, 1]$,*

$$\hat{A}_d(r, s) = \sum_{1 \leq i, j \leq n} \hat{a}_{d,ij} \mathbb{K}(r, s_i) \mathbb{K}(s, s_j), \text{ for } d = 1, 2, \dots, D. \quad (14)$$

We note that while Proposition 2 implies that a minimizer of (13) lives in the space spanned by the reproducing kernel $\{\mathbb{K}(s_i, \cdot)\}_{i=1}^n$, it does not rule out the possibility that there is a different solution $\{\hat{A}'_d\}_{d=1}^D$ that lives in a different subspace of higher dimensions. However, this does not affect the later theoretical analysis of consistency, which holds for any minimizer of (13). We remark that uniqueness of optimum is not a necessary condition for consistency in the RKHS literature. See for instance, Raskutti et al. (2012) and Koltchinskii and Yuan (2010).

Given the estimated transition operators $\{\hat{A}_d\}_{d=1}^D$, the one-step ahead prediction of X_{T+1} can be readily calculated as

$$\hat{X}_{T+1}(r) = \sum_{d=1}^D \frac{1}{n} \sum_{j=1}^n \hat{A}_d(r, s_j) X_{T+1-d}(s_j) \text{ for } r \in [0, 1]. \quad (15)$$

3.2 Consistency

In this section, we investigate the theoretical properties of the penalized nuclear norm estimator $\{\hat{A}_d\}_{d=1}^D$ and establish its consistency.

Given Assumptions 1-3, Theorem 1 establishes the consistency result of $\{\hat{A}_d\}_{d=1}^D$ and further provides the explicit convergence rate. We first introduce some notations before

stating the theorem. Denote $\|f\|_n^2 = \frac{1}{n} \sum_{i=1}^n f(s_i)^2$. We define

$$\gamma'_n := \inf \left\{ \gamma : \left| \int f(s) ds - \frac{1}{n} \sum_{i=1}^n f(s_i) \right| \leq \gamma \|f\|_{\mathcal{L}^2} + \gamma^2 \text{ for all } f \text{ such that } \|f\|_{\mathcal{H}} \leq 1 \right\}, \quad (16)$$

$$\gamma''_n := \inf \left\{ \gamma : \|f\|_{\mathcal{L}^2}^2 \leq 2\|f\|_n^2 + \gamma^2 \text{ and } \|f\|_n^2 \leq 2\|f\|_{\mathcal{L}^2}^2 + \gamma^2 \text{ for all } f \text{ such that } \|f\|_{\mathcal{H}} \leq 1 \right\}, \quad (17)$$

$$\gamma_n = \max\{\gamma'_n, \gamma''_n\}. \quad (18)$$

Intuitively speaking, γ_n (uniformly) quantifies how well we know a function $f \in \mathcal{H}$ (in our case $f = X_t$) given its measurements on n sample points: if the number of measurements n increases, we have more knowledge of X_t and γ_n decreases. We note that γ_n^2 is the optimal mean squared error bound of estimating a single function in \mathcal{H} given n discrete measurements. See [Mendelson \(2002\)](#), [Koltchinskii and Yuan \(2010\)](#) and [Raskutti et al. \(2012\)](#) for more details. For $\mathcal{H} = W^{\alpha,2}$, Corollary 2 of the Appendix establishes that $\gamma_n = O_p(n^{-\alpha/(2\alpha+1)})$, where $W^{\alpha,2}$ denotes the commonly used Sobolev space on $[0, 1]$ (see Section 2.1).

In addition, we define

$$\delta'_T := \inf \left\{ \delta : \left| \frac{1}{T} \sum_{t=1}^T \left(\sum_{d=1}^D \int v_d(r) X_{t-d}(r) dr \right)^2 - E \left(\sum_{d=1}^D \int v_d(r) X_{t-d}(r) dr \right)^2 \right| \leq \delta \sqrt{\sum_{d=1}^D \|v_d\|_{\mathcal{L}^2}^2} \right. \\ \left. \text{for all } \{v_d\}_{d=1}^D \text{ such that } \sup_{1 \leq d \leq D} \|v_d\|_{\mathcal{H}} \leq 1 \right\}, \quad (19)$$

$$\delta''_T := \sup_{1 \leq d \leq D, r, s \in [0,1]} \left| \frac{1}{T} \sum_{t=1}^T X_{t-d}(r) \epsilon_t(s) \right|, \quad (20)$$

$$\delta_T = \max\{\delta'_T, \delta''_T\}. \quad (21)$$

Intuitively speaking, δ_T characterizes the convergence rate of $\{\tilde{A}_d\}_{d=1}^D$ when the functional time series $\{X_t\}_{t=1}^T$ is fully observed. Corollary 3 of the Appendix shows that, for $\mathcal{H} = W^{\alpha,2}$, there exists constants c'_w, C'_w such that

$$P \left(\delta'_T \geq c'_w T^{\frac{-\alpha}{2\alpha+1}} \right) \leq 2T^2 \exp \left(-c'_w T^{\frac{1}{2\alpha+1}} \right) \quad \text{and} \quad P \left(\delta''_T \geq 3C_X C_\epsilon \sqrt{\frac{\log(T)}{T}} \right) \leq T^{-3}.$$

We now state the main theoretical result of the paper, which quantifies the convergence

rate of the penalized estimators $\{\widehat{A}_d\}_{d=1}^D$ through the \mathcal{L}^2 norm. The \mathcal{L}^2 norm of any bivariate function $A(r, s)$ is defined as $\|A\|_{\mathcal{L}^2}^2 := \iint A^2(r, s) dr ds$.

Theorem 1. *Suppose Assumptions 1-3 hold. Let $\{\widehat{A}_d\}_{d=1}^D$ be the solution of (13). If $\kappa_X \geq 64D\gamma_n^2$ and the tuning parameter $\boldsymbol{\tau}$ satisfies $\|A_d^*\|_{\mathcal{H},*} \leq \tau_d < C_A$, $d = 1, \dots, D$ for some constant C_A , then we have*

$$\sum_{d=1}^D \|\widehat{A}_d - A_d^*\|_{\mathcal{L}^2}^2 \leq C_1 (\gamma_n^2 + \delta_T^2), \quad (22)$$

for some constant C_1 independent of n and T .

The bound in Theorem 1 has two components: γ_n^2 quantifies how well we can estimate a single function in \mathcal{H} based on n discrete measurements and δ_T^2 is the rate of estimating the transition operators given fully observed $\{X_t\}_{t=1}^T$. Note that unlike existing FAR literature, the consistency result in Theorem 1 does not require the (unrealistic) assumption of fully observed functional time series. To our best knowledge, this is the first result in the FAR literature providing theoretical guarantees for the estimation of transition operators based on discrete measurements.

An immediate result of Theorem 1 is the explicit convergence rate of the penalized estimator $\{\widehat{A}_d\}_{d=1}^D$ for FAR(D) in the Sobolev space $W^{\alpha,2}$, which is given in the following Corollary 1.

Corollary 1. *Suppose the conditions in Theorem 1 hold. For $\mathcal{H} = W^{\alpha,2}$, with probability at least $1 - 1/n^4 - 1/T^3 - 2T^2 \exp\left(-c'_w T^{\frac{1}{2\alpha+1}}\right)$, it holds that*

$$\sum_{d=1}^D \|\widehat{A}_d - A_d^*\|_{\mathcal{L}^2}^2 \leq C'_1 \left(n^{\frac{-2\alpha}{2\alpha+1}} + T^{\frac{-2\alpha}{2\alpha+1}} \right),$$

for some constants c'_w, C'_1 independent of n and T .

As discussed in Section 1, the consistency result of the dimension reduction based estimation methods (e.g. Bosq, 2000; Kargin and Onatski, 2008) typically require the number of basis p grows with the sample size T at a rate that implicitly depends on intricate interrelation of eigenvalues and spectral gaps of the true covariance operator of the functional

time series $\{X_t\}$, making the derived convergence rate rather opaque and case-specific. In contrast, our RKHS-based estimation method does not require dimension reduction, making the convergence rate in Corollary 1 explicit as there is no dimension reduction incurred errors.

We further provide a simple argument to show that the error bound given in Theorem 1 is intuitive. Note that estimating A_d^* is harder than estimating a single function in \mathcal{H} . Thus the consistency rate is lower bounded by γ_n^2 , since as mentioned before, γ_n^2 is the well known optimal rate of estimating a single function from its n discrete realizations in RKHS. We also note that FAR is an extension and generalization to the Function to Function Regression (FFR) model. When the functions are fully observed, the optimal rate of excess risk in the FFR setting is δ_T^2 (see e.g. Sun et al. (2018)). Based on the above discussion, the error bound we established in Theorem 1 is sharp.

The estimation error bound in Theorem 1 naturally implies an error bound on the one-step ahead prediction given in (15). Proposition 3 quantifies the prediction risk of X_{T+1} given $\{X_t\}_{t=1}^T$.

Proposition 3. *Let $\mathcal{H} = W^{\alpha,2}$ and $\hat{X}_{T+1}(r)$ be defined as in (15). Define the oracle one-step ahead prediction of $X_{T+1}(r)$ as $E(X_{T+1}(r)|\{X_t\}_{t=1}^T) = \int \sum_{d=1}^D A_d^*(r, s) X_{T+1-d}(s) ds$. With probability at least $1 - 1/n^4 - 1/T^3 - 2T^2 \exp\left(-c'_w T^{\frac{1}{2\alpha+1}}\right)$, it holds that*

$$\begin{aligned} \|E(X_{T+1}|\{X_t\}_{t=1}^T) - \hat{X}_{T+1}\|_{\mathcal{L}^2}^2 &\leq C_1'' \left(n^{\frac{-2\alpha}{2\alpha+1}} + T^{\frac{-2\alpha}{2\alpha+1}} \right), \\ \frac{1}{n} \sum_{j=1}^n \left(E(X_{T+1}(s_j)|\{X_t\}_{t=1}^T) - \hat{X}_{T+1}(s_j) \right)^2 &\leq C_1'' \left(n^{\frac{-2\alpha}{2\alpha+1}} + T^{\frac{-2\alpha}{2\alpha+1}} \right), \end{aligned}$$

for some constants c'_w, C_1'' independent of n and T .

3.3 Optimization via Accelerated Gradient Method

In this section, we discuss the numerical implementation of the proposed RKHS-based penalized estimator by reformulating the constrained optimization in (13) into a standard trace norm minimization problem, which is well-studied in the machine learning literature (Ji and Ye (2009)).

We first introduce some notations. Denote the estimator $A_d(r, s) = \sum_{1 \leq i, j \leq n} a_{d,ij} \mathbb{K}(r, s_i) \mathbb{K}(s, s_j)$, where $a_{d,ij}$ s are the coefficients to be estimated. Define the coefficient matrix $R_d \in \mathbb{R}^{n \times n}$ with $R_{d,ij} = a_{d,ij}$. Define the kernel vector $k_i = (\mathbb{K}(s_1, s_i), \mathbb{K}(s_2, s_i), \dots, \mathbb{K}(s_n, s_i))^\top$ and the kernel matrix $K = [k_1, k_2, \dots, k_n]$. Note that the kernel matrix K is symmetric such that $K = K^\top$. Denote the observation of the functional time series at time t as $X_t = (X_t(s_1), X_t(s_2), \dots, X_t(s_n))^\top$. Define the observation matrix $X = [X_T, X_{T-1}, \dots, X_{D+1}]$ and the lagged observation matrix $X^{(d)} = [X_{T-d}, X_{T-d-1}, \dots, X_{D+1-d}]$ for $d = 1, \dots, D$.

Using the well-known equivalence between constrained and penalized optimization (see [Hastie et al. \(2009\)](#)), we can reformulate (13) into a penalized nuclear norm optimization such that

$$\{\hat{A}_d\}_{d=1}^D = \arg \min \sum_{t=D+1}^T \sum_{i=1}^n \left(X_t(s_i) - \sum_{d=1}^D \frac{1}{n} \sum_{j=1}^n A_d(s_i, s_j) X_{t-d}(s_j) \right)^2 + \sum_{d=1}^D \lambda_d \|A_d\|_{\mathcal{H},*},$$

where $(\lambda_1, \dots, \lambda_D)$ is the tuning parameter. With simple linear algebra, we can rewrite the penalized optimization as

$$\begin{aligned} & \min_{R_1, \dots, R_D} \sum_{t=D+1}^T \left(X_t - \frac{1}{n} \sum_{d=1}^D K^\top R_d K X_{t-d} \right)^\top \left(X_t - \frac{1}{n} \sum_{d=1}^D K^\top R_d K X_{t-d} \right) + \sum_{d=1}^D \lambda_d \|A_d\|_{\mathcal{H},*} \\ &= \min_{R_1, \dots, R_D} \left\| X - \frac{1}{n} \sum_{d=1}^D K R_d K X^{(d)} \right\|_F^2 + \sum_{d=1}^D \lambda_d \|A_d\|_{\mathcal{H},*}. \end{aligned} \quad (23)$$

We now write the nuclear norm $\|A_d\|_{\mathcal{H},*}$ as a function of R_d . By the Representer theorem, $A_d(r, s) = \sum_{i,j} a_{d,ij} \mathbb{K}(r, s_i) \mathbb{K}(s, s_j)$, thus the adjoint operator $A_d^\top(r, s) = A_d(s, r)$. Define $k(s) = (\mathbb{K}(s, s_1), \mathbb{K}(s, s_2), \dots, \mathbb{K}(s, s_n))^\top$, we have $A_d(r, s) = k(r)^\top R_d k(s)$ and $\langle k(s), k(s)^\top \rangle_{\mathcal{H}} = K$. Define $u(s) = k(s)^\top b$, where $b = (b_1, b_2, \dots, b_n)^\top$. To calculate $\|A_d\|_{\mathcal{H},*}$, note that

$$\begin{aligned} A_d^\top A_d[u](s) &= \langle A_d^\top(s, r), A_d[u](r) \rangle_{\mathcal{H}} = \langle A_d(r, s), \langle A_d(r, s), u(s) \rangle_{\mathcal{H}} \rangle_{\mathcal{H}} \\ &= \langle k(r)^\top R_d k(s), \langle k(r)^\top R_d k(s), k(s)^\top b \rangle_{\mathcal{H}} \rangle_{\mathcal{H}} = k(s)^\top R_d^\top K R_d K b. \end{aligned}$$

In other words, the eigenvalues of the operator $A_d^\top A$ correspond to the eigenvalues of the

matrix $R_d^\top K R_d K$. Thus, (23) can be further written as

$$\begin{aligned}
& \min_{R_1, \dots, R_D} \left\| X - \frac{1}{n} \sum_{d=1}^D K R_d K X^{(d)} \right\|_F^2 + \sum_{d=1}^D \lambda_d \cdot \text{trace}((R_d^\top K R_d K)^{\frac{1}{2}}) \\
&= \min_{R_1, \dots, R_D} \left\| X - \frac{1}{n} \sum_{d=1}^D K R_d K X^{(d)} \right\|_F^2 + \sum_{d=1}^D \lambda_d \|K^{\frac{1}{2}} R_d K^{\frac{1}{2}}\|_* \\
&= \min_{W_1, \dots, W_D} \left\| X - \sum_{d=1}^D \mathcal{K}_d W_d Z_d \right\|_F^2 + \sum_{d=1}^D \|W_d\|_* \tag{24}
\end{aligned}$$

where $W_d = \lambda_d K^{\frac{1}{2}} R_d K^{\frac{1}{2}}$, $\mathcal{K}_d = \frac{1}{\lambda_d} K^{\frac{1}{2}}$, $Z_d = \frac{1}{n} K^{\frac{1}{2}} X^{(d)}$ and the first equality comes from the fact that $R_d^\top K R_d K$ and $K^{1/2} R_d^\top K R_d K^{1/2}$ share the same eigenvalues for $d = 1, \dots, D$.

Define $\mathcal{K} = [\mathcal{K}_1, \dots, \mathcal{K}_D]$, $Z = \begin{bmatrix} Z_1 \\ \vdots \\ Z_D \end{bmatrix}$ and $W = \begin{bmatrix} W_1 & & \\ & \ddots & \\ & & W_D \end{bmatrix}$, the optimization in

(24) can be further written as

$$\arg \min_W \|X - \mathcal{K} W Z\|_F^2 + \|W\|_*, \tag{25}$$

where $g(W) = \|X - \mathcal{K} W Z\|_F^2$ is a convex function of the block diagonal matrix W and $\|W\|_*$ is its trace norm. Note that (25) is a convex function of W_1, \dots, W_d with a unique global minimizer.

Thus, we formulate the constrained nuclear norm optimization in (13) into a standard trace norm minimization problem in the machine learning literature (e.g. see [Bach \(2008\)](#), [Candès and Recht \(2009\)](#)). In particular, given tuning parameters $\{\lambda_d\}_{d=1}^D$, (25) can be readily solved by the Accelerated Gradient Method (AGM) in [Ji and Ye \(2009\)](#). Due to the block diagonal structure of W , AGM can be performed in a component-wise fashion where the gradient update of the optimization is carried out for each W_1, \dots, W_D separately. The implementation details of the AGM algorithm can be found in Section F of the Appendix.

Given $(\widehat{W}_1, \dots, \widehat{W}_D)$, the estimated transition operators $\{\widehat{A}_d\}_{d=1}^D$ can be recovered by

$$\widehat{A}_d(r, s) = k(r)^\top \widehat{R}_d k(s) = \frac{1}{\lambda_d} k(r)^\top K^{-\frac{1}{2}} \widehat{W}_d K^{-\frac{1}{2}} k(s), \text{ for } d = 1, \dots, D.$$

Plugging into (15), the one-step ahead prediction of X_{T+1} is then

$$\widehat{X}_{T+1}(r) = \frac{1}{n} \sum_{d=1}^D \frac{1}{\lambda_d} k(r)^\top K^{-\frac{1}{2}} \widehat{W}_d K^{\frac{1}{2}} X_{T+1-d}, \text{ for } r \in [0, 1].$$

4 Simulation Studies

In this section, we conduct simulation studies to investigate the estimation and prediction performance of the proposed penalized nuclear norm estimator and compare it with the standard transition operator estimation approach in Bosq (2000) and the state-of-the art functional time series prediction method in Aue et al. (2015).

4.1 Basic simulation setting

Data generating process: We first define an FAR(D) process, borrowed from the simulation setting in Aue et al. (2015), that is used in the simulation study. For $d = 1, 2, \dots, D$, we assume the d th transition operator $A_d(r, s)$ is of rank q_d and is generated by q_d basis functions $\{u_i(s)\}_{i=1}^{q_d}$ such that

$$A_d(r, s) = \sum_{i,j=1}^{q_d} \lambda_{d,ij} u_i(r) u_j(s),$$

where $\{u_i(s)\}_{i=1}^{q_d}$ consists of orthonormal basis of $\mathcal{L}^2[0, 1]$ that will be specified later. Define matrix Λ_d such that $\Lambda_{d,ij} = \lambda_{d,ij}$ and define $\mathbf{u}_{q_d}(s) = (u_1(s), u_2(s), \dots, u_{q_d}(s))^\top$. We have $A_d(r, s) = \mathbf{u}_{q_d}(r)^\top \Lambda_d \mathbf{u}_{q_d}(s)$. We further set the noise function ϵ_t to be of finite rank q_ϵ such that $\epsilon_t(s) = \sum_{i=1}^{q_\epsilon} z_{ti} u_i(s)$, where $z_{ti} \stackrel{i.i.d.}{\sim} U(-a_i, a_i)$ or $z_{ti} \stackrel{i.i.d.}{\sim} N(0, \sigma_i^2)$.

Without loss of generality, we set $q_1 = q_2 = \dots = q_D = q_\epsilon = q$ for simplicity. Thus, the FAR(D) process $\{X_t(s)\}_{t=1}^T$ resides in a finite dimensional subspace spanned by the orthonormal basis $\{u_i(s)\}_{i=1}^q$. Denote $X_t(r) = \sum_{i=1}^q x_{ti} u_i(r)$ where $x_{ti} = \int X_t(r) u_i(r) dr$, and denote $x_t = (x_{t1}, \dots, x_{tq})^\top$ and $z_t = (z_{t1}, \dots, z_{tq})^\top$. We have

$$\begin{aligned} X_t(r) &= \sum_{d=1}^D \int A_d(r, s) X_{t-d}(s) ds + \epsilon_t(r) = \sum_{d=1}^D \int \mathbf{u}_q(r)^\top \Lambda_d \mathbf{u}_q(s) X_{t-d}(s) ds + z_t^\top \mathbf{u}_q(r) \\ &= \sum_{d=1}^D \int \mathbf{u}_q(r)^\top \Lambda_d \mathbf{u}_q(s) \mathbf{u}_q(s)^\top x_{t-d} ds + z_t^\top \mathbf{u}_q(r) = \mathbf{u}_q(r)^\top \left(\sum_{d=1}^D \Lambda_d x_{t-d} + z_t \right). \end{aligned}$$

This leads to $x_t = \sum_{d=1}^D \Lambda_d x_{t-d} + z_t$. Thus, the FAR(D) process can be exactly simulated via a VAR(D) process. Following the simulation setting in [Yuan and Cai \(2010\)](#) and [Sun et al. \(2018\)](#), we set $u_i(s) = 1$ if $i = 1$ and $u_i(s) = \sqrt{2} \cos((i-1)\pi s)$ for $i = 2, \dots, q$.

Given the transition operators A_1, \dots, A_D (i.e. $\Lambda_1, \dots, \Lambda_D$) and the distribution of noise z_t , the true FAR(D) process $\{X_t(s), s \in [0, 1]\}_{t=1}^T$ can be simulated and discrete measurements of the functional time series are taken at the sampling points $\{s_i\}_{i=1}^n$. For simplicity, we set $\{s_i\}_{i=1}^n$ to be the n equal-spaced points in $[0, 1]$, which resembles the typical sampling scheme of functional time series in real data applications. Simulation based on uniformly distributed $\{s_i\}_{i=1}^n$ gives consistent conclusions.

Evaluation criteria: We evaluate the performance of a method via (a). estimation error of $\hat{A}_1, \hat{A}_2, \dots, \hat{A}_D$ and (b). prediction error of the estimated FAR(D) model.

Specifically, given sample size (n, T) , we simulate the observed functional time series $\{X_t(s_i), i = 1, \dots, n\}_{t=1}^{T+0.2T}$, which we then partition into training data $\{X_t(s_i), i = 1, \dots, n\}_{t=1}^T$ for estimation of A_1, \dots, A_D and test data $\{X_t(s_i), i = 1, \dots, n\}_{t=T+1}^{T+0.2T}$ for evaluation of prediction performance. Denote $\{\hat{X}_t(s_i), i = 1, \dots, n\}_{t=T+1}^{T+0.2T}$ as the one-step ahead prediction given by the estimated FAR(D) model. We define

$$\text{MISE}(\hat{A}_d, A_d) = \int_{[0,1]} \int_{[0,1]} (A_d(r, s) - \hat{A}_d(r, s))^2 dr ds \Big/ \int_{[0,1]} \int_{[0,1]} A_d(r, s)^2 dr ds, \quad (26)$$

$$\text{PE} = \frac{1}{0.2nT} \sum_{t=T+1}^{T+0.2T} \sum_{i=1}^n (X_t(s_i) - \hat{X}_t(s_i))^2, \quad (27)$$

where MISE (mean integrated squared error) measures the estimation error and PE measures the prediction error. For reference purposes, we also calculate the oracle prediction error and the constant mean prediction error such that

$$\text{Oracle PE} = \frac{1}{0.2nT} \sum_{t=T+1}^{T+0.2T} \sum_{i=1}^n (X_t(s_i) - \tilde{X}_t(s_i))^2, \quad \text{Mean Zero PE} = \frac{1}{0.2nT} \sum_{t=T+1}^{T+0.2T} \sum_{i=1}^n (X_t(s_i) - 0)^2,$$

where $\tilde{X}_t(s_i) = \sum_{d=1}^D \int A_d(s_i, r) X_{t-d}(r) dr$ is the (infeasible) oracle predictor for $X_t(s_i)$ and 0 is the constant mean prediction since $E(X_t(s)) = 0$ for $s \in [0, 1]$. Evaluation based on other types of error measures for estimation and prediction error (besides MISE and PE) gives consistent conclusions and thus is omitted.

4.2 Estimation methods and implementation details

For comparison, we implement two functional PCA (FPCA) based estimation approach for FAR: (a). the standard estimator in Bosq (2000) and (b). the vector autoregressive based approach in Aue et al. (2015). Both estimators make use of the FPCA conducted on the sample covariance operator $\tilde{C}(s, r) = \frac{1}{T} \sum_{t=1}^T X_t(s)X_t(r)$ such that $\tilde{C}(s, r) = \sum_{i=1}^{\infty} \hat{\lambda}_i \hat{f}_i(s) \hat{f}_i(r)$, where $(\hat{\lambda}_i, \hat{f}_i)$ is the eigenvalue-eigenfunction pair.

Standard estimator in Bosq (2000) [Bosq]: The estimator in Bosq (2000) is designed for estimating the transition operator $A_1(s, r)$ of FAR(1) based on the Yule-Walker equation for FAR(1) such that $D(s, r) = E(X_t(s)X_{t-1}(r)) = E(\int A_1(s, s')X_{t-1}(s')ds'X_{t-1}(r)) = \int A_1(s, s')C(s', r)ds'$, where $C(s, r) = E(X_t(s)X_t(r))$ is the covariance operator and $D(s, r) = E(X_t(s)X_{t-1}(r))$ is the auto-covariance operator.

The Yule-Walker equation is inverted via FPCA-based dimension reduction, where all quantities in the Yule-Walker equation are projected on the subspace spanned by the p orthonormal eigenfunctions $\hat{f}(s) = (\hat{f}_1(s), \dots, \hat{f}_p(s))^T$ corresponding to the p largest eigenvalues $(\hat{\lambda}_1, \dots, \hat{\lambda}_p)$ of the sample covariance operator. Specifically, $C(s, r)$ is approximated by $\hat{C}(s, r) = \sum_{i=1}^p \hat{\lambda}_i \hat{f}_i(s) \hat{f}_i(r)$ and $D(s, r)$ is approximated by

$$\hat{D}(s, r) = \frac{1}{T-1} \sum_{t=2}^T \sum_{i=1}^p \langle X_t, \hat{f}_i \rangle_{\mathcal{L}^2} \hat{f}_i(s) \sum_{j=1}^p \langle X_{t-1}, \hat{f}_j \rangle_{\mathcal{L}^2} \hat{f}_j(r).$$

The estimator of A_1 takes the form $\hat{A}_1(s, r) = \sum_{i=1}^p \sum_{j=1}^p a_{ij} \hat{f}_i(s) \hat{f}_j(r)$. Denote $\hat{\Lambda} = \text{diag}(\hat{\lambda}_1, \dots, \hat{\lambda}_p)$, $\hat{d}_t = (\langle X_t, \hat{f}_1 \rangle_{\mathcal{L}^2}, \dots, \langle X_t, \hat{f}_p \rangle_{\mathcal{L}^2})$ and let R denote the coefficient matrix such that $R_{ij} = a_{ij}$. The Yule-Walker equation implies that $\frac{1}{T-1} \sum_{t=2}^T \hat{d}_t \hat{d}_{t-1}^T = R \hat{\Lambda}$, and thus $R = \frac{1}{T-1} \sum_{t=2}^T \hat{d}_t \hat{d}_{t-1}^T \hat{\Lambda}^{-1}$, which provides an estimator of the transition operator A_1 . The number of functional principal components p used in the projection is typically set as the smallest number of eigenvalues such that the explained variability of the sample covariance operator is over a high threshold τ , say $\tau = 80\%$. In the following, we refer to this estimator by Bosq.

Using the fact that an FAR(D) process can be formulated into an FAR(1) process, the above argument naturally provides an estimator for the transition operators A_1, \dots, A_D of

FAR(D) with $D > 1$. We refer to [Bosq \(2000\)](#) for more details.

Functional PCA-VAR estimator in [Aue et al. \(2015\)](#) [ANH]: The basic idea of [Aue et al. \(2015\)](#) is a canny combination of FPCA-based dimension reduction and the classical vector autoregressive (VAR) model, designed for prediction of FAR processes. Specifically, the infinite dimensional functional time series $\{X_t\}_{t=1}^T$ is first projected to the p eigenfunctions $\hat{f}(s) = (\hat{f}_1(s), \dots, \hat{f}_p(s))^\top$ of the sample covariance operator. After projection, X_t is represented by a p -dimensional functional principal score $x_t = (x_{t1}, \dots, x_{tp})^\top$ with $x_{ti} = \int X_t(s) \hat{f}_i(s) ds$. A VAR(D) model is then fitted on the p -dimensional time series $\{x_t\}_{t=1}^T$ such that $x_t = B_1 x_{t-1} + \dots + B_D x_{t-D} + \epsilon_t$. Denote the estimated coefficient matrices as $\hat{B}_1, \dots, \hat{B}_D \in \mathbb{R}^{p \times p}$, the one-step ahead prediction of $X_t(s)$ is then $\hat{X}_t(s) = \hat{f}(s)^\top \hat{x}_t = \hat{f}(s)^\top \sum_{d=1}^D \hat{B}_d x_{t-d}$.

Note that this implies $\hat{X}_t(s) = \hat{f}(s)^\top \hat{x}_t = \hat{f}(s)^\top \sum_{d=1}^D \hat{B}_d x_{t-d} = \hat{f}(s)^\top \sum_{d=1}^D \hat{B}_d \int \hat{f}(r) X_{t-d}(r) dr = \sum_{d=1}^D \int \hat{f}(s)^\top \hat{B}_d \hat{f}(r) X_{t-d}(r) dr$. Thus, the FPCA-based prediction algorithm in [Aue et al. \(2015\)](#) induces an estimator for the transition operators $\{A_d\}_{d=1}^D$ such that

$$\hat{A}_d(s, r) = \hat{f}(s)^\top \hat{B}_d \hat{f}(r), \text{ for } d = 1, \dots, D.$$

The fFPE criterion in [Aue et al. \(2015\)](#) is used to select the number of functional principal components p for a given autoregressive order D . In the following, we refer to this estimator by ANH.

Implementation of FPCA-based estimators (Bosq and ANH): For the implementation of Bosq and ANH, the functional time series is required to be fully observed over the entire interval $[0, 1]$. However, under the current simulation setting, only discrete measurements $\{X_t(s_i), i = 1, \dots, n\}_{t=1}^T$ are available. Following [Aue et al. \(2015\)](#), for each t , the function $X_t(s), s \in [0, 1]$ is estimated using 10 cubic B-spline basis functions based on the discrete measurements $(X_t(s_1), \dots, X_t(s_n))$. We also use 20 cubic B-spline basis functions for more flexibility (see more details later).

Implementation of penalized nuclear norm estimator (RKHS): For the implementation of the proposed RKHS-based penalized nuclear norm estimator, we use the rescaled Bernoulli polynomial as the reproducing kernel \mathbb{K} , such that

$$\mathbb{K}(x, y) = 1 + k_1(x)k_1(y) + k_2(x)k_2(y) - k_4(x - y),$$

where $k_1(x) = x - 0.5$, $k_2(x) = \frac{1}{2}(k_1^2(x) - \frac{1}{12})$ and $k_4(x) = \frac{1}{24}(k_1^4(x) - \frac{k_1^2(x)}{2} + \frac{7}{240})$ for $x \in [0, 1]$, and $k_4(x - y) = k_4(|x - y|)$ for $x, y \in [0, 1]$. Such \mathbb{K} is the reproducing kernel for $W^{2,2}$. See Chapter 2.3.3 of [Gu \(2013\)](#) for more detail.

The accelerated gradient algorithm in [Ji and Ye \(2009\)](#) is used to solve the trace norm minimization as discussed in Section 3.3, where the algorithm stops when the relative decrease of function value in (25) is less than 10^{-8} . A standard 5-fold cross validation is used to select the tuning parameter $(\lambda_1, \dots, \lambda_D)$. Based on $\{\hat{A}_d\}_{d=1}^D$, the one-step ahead prediction of $X_t(s_i)$ for $t = T + 1, \dots, T + 0.2T$ in the test data can be calculated via $\hat{X}_t(s_i) = \sum_{d=1}^D \frac{1}{n} \sum_{j=1}^n \hat{A}_d(s_i, s_j) X_{t-d}(s_j)$ for $i = 1, \dots, n$ as in (15).

4.3 Simulation result for FAR(1)

We first start with the simple case of FAR(1), where there is only one transition operator $A(r, s) = A_1(r, s)$. The simulation setting involves the transition matrix $\Lambda = \Lambda_1 \in \mathbb{R}^{q \times q}$ (signal) and the noise range $a_{1:q} = (a_1, a_2, \dots, a_q)$ or the noise variance $\sigma_{1:q}^2 = (\sigma_1^2, \sigma_2^2, \dots, \sigma_q^2)$ for $\{z_{ti}\}_{i=1}^q$ (driving noise). Denote $\sigma(\Lambda)$ as the leading singular value for a matrix Λ . We consider three different signal-noise settings:

- Scenario A (Diag Λ): $\Lambda = \text{diag}(\kappa, \dots, \kappa)$ and $z_{ti} \stackrel{i.i.d.}{\sim} U(-a, a)$ with $a = 0.1$ for $i = 1, \dots, q$.
- Scenario B (Random Λ): A random matrix Λ^* is first generated via $\Lambda_{ij}^* \stackrel{i.i.d.}{\sim} N(0, 1)$ and we set $\Lambda = \kappa \cdot \Lambda^* / \sigma(\Lambda^*)$, and $z_{ti} \stackrel{i.i.d.}{\sim} U(-a, a)$ with $a = 0.1$ for $i = 1, \dots, q$.
- Scenario C (ANH setting): (a) A random matrix Λ^* is first generated via $\Lambda_{ij}^* \stackrel{ind.}{\sim} N(0, \sigma_i \sigma_j)$ and we set $\Lambda = \kappa \cdot \Lambda^* / \sigma(\Lambda^*)$, and $z_{ti} \stackrel{ind.}{\sim} N(0, \sigma_i^2)$ with $\sigma_{1:q} = (1 : q)^{-1}$. (b) Same setting except $\sigma_{1:q} = 1.2^{-(1:q)}$.

Scenario C is borrowed from [Aue et al. \(2015\)](#). Within each scenario, the intrinsic dimension of FAR(1) is controlled by the dimension q of the transition matrix Λ and the signal strength is controlled by the spectral norm κ of Λ , where a higher q implies a more complex FAR process and a larger κ gives a stronger signal.

Signal strength for Scenarios A-C: Given the same (q, κ) , we further discuss the signal strength of the three scenarios from the viewpoint of VAR processes. The main difference between Scenarios A, B and Scenario C is that for Scenarios A and B, the variance of the noise stays at a constant level a across $\{z_{ti}\}_{i=1}^q$, while for Scenario C, the variance of the noise $\sigma_{1:q}$ decays with q and the decay rate is faster in Scenario C(a) than in Scenario C(b). Note that unlike the classical regression setting, the noise $\{z_{ti}\}_{i=1}^q$ of an autoregressive process is not noise in the traditional sense but rather the driving force of the process. Indeed, variation in $\{z_{ti}\}_{i=1}^q$ helps reveal more information about the transition matrix Λ and leads to stronger signals. Thus, compared to Scenarios A and B, Scenario C has weaker signals with Scenario C(a) having the lowest signal strength, and intuitively Scenario C can be more well approximated by a lower-dimensional process. Between Scenarios A and B, note that the transition matrix in Scenario A has overall larger and non-decaying singular values, making Scenario A the strongest signal scenario and most difficult to be approximated by a low-dimensional process.

To summarize, in terms of signal strength, we have Scenario A > B > C(b) > C(a) given the same intrinsic dimension q and spectral norm κ . This indeed has implications on the numerical results (see more details later). For more discussion of the signal-to-noise ratio for VAR processes, we refer to [Lütkepohl \(2005\)](#). Additionally, we remark that the numerical performance is insensitive to the distribution of z_{ti} (uniform or normal distribution).

For Bosq and ANH, the function $X_t(s)$ is first estimated using 10 cubic B-spline basis functions. For ANH, we use 20 cubic B-splines when $q = 21$ for more flexibility. The performance of Bosq worsens when using 20 cubic B-splines, thus we always use 10 cubic B-splines for Bosq. With the FAR order fixed at $D = 1$, the threshold τ is set at 80% to select the number of FPCs p for Bosq and the ffPE criterion is used to select the number of FPCs p for ANH. For RKHS, we use 5-fold cross validation to select the tuning parameter λ_1 .

Numerical result for FAR(1): For Scenarios A and B, we consider three sample sizes: (1) $q = 6, n = 20, T = 100$, (2) $q = 12, n = 20, T = 400$, (3) $q = 21, n = 40, T = 400$. For

Scenario C, we consider $q = 21, n = 40, T = 400$. As for the signal level, we vary the spectral norm of Λ by $\kappa = 0.2, 0.5, 0.8$. For each simulation setting, i.e. different combination of Scenario A-C and (q, n, T, κ) , we conduct 100 experiments. Note that the transition matrix Λ is randomly generated for each experiment under Scenario B and C.

We summarize the numerical performance of Bosq, ANH and RKHS in Table 1, where we report the mean MISE (MISE_{avg}) and mean PE (PE_{avg}) across the 100 experiments (the conclusion based on median MISE and median PE is consistent and thus omitted). For each experiment, we also calculate the percentage improvement of prediction by RKHS over ANH via $\text{Ratio} = (\text{PE}(\text{ANH}) / \text{PE}(\text{RKHS}) - 1) \times 100\%$. A positive ratio indicates improvement by RKHS. We report the mean ratio (denoted by R_{avg}) across the 100 experiments. In addition, we report the percentage of experiments (denoted by R_w) where RKHS achieves a lower PE than ANH. Note that we compare ANH and RKHS as Bosq in general gives the least favorable performance. We further give the boxplot of PE in Figure 1 under signal strength $\kappa = 0.5$. The boxplots of PE under $\kappa = 0.2, 0.8$ can be found in the Appendix.

Overall, RKHS gives the smallest estimation error (measured by MISE defined in (26)) and prediction error (measured by PE defined in (27)) while ANH offers the second best performance. In general, within each scenario, the improvement of RKHS over comparison methods increases with a higher dimension q and a stronger signal κ , while for the same (q, κ) , RKHS yields the most improvement in Scenario A, followed by Scenarios B, C(b), and C(a). We provide some intuition as follows. When the intrinsic dimension of the FAR process is low and the signal is weak, the FPCA-based dimension reduction (which is a hard thresholding method) does not induce much bias and achieves a good bias-variance trade-off. However, when the signal is strong and the intrinsic dimension of the process is high, information lost in the dimension reduction is non-negligible, and thus the proposed RKHS-based regularization outperforms FPCA-based methods as it corresponds to a soft thresholding method. Note that the improvement in MISE may not lead to the same scale of improvement in PE, an observation also seen in Didericksen et al. (2012).

Compared to Scenario A, the estimation performance (MISE) of all methods deteriorate

under Scenario B and C, due to the more complex nature of the transition operator and the decaying signal strength. Note that MISE of ANH is noticeably large under $q = 21$ for Scenario B. One possible reason is the numerical instability caused by estimation of a large VAR model (A VAR(20) model, i.e. $p = 20$ FPC, is selected by ANH 33 out of 100 times.¹). Under Scenario C, Bosq gives the smallest MISE while RKHS still gives the smallest PE, however, MISE is not very meaningful as all methods are unable to recover the transition operators accurately under Scenario C.

As mentioned above, the reported result by ANH under $q = 21$ is based on 20 cubic B-splines for more flexibility. For illustration, Figure 1(c)(f) additionally plots the PE of ANH based on 10 cubic B-splines, which is noticeably worse than the one based on 20 cubic B-splines. This indicates that the smoothing step can substantially affect the performance of methods that rely on fully observed functional time series, though the smoothing error is typically ignored in theoretical results.

¹Under $q = 6$, ANH occasionally results in extremely large estimation and prediction error due to numerical instability of the VAR estimation if more than 6 FPC are selected. We exclude those cases from the numerical result.

		Scenario A: $q = 6, n = 20, T = 100$				Scenario B: $q = 6, n = 20, T = 100$			
	Method	MISE _{avg}	PE _{avg}	R _{avg} (%)	R _w (%)	MISE _{avg}	PE _{avg}	R _{avg} (%)	R _w (%)
$\kappa = 0.2$	RKHS	0.894	2.182	0.20	52	1.119	2.130	0.79	64
	ANH	0.960	2.185			1.617	2.146		
	Bosq	1.210	2.204			3.543	2.223		
$\kappa = 0.5$	RKHS	0.222	2.260	3.60	76	0.639	2.243	0.74	57
	ANH	0.323	2.343			0.742	2.256		
	Bosq	0.308	2.322			0.739	2.263		
$\kappa = 0.8$	RKHS	0.078	2.340	0.42	59	0.241	2.233	1.27	73
	ANH	0.065	2.351			0.270	2.261		
	Bosq	0.341	3.461			0.394	2.320		
		Scenario A: $q = 12, n = 20, T = 400$				Scenario B: $q = 12, n = 20, T = 400$			
	Method	MISE _{avg}	PE _{avg}	R _{avg} (%)	R _w (%)	MISE _{avg}	PE _{avg}	R _{avg} (%)	R _w (%)
$\kappa = 0.2$	RKHS	0.563	4.288	0.40	59	1.017	4.241	0.10	54
	ANH	0.716	4.305			1.081	4.245		
	Bosq	0.668	4.298			1.525	4.270		
$\kappa = 0.5$	RKHS	0.097	4.290	6.90	100	0.299	4.296	2.42	98
	ANH	0.419	4.586			1.078	4.400		
	Bosq	0.450	4.829			0.775	4.459		
$\kappa = 0.8$	RKHS	0.044	4.323	38.53	100	0.122	4.297	7.94	100
	ANH	0.341	5.987			0.840	4.639		
	Bosq	0.464	7.762			0.679	4.865		
		Scenario A: $q = 21, n = 40, T = 400$				Scenario B: $q = 21, n = 40, T = 400$			
	Method	MISE _{avg}	PE _{avg}	R _{avg} (%)	R _w (%)	MISE _{avg}	PE _{avg}	R _{avg} (%)	R _w (%)
$\kappa = 0.2$	RKHS	0.614	7.339	0.75	78	1.016	7.256	0.04	50
	ANH	0.829	7.394			1.062	7.259		
	Bosq	0.806	7.380			1.528	7.293		
$\kappa = 0.5$	RKHS	0.092	7.350	6.57	100	0.344	7.359	3.34	100
	ANH	0.304	7.833			2.914	7.605		
	Bosq	0.665	8.691			0.960	7.694		
$\kappa = 0.8$	RKHS	0.032	7.424	23.94	100	0.129	7.365	5.39	100
	ANH	0.271	9.200			3.985	7.762		
	Bosq	0.674	15.406			0.899	8.594		
		Scenario C(a): $q = 21, n = 40, T = 400$				Scenario C(b): $q = 21, n = 40, T = 400$			
	Method	MISE _{avg}	PE _{avg}	R _{avg} (%)	R _w (%)	MISE _{avg}	PE _{avg}	R _{avg} (%)	R _w (%)
$\kappa = 0.2$	RKHS	1.193	1.657	0.08	55	1.042	2.349	0.04	60
	ANH	1.696	1.658			1.068	2.350		
	Bosq	1.061	1.655			1.182	2.356		
$\kappa = 0.5$	RKHS	1.669	1.696	0.42	56	1.736	2.433	0.07	64
	ANH	1.788	1.703			1.827	2.435		
	Bosq	0.996	1.746			0.985	2.480		
$\kappa = 0.8$	RKHS	1.880	1.759	-0.54	38	1.618	2.481	0.58	63
	ANH	1.740	1.749			1.308	2.495		
	Bosq	0.975	1.929			0.945	2.745		

Table 1: Numerical performance of various methods for FAR(1) processes. Methods considered are RKHS (this paper), ANH (Aue et al., 2015), and Bosq (Bosq, 2000). Bold font indicates the best performance, where the proposed RKHS method is generally the best performer in Scenarios A and B. (PE_{avg} is multiplied by 100 in scale for Scenarios A and B, but not for Scenario C.)

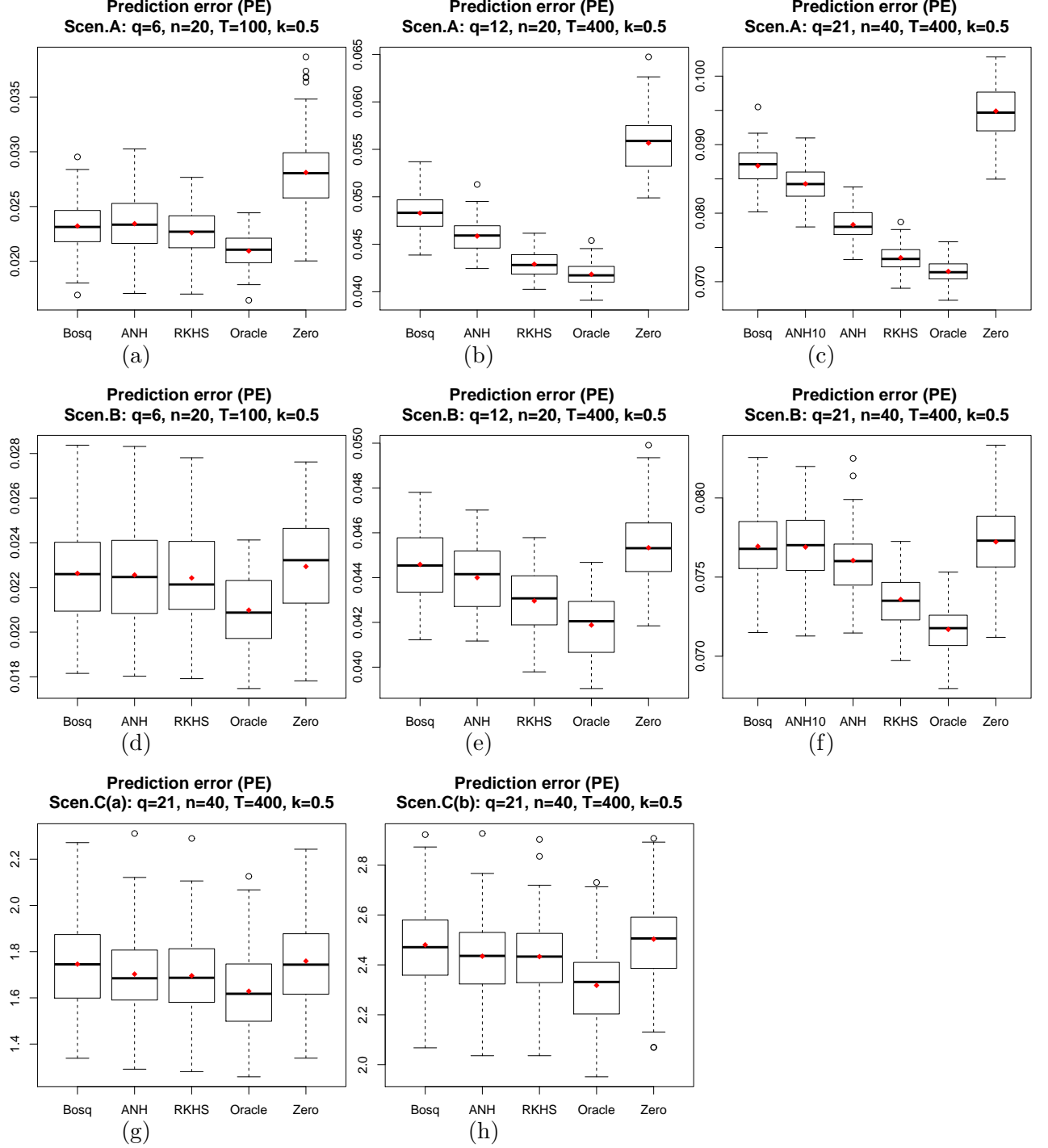


Figure 1: Boxplot of prediction error (PE) for FAR(1) across 100 experiments with signal strength $\kappa = 0.5$. In (c) and (f), ANH10 stands for ANH based on 10 cubic B-splines under $q = 21$. Red points denote average PE across 100 experiments for each method.

4.4 Simulation result for FAR with autoregressive order selection

This section investigates the performance of RKHS under an unknown FAR order D . Specifically, we consider an FAR(2) process under three signal-noise settings adapted from Section 4.3:

- Scenario A2 (Diag Λ): For $d = 1, 2$, $\Lambda_d = \text{diag}(\kappa_d, \dots, \kappa_d)$ and $z_{ti} \stackrel{i.i.d.}{\sim} U(-a, a)$ with $a = 0.1$ for $i = 1, \dots, q$.
- Scenario B2 (Random Λ): For $d = 1, 2$, a random matrix Λ_d^* is first generated via $\Lambda_{d,ij}^* \stackrel{i.i.d.}{\sim} N(0, 1)$ and we set $\Lambda_d = \kappa_d \cdot \Lambda_d^* / \sigma(\Lambda_d^*)$, and $z_{ti} \stackrel{i.i.d.}{\sim} U(-a, a)$ with $a = 0.1$, for $i = 1, \dots, q$.
- Scenario C2 (ANH setting): (a) For $d = 1, 2$, a random matrix Λ_d^* is first generated via $\Lambda_{d,ij}^* \stackrel{ind.}{\sim} N(0, \sigma_i \sigma_j)$ and we set $\Lambda_d = \kappa_d \cdot \Lambda_d^* / \sigma(\Lambda_d^*)$, and $z_{ti} \stackrel{ind.}{\sim} N(0, \sigma_i^2)$, where $\sigma_{1:q} = (1 : q)^{-1}$. (b) Same setting except $\sigma_{1:q} = 1.2^{-(1:q)}$.

The implementation of ANH and RKHS is the same as that for FAR(1). The only difference is that we do not impose the autoregressive order $D = 2$. Instead, we assume $D_{max} = 2$ and let the algorithms select the FAR order. For ANH, the ffPE criterion is used to select the number of FPC p and the FAR order D . For RKHS, we use 5-fold cross validation to select both D and the tuning parameters (λ_1, λ_2) . Note that both ffPE and CV are prediction-based order selection criteria and thus may not always favor the correct autoregressive order. We do not include Bosq in the comparison as its performance is typically inferior to ANH and RKHS (as shown in Section 4.3) and additional procedure is needed to determine the FAR order for Bosq, see for example [Kokoszka and Reimherr \(2013\)](#).

Numerical result for autoregressive order selection: For Scenarios A2 and B2, we consider (1) $q = 6, n = 20, T = 100$, (2) $q = 12, n = 20, T = 400$, (3) $q = 21, n = 40, T = 400$. For Scenario C2, we consider $q = 21, n = 40, T = 400$. As for the signal level, we consider $(\kappa_1, \kappa_2) = (0.5, 0.3)$ and $(\kappa_1, \kappa_2) = (0, 0.5)$ similar as in [Aue et al. \(2015\)](#). For each simulation setting, we conduct 100 experiments.

We summarize the numerical performance of RKHS and ANH in Table 2. Note that MISE is not well-defined when an incorrect autoregressive order is selected, thus we only report PE. For each experiment, PE is calculated based on the selected FAR model, which may or may not be FAR(2). Same as the analysis for FAR(1), we report the mean ratio (R_{avg}) of prediction improvement by RKHS and the percentage of experiments (R_w) where RKHS achieves a lower PE than ANH. In addition, we report the percentage of experiments (D_T) where the algorithm selects the correct autoregressive order D . We further give the boxplot of PE in Figure 2 under signal strength $(\kappa_1, \kappa_2) = (0.5, 0.3)$. The boxplot of PE under $(\kappa_1, \kappa_2) = (0, 0.5)$ can be found in the Appendix.

RKHS continues to offer better performance for estimation and prediction under autoregressive order selection. Note that for $(\kappa_1, \kappa_2) = (0, 0.5)$, both RKHS and ANH can identify the correct FAR order accurately, as ignoring κ_2 can result in large prediction error. However, this is not the case for $(\kappa_1, \kappa_2) = (0.5, 0.3)$, where due to possible bias-variance trade-off, FAR(1) may be the favored model for prediction.

		Scenario A2: $q = 6, n = 20, T = 100$				Scenario B2: $q = 6, n = 20, T = 100$			
	Method	PE_{avg}	$D_T(\%)$	$R_{avg}(\%)$	$R_w(\%)$	PE_{avg}	$D_T(\%)$	$R_{avg}(\%)$	$R_w(\%)$
$\kappa_1, \kappa_2 = 0.5, 0.3$	RKHS	2.557	49	5.28	70	2.315	6	2.24	71
	ANH	2.696	93			2.364	36		
$\kappa_1, \kappa_2 = 0, 0.5$	RKHS	2.244	100	9.45	91	2.248	99	3.96	72
	ANH	2.456	100			2.334	88		
		Scenario A2: $q = 12, n = 20, T = 400$				Scenario B2: $q = 12, n = 20, T = 400$			
	Method	PE_{avg}	$D_T(\%)$	$R_{avg}(\%)$	$R_w(\%)$	PE_{avg}	$D_T(\%)$	$R_{avg}(\%)$	$R_w(\%)$
$\kappa_1, \kappa_2 = 0.5, 0.3$	RKHS	4.418	100	26.26	100	4.389	61	3.01	99
	ANH	5.577	100			4.521	52		
$\kappa_1, \kappa_2 = 0, 0.5$	RKHS	4.296	100	9.56	100	4.290	100	4.53	100
	ANH	4.707	100			4.484	100		
		Scenario A2: $q = 21, n = 40, T = 400$				Scenario B2: $q = 21, n = 40, T = 400$			
	Method	PE_{avg}	$D_T(\%)$	$R_{avg}(\%)$	$R_w(\%)$	PE_{avg}	$D_T(\%)$	$R_{avg}(\%)$	$R_w(\%)$
$\kappa_1, \kappa_2 = 0.5, 0.3$	RKHS	7.569	100	22.78	100	7.558	42	3.69	100
	ANH	9.292	100			7.836	3		
$\kappa_1, \kappa_2 = 0, 0.5$	RKHS	7.347	100	12.22	100	7.374	100	5.11	100
	ANH	8.245	100			7.750	99		
		Scenario C2(a): $q = 21, n = 40, T = 400$				Scenario C2(b): $q = 21, n = 40, T = 400$			
	Method	PE_{avg}	$D_T(\%)$	$R_{avg}(\%)$	$R_w(\%)$	PE_{avg}	$D_T(\%)$	$R_{avg}(\%)$	$R_w(\%)$
$\kappa_1, \kappa_2 = 0.5, 0.3$	RKHS	1.727	65	0.24	51	2.494	51	-0.18	43
	ANH	1.731	9			2.489	1		
$\kappa_1, \kappa_2 = 0, 0.5$	RKHS	1.692	99	1.19	71	2.438	95	1.87	81
	ANH	1.712	96			2.483	88		

Table 2: Numerical performance of various methods for FAR(2) processes with autoregressive order selection. Methods considered are RKHS (this paper) and ANH (Aue et al., 2015). Bold font indicates the best performance, where the proposed RKHS method is generally the best performer in Scenarios A2 and B2. (PE_{avg} is multiplied by 100 in scale for Scenarios A2 and B2, but not for Scenario C2.)

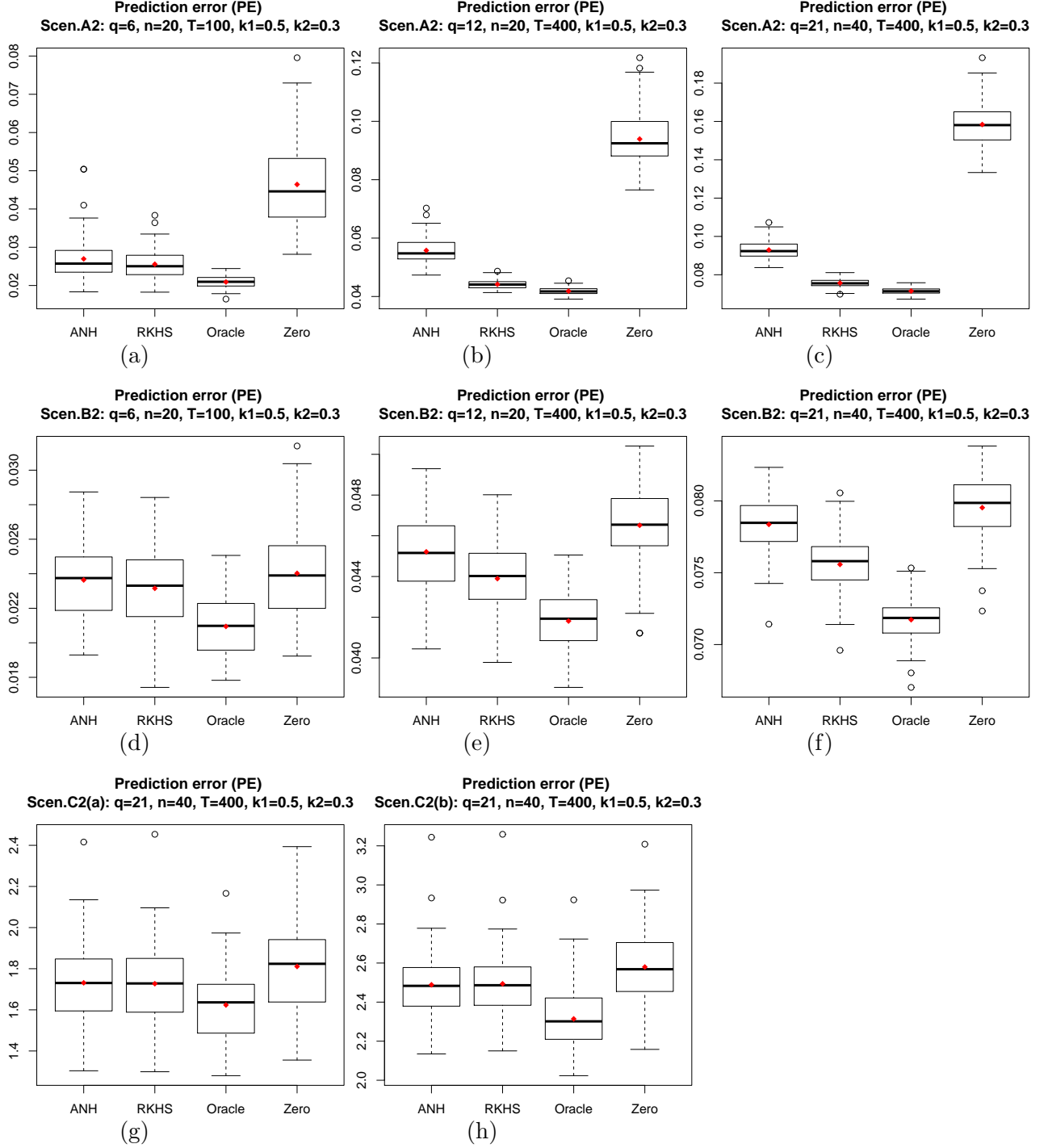


Figure 2: Boxplot of prediction error (PE) for FAR with autoregressive order selection across 100 experiments with signal strength $\kappa_1 = 0.5, \kappa_2 = 0.3$. Red points denote average PE across 100 experiments for each method.

5 Real Data Application

In this section, we give an illustrative example of RKHS in predicting functional time series. Specifically, we consider the Utility demand data in the book [Hyndman et al. \(2008\)](#), which is publicly available in R package `expsmooth`. The data contains 125 daily curves of hourly utility demand from a company in Midwest U.S., starting from January 2003. Thus we have $T = 125$ and $n = 24$.

The original functional time series is given in Figure 3. As can be seen, the utility demand seems to be non-stationary with a downward trend. Thus, we take the first-order difference and study the differenced time series, in other words, we study the derivative of the utility demand curve. We partition the time series into training data, which contains the first 100 daily curves, and test data, which contains the last 25 daily curves.

Based on the training data, we estimate three FAR(1) models using Bosq, ANH and RKHS respectively, where the implementation of the three methods is the same as in Section 4.3. The estimated model is then used to generate one-day ahead prediction for the 25 daily curves in the test data. For reference, we also implement a naive prediction, where the lagged X_{t-1} is used to predict X_t . For each day $t = 101, \dots, 125$ in the test data, we calculate the prediction error for each hour $e_{ti} = X_t(s_i) - \hat{X}_t(s_i), i = 1, \dots, 24$ where $\hat{X}_t(s_i)$ denotes the predicted value, and we define $\text{RMSE}_t = \sqrt{\sum_{i=1}^{24} e_{ti}^2 / 24}$ and $\text{MAE}_t = \sum_{i=1}^{24} |e_{ti}| / 24$. Table 3 summarizes the prediction performance of the four methods, where for each method, we report the average RMSE and average MAE across the 25 days on the test data. RKHS gives the best performance, followed by ANH. In addition, we give the percentage of days when RKHS gives the best performance among the four methods in terms of RMSE_t and MAE_t , and it is seen that RKHS wins around 60% of the time.

Figure 4 gives the 3D plot of the transition operator $\hat{A}(s, r)$ estimated by Bosq, ANH and RKHS. As can be seen, the transition operators by ANH and RKHS exhibit wider range and more complex nature than Bosq. This is also confirmed by the singular values of the estimated transition operator, as is shown in Figure 3(right). Bosq selects $p = 3$ FPC and the ffPE criterion of ANH selects $p = 5$ FPC, which reflects on the rank of the estimated

$\hat{A}(s, r)$.

For illustration, Figure 5(left) further plots the mean observation $\overline{X}(s_i) = \sum_{t=101}^{125} X_t(s_i)/25$ for each hour $i = 1, \dots, 24$ across the 25 days on the test data, together with the mean prediction $\overline{\hat{X}}(s) = \sum_{t=101}^{125} \hat{X}_t(s)/25$ by Bosq, ANH and RKHS. As can be seen, the mean prediction given by RKHS performs the best, while Bosq and ANH seem to miss some variation in the data, possibly due to information loss in dimension reduction. Figure 5(center, right) plot sectional views of the estimated transition operator $\hat{A}(s, \cdot)$ at $s = 5$ and $s = 20$ hour respectively. Same as in Figure 4, the transition operators estimated by RKHS and ANH exhibit more structures than Bosq. Additionally, it seems that the end of day observations have high predictive power as $\hat{A}(s, r)$ takes larger absolute values around $r = 20$, though the direction may be different for different hours s .

	Bosq	ANH	RKHS	Naive	RKHS wins
average RMSE	268.30	239.14	201.64	301.80	60%
average MAE	191.05	173.23	147.84	203.79	60%

Table 3: Prediction performance of Bosq, ANH, RKHS and Naive on the test data.

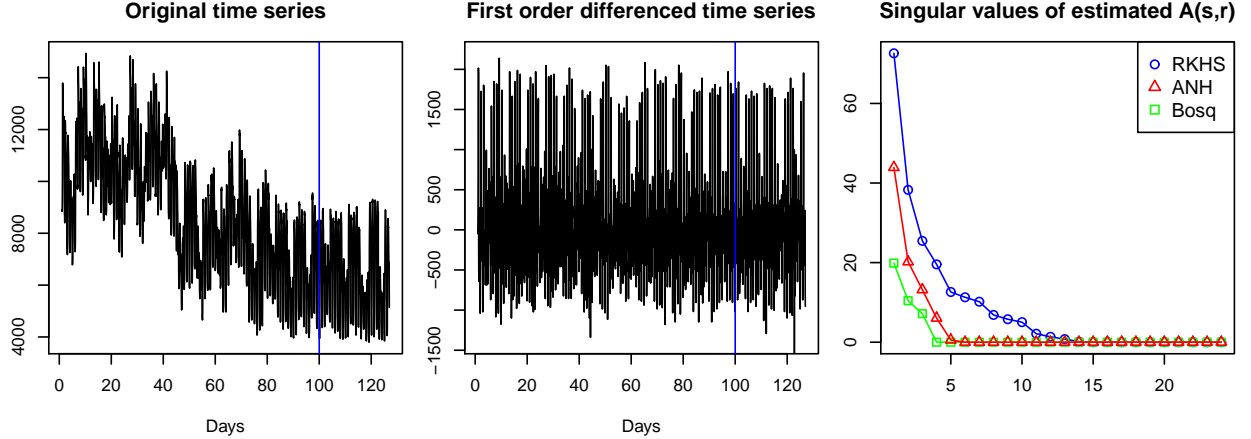


Figure 3: Left plot: Original utility demand time series. Center plot: First order differenced utility demand time series. (The blue vertical line marks the beginning of test data.) Right plot: Singular values of estimated $A(s, r)$ by Bosq, ANH and RKHS.

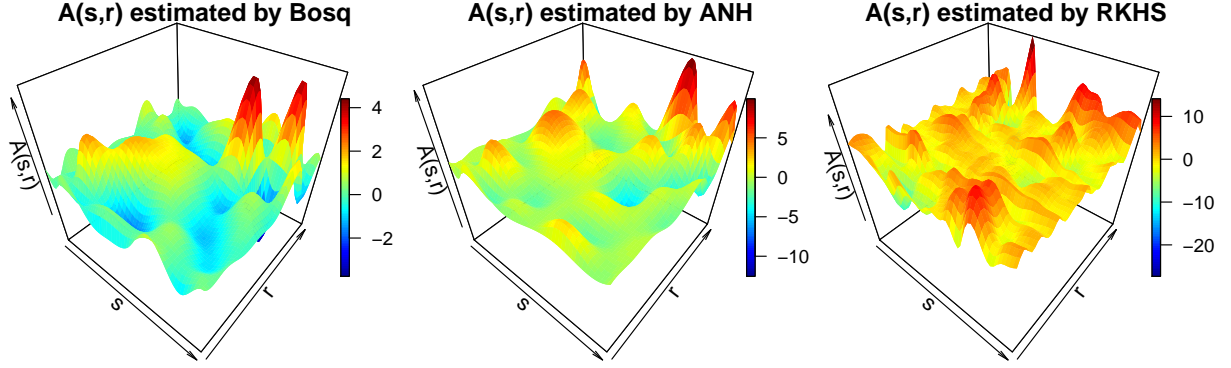


Figure 4: 3D plot of the transition operator $A(s, r)$ estimated by Bosq, ANH and RKHS.

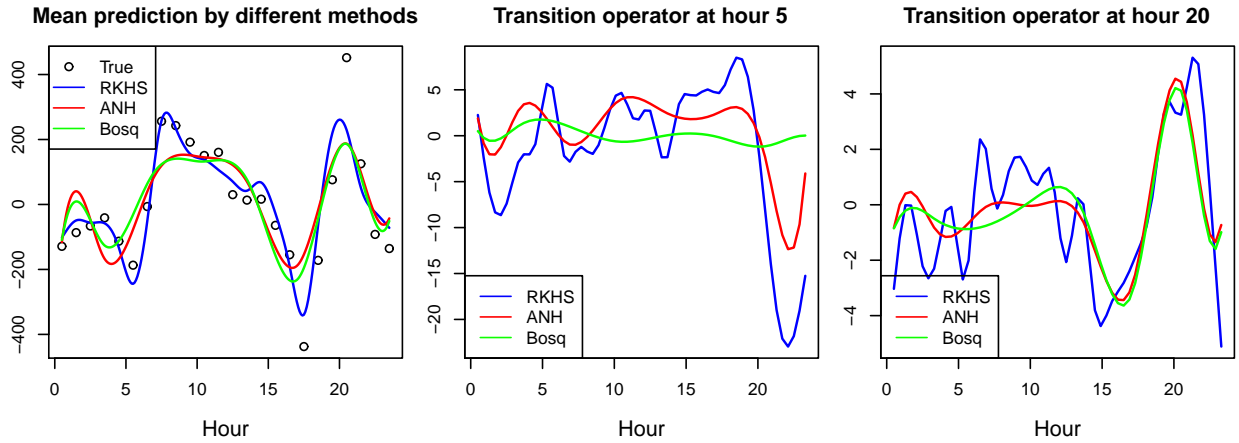


Figure 5: Left plot: Mean prediction for each hour on the test data. Center plot: Estimated transition operator $\hat{A}(s, \cdot)$ at hour $s = 5$ (sectional view). Right plot: Estimated transition operator $\hat{A}(s, \cdot)$ at hour $s = 20$ (sectional view).

6 Conclusion

In this paper, we study the inference (estimation and prediction) of the FAR process through the lens of RKHS. Unlike existing literature, the proposed inference framework does not require dimension reduction thanks to the derived Representer theorem. The proposed method works directly with discrete measurements of the functional time series and we

show that the nuclear norm penalization estimator is consistent with sharp convergence rate. Simulation studies and a real data application further demonstrate the promising performance of the proposed method and the advantage of dimension reduction free inference. A natural extension of the current framework is the scenario of noisy measurements, where the functional time series is observed with additional (i.i.d.) measurement errors at each sampling point. We expect the method and theory developed in the current paper continue to work under the noisy measurement scenario and leave the thorough investigation for future research.

References

- Antoniadis, A., Paparoditis, E., and Sapatinas, T. (2006). A functional wavelet–kernel approach for time series prediction. *Journal of the Royal Statistical Society - Series B*, 68.
- Antoniadis, A. and Sapatinas, T. (2003). Wavelet methods for continuous-time prediction using hilbert-valued autoregressive processes. *Journal of Multivariate Analysis*, 87(1):133–158.
- Aue, A., Norinho, D. D., and Hörmann, S. (2015). On the prediction of stationary functional time series. *Journal of the American Statistical Association*, 110(509):378–392.
- Bach, F. R. (2008). Consistency of trace norm minimization. *Journal of Machine Learning Research*, (8):1019–1048.
- Bartlett, P. L., Bousquet, O., and Mendelson, S. (2005). Local rademacher complexities. *Annals of Statistics*, 33(4):1497–1537.
- Basu, S. and Michailidis, G. (2015). Regularized estimation in sparse high-dimensional time series models. *Annals of Statistics*, 43(4):1535–1567.
- Besse, P. C. and Cardot, H. (1996). Approximation spline de la prevision d’un processus fonctionnel autorégressif d’ordre 1. *Canadian Journal of Statistics*, 24(4):467–487.
- Besse, P. C., Cardot, H., and Stephenson, D. B. (2000). Autoregressive forecasting of some functional climatic variations. *Scandinavian Journal of Statistics*, 27(4):673–687.
- Bosq, D. (1998). *Nonparametric Statistics for Stochastic Processes: Estimation and Prediction*. Springer-Verlag New York, 2 edition.
- Bosq, D. (2000). *Linear processes in function spaces: theory and applications*. Springer-Verlag New York.

- Brezis, H. (2011). *Functional analysis, Sobolev spaces and partial differential equations*. Springer-Verlag New York.
- Brockwell, P. J. and Davis, R. A. (1991). *Time Series: Theory and Methods*. Springer-Verlag New York.
- Bueno-Larraz, B. and Klepsch, J. (2019). Variable selection for the prediction of $c[0,1]$ -valued autoregressive processes using reproducing kernel hilbert spaces. *Technometrics*, 61(2):139–153.
- Candès, E. J. and Recht, B. (2009). Exact matrix completion via convex optimization. *Foundations of Computational Mathematics*, (9):717–772.
- Didericksen, D., Kokoszka, P., and Zhang, X. (2012). Empirical properties of forecasts with the functional autoregressive model. *Computational Statistics*, (27):285–298.
- Ferraty, F. and Vieu, P. (2006). *Nonparametric Functional Data Analysis*. Springer-Verlag New York.
- Gu, C. (2013). *Smoothing Spline ANOVA Models*. Springer-Verlag New York, 2 edition.
- Hastie, T., Tibshirani, R., and Friedman, J. (2009). *The Elements of Statistical Learning*. Springer-Verlag New York, 2 edition.
- Heil, C. (2018). *Metrics, Norms, Inner Products, and Operator Theory*. Birkhäuser Basel.
- Horváth, L. and Kokoszka, P. (2012). *Inference for Functional Data with Applications*. Springer.
- Hyndman, R., Koehler, A. B., Ord, J. K., and Snyder, R. D. (2008). *Forecasting with Exponential Smoothing: The State Space Approach*. Springer-Verlag Berlin Heidelberg, 1 edition.
- Hyndman, R. J. and Shang, H. L. (2009). Forecasting functional time series. *Journal of the Korean Statistical Society*, 38(3):199–211.
- Hyndman, R. J. and Ullah, M. S. (2007). Robust forecasting of mortality and fertility rates: A functional data approach. *Computational Statistics & Data Analysis*, 51(10):4942–4956.
- Hörmann, S. and Kokoszka, P. (2010). Weakly dependent functional data. *Annals of Statistics*, 38(3):1845–1884.
- Ji, S. and Ye, J. (2009). An accelerated gradient method for trace norm minimization. In *ICML '09: Proceedings of the 26th Annual International Conference on Machine Learning*, page 457–464.
- Kargin, V. and Onatski, A. (2008). Curve forecasting by functional autoregression. *Journal of Multivariate Analysis*, 99(10):2508–2526.

- Kokoszka, P. and Reimherr, M. (2013). Determining the order of the functional autoregressive model. *Journal of Time Series Analysis*, 34(1):116–129.
- Kokoszka, P., Rice, G., and Shang, H. L. (2017). Inference for the autocovariance of a functional time series under conditional heteroscedasticity. *Journal of Multivariate Analysis*, 162:32–50.
- Koltchinskii, V. and Yuan, M. (2010). Sparsity in multiple kernel learning. *Annals of Statistics*, 38(6):3660–3695.
- Lütkepohl, H. (2005). *New Introduction to Multiple Time Series Analysis*. Springer-Verlag Berlin Heidelberg.
- Mendelson, S. (2002). Geometric parameters of kernel machines. In *International Conference on Computational Learning Theory*, pages 29–43. Springer.
- Nickl, R. and Pötscher, B. M. (2007). Bracketing metric entropy rates and empirical central limit theorems for function classes of besov-and sobolev-type. *Journal of Theoretical Probability*, 20(2):177–199.
- Ramsay, J. and Silverman, B. W. (2005). *Functional Data Analysis*. Springer-Verlag New York.
- Raskutti, G., Wainwright, M. J., and Yu, B. (2012). Minimax-optimal rates for sparse additive models over kernel classes via convex programming. *Journal of Machine Learning Research*, 13(Feb):389–427.
- Shang, H. L. (2013). Functional time series approach for forecasting very short-term electricity demand. *Journal of Applied Statistics*, 40(1):152–168.
- Sun, X., Du, P., Wang, X., and Ma, P. (2018). Optimal penalized function-on-function regression under a reproducing kernel hilbert space framework. *Journal of the American Statistical Association*, 113(524):1601–1611.
- Wahba, G. (1990). *Spline Models for Observational Data*. SIAM, Philadelphia.
- Wong, K. C., Li, Z., and Tewari, A. (2017). Lasso guarantees for beta-mixing heavy tailed time series. *arXiv preprint arXiv:1708.01505*.
- Yuan, M. and Cai, T. T. (2010). A reproducing kernel Hilbert space approach to functional linear regression. *Annals of Statistics*, 38(6):3412–3444.
- Appendix A-E contains technical proofs of theorems in the main text. Appendix F gives the implementation details of the accelerated gradient method (AGM). Appendix G contains additional simulation results.

A Results related to linear compact operators : $\mathcal{H} \rightarrow \mathcal{H}$

In this section, we give some properties of the linear compact operator $A : \mathcal{H} \rightarrow \mathcal{H}$ that will be used later in the proof. Lemma 1 shows that a linear compact operator is also bounded operator $A : \mathcal{L}^2 \rightarrow \mathcal{L}^2$.

Lemma 1. *Suppose $A : \mathcal{H} \rightarrow \mathcal{H}$ is a compact operator. Then*

$$\|A\|_{\mathcal{L}^2, op} := \sup_{\|v\|_{\mathcal{L}^2} \leq 1, \|u\|_{\mathcal{L}^2} \leq 1} \iint A(r, s)u(r)v(s)drds \leq \mu_1 \|A\|_{\mathcal{H}, op}.$$

Proof. Let $u = \sum_{i=1}^{\infty} \alpha_i \phi_i$ and $v = \sum_{i=1}^{\infty} \beta_i \phi_i$ and that $\|u\|_{\mathcal{L}^2} \leq 1$, $\|v\|_{\mathcal{L}^2} \leq 1$. Observe that by (6),

$$\begin{aligned} \iint A(r, s)u(r)v(s)drds &= \sum_{i,j=1}^{\infty} a_{ij} \sqrt{\mu_i \mu_j} \sum_{k=1}^{\infty} \alpha_k \langle \phi_i, \phi_k \rangle_{\mathcal{L}^2} \cdot \sum_{l=1}^{\infty} \beta_l \langle \phi_j, \phi_l \rangle_{\mathcal{L}^2} \\ &= \sum_{i,j=1}^{\infty} a_{ij} \sqrt{\mu_i} \alpha_i \sqrt{\mu_j} \beta_j \\ &\leq \sup_{\sum_{i=1}^{\infty} c_i^2 \leq \mu_1, \sum_{j=1}^{\infty} d_j^2 \leq \mu_1} \sum_{i,j=1}^{\infty} a_{ij} c_i d_j \\ &\leq \mu_1 \|A\|_{\mathcal{H}, op}, \end{aligned}$$

where the last inequality follows from the definition in (7) that

$$\|A\|_{\mathcal{H}, op} = \sup_{\sum_{i=1}^{\infty} c_i^2 \leq 1, \sum_{j=1}^{\infty} d_j^2 \leq 1} \sum_{i,j=1}^{\infty} a_{ij} c_i d_j.$$

□

Remark 1. *We note that from equation (3), it holds that*

$$C_{\mathbb{K}} \geq \int \mathbb{K}(r, r)dr = \sum_{k=1}^{\infty} \mu_k \|\phi_k\|_{\mathcal{L}^2}^2 = \sum_{k=1}^{\infty} \mu_k.$$

Therefore $\mu_1 \leq C_{\mathbb{K}} = 1$. We will use these inequalities repeatedly in our analysis.

Theorem 2. *Suppose $A : \mathcal{H} \rightarrow \mathcal{H}$ is a compact operator. Then there exist two collections of sub-basis $\{\psi_k\}_{k=1}^{\infty}$ and $\{\omega_k\}_{k=1}^{\infty}$ in \mathcal{H} , such that*

$$A(r, s) = \sum_{k=1}^{\infty} a_k \psi_k(s) \omega_k(r).$$

Suppose in addition, $\text{rank}(A) \leq K$. Then

$$A(r, s) = \sum_{k=1}^K a_k \psi_k(s) \omega_k(r).$$

Proof. This is the well known spectral theory for compact operators on Hilbert space. See Chapter 5 of [Brezis \(2011\)](#) for a detailed proof. \square

Lemma 2. Let $A : \mathcal{H} \rightarrow \mathcal{H}$ be any compact linear operator. Then

$$\max \left\{ \sup_{r \in [0,1]} \|A(r, \cdot)\|_{\mathcal{H}}, \sup_{s \in [0,1]} \|A(\cdot, s)\|_{\mathcal{H}}, \sup_{r,s \in [0,1]} |A(r, s)| \right\} \leq \|A\|_{\mathcal{H},*}.$$

Proof. By Theorem 2,

$$A(r, s) = \sum_{k=1}^{\infty} a_k \psi_k(r) \omega_k(s).$$

Therefore $\|A\|_{\mathcal{H},*} = \sum_{k=1}^{\infty} |a_k|$ and that

$$\sup_{r \in [0,1]} \|A(r, \cdot)\|_{\mathcal{H}} \leq \sum_{k=1}^{\infty} \sup_{r \in [0,1]} |a_k \psi_k(r)| \|\omega_k\|_{\mathcal{H}} \leq \sum_{k=1}^{\infty} |a_k| \|\psi_k\|_{\mathcal{H}} \leq \sum_{k=1}^{\infty} |a_k| \leq \|A\|_{\mathcal{H},*},$$

where $\|\psi_k\|_{\infty} \leq \|\psi_k\|_{\mathcal{H}} \leq 1$ is used in deriving the inequality. Similar argument shows that

$$\sup_{s \in [0,1]} \|A(\cdot, s)\|_{\mathcal{H}} \leq \|A\|_{\mathcal{H},*}.$$

For the last part of the inequality, observe that for any fixed $r \in [0, 1]$,

$$A(r, s) = \langle A(r, \cdot), \mathbb{K}_s(\cdot) \rangle_{\mathcal{H}}.$$

Therefore

$$\sup_{s \in [0,1]} |A(r, s)| \leq \sup_{s \in [0,1]} |\langle A(r, \cdot), \mathbb{K}_s(\cdot) \rangle_{\mathcal{H}}| \leq \|A(r, \cdot)\|_{\mathcal{H}} \sup_{s \in [0,1]} \|\mathbb{K}_s(\cdot)\|_{\mathcal{H}} \leq \|A(r, \cdot)\|_{\mathcal{H}},$$

where $\|\mathbb{K}_s(\cdot)\|_{\mathcal{H}}^2 = \mathbb{K}(s, s) \leq 1$ is used in the last inequality. Therefore

$$\sup_{r,s \in [0,1]} |A(r, s)| \leq \sup_{r \in [0,1]} \|A(r, \cdot)\|_{\mathcal{H}} \leq \|A\|_{\mathcal{H},*}.$$

\square

B Proof of Proposition 1

Proof of Proposition 1. Proposition 1 directly follows from Lemma 4 and Lemma 5. Specifically, Lemma 4 proves the stationarity and boundedness of $\{X_t\}$ and Lemma 5 proves the restricted eigenvalue condition (11) of $\{X_t\}$. \square

We start with some general definitions and results for functional time series from Bosq (2000).

Definition 3. Let $\mathbb{B} : \mathcal{H} \rightarrow \mathcal{H}$ be any linear operator. Define

$$\|\mathbb{B}\|_{\mathcal{H} \rightarrow \mathcal{H}} := \sup_{\|f\|_{\mathcal{H}} \leq 1, \|g\|_{\mathcal{H}} \leq 1} \langle \mathbb{B}(f), g \rangle_{\mathcal{H}}.$$

\mathbb{B} is said to be bounded if $\|\mathbb{B}\|_{\mathcal{H} \rightarrow \mathcal{H}} < \infty$.

Theorem 3. Let $\{\mathbb{A}_d\}_{d=1}^D$ be a collection of bounded linear operators from $\mathcal{H} \rightarrow \mathcal{H}$. Suppose that $\{X_t\}_{t=-\infty}^{\infty}$ and that $\{\epsilon_t\}_{t=-\infty}^{\infty}$ are two collections of functions in \mathcal{H} such that $X_t = \sum_{d=1}^D \mathbb{A}_d(X_{t-d}) + \epsilon_t$. Suppose in addition that

$$\sup_{|z| \leq 1, z \in \mathbb{C}} \left\| \sum_{d=1}^D z^d \mathbb{A}_d \right\|_{\mathcal{H} \rightarrow \mathcal{H}} = \gamma < 1, \quad (28)$$

then there exists a unique collection of $\{\mathbb{B}_i\}_{i=1}^{\infty}$ being operators from $\mathcal{H} \rightarrow \mathcal{H}$ such that $X_t = \sum_{i=0}^{\infty} \mathbb{B}_i(\epsilon_{t-i})$ and that

$$\sum_{i=0}^{\infty} \|\mathbb{B}_i\|_{\mathcal{H} \rightarrow \mathcal{H}} \leq \frac{1}{1 - \gamma}.$$

Proof. The proof of the theorem follows immediately from Theorem 5.1 and Theorem 5.2 of Bosq (2000) and thus is omitted. \square

Lemma 3 is used in the proof of Lemma 4.

Lemma 3. Let $B(r, s)$ be any bivariate functions on $[0, 1] \times [0, 1]$ such that

$$B(r, s) = \sum_{i,j=1}^{\infty} b_{ij} \Phi_i(r) \Phi_j(s), \quad (29)$$

where $\{\Phi_i\}_{i=1}^{\infty}$ are the eigen-basis of \mathbb{K} as in (6). For any $f \in \mathcal{H}$, let \mathbb{B} denote the operator from $\mathcal{H} \rightarrow \mathcal{H}$ such that

$$\mathbb{B}(f)(\cdot) := \int B(\cdot, s) f(s) ds.$$

Then it holds that

$$\|\mathbb{B}\|_{\mathcal{H} \rightarrow \mathcal{H}} \leq \mu_1 \|B\|_{\mathcal{H}, op}.$$

Proof. Since $\{\Phi_i\}_{i=1}^\infty$ are orthonormal basis of \mathcal{H} , for any $f \in \mathcal{H}$ such that $\|f\|_{\mathcal{H}} = 1$, it holds that $f = \sum_{i=1}^\infty c_i \Phi_i$ with $\sum_{i=1}^\infty c_i^2 = 1$.

$$\begin{aligned}
\|\mathbb{B}\|_{\mathcal{H} \rightarrow \mathcal{H}} &= \sup_{\|f\|_{\mathcal{H}} \leq 1, \|g\|_{\mathcal{H}} \leq 1} \langle \mathbb{B}(f), g \rangle_{\mathcal{H}} \\
&= \sup_{\|f\|_{\mathcal{H}} \leq 1, \|g\|_{\mathcal{H}} \leq 1} \left\langle \int B(\cdot, s) f(s) ds, g(\cdot) \right\rangle_{\mathcal{H}} \\
&= \sup_{\|f\|_{\mathcal{H}} \leq 1, \|g\|_{\mathcal{H}} \leq 1} \sum_{i,j=1}^\infty b_{ij} \langle \Phi_i, g \rangle_{\mathcal{H}} \langle \Phi_j, f \rangle_{\mathcal{H}} \\
&= \sup_{\sum_{k=1}^\infty c_k^2 \leq 1, \sum_{l=1}^\infty d_l^2 \leq 1} \sum_{i,j=1}^\infty b_{ij} \langle \Phi_i, \sum_{l=1}^\infty d_l \Phi_l \rangle_{\mathcal{H}} \langle \Phi_j, \sum_{k=1}^\infty c_k \Phi_k \rangle_{\mathcal{H}} \\
&= \sup_{\sum_{k=1}^\infty c_k^2 \leq 1, \sum_{l=1}^\infty d_l^2 \leq 1} \sum_{i,j=1}^\infty b_{ij} d_i c_j \\
&\leq \sup_{\sum_{k=1}^\infty (c'_k)^2 \leq \mu_1^2, \sum_{l=1}^\infty d_l^2 \leq 1} \sum_{i,j=1}^\infty b_{ij} d_i c'_j.
\end{aligned}$$

Since (7) gives

$$\|B\|_{\mathcal{H}, \text{op}} = \sup_{\sum_{k=1}^\infty c_k^2 \leq 1, \sum_{l=1}^\infty d_l^2 \leq 1} \sum_{i,j=1}^\infty b_{ij} d_i c_j,$$

the desired result immediately follows. \square

Lemma 4. *Under the conditions in Proposition 1, there is a unique stationary solution $\{X_t\}_{t=-\infty}^\infty$ to (8) and*

$$\|X_t\|_{\mathcal{H}} \leq \frac{C_\epsilon}{1 - \gamma_A}.$$

Proof. For any $z \in \mathbb{C}$, let $B(r, s) := \sum_{d=1}^D z^d A_d^*(r, s)$ and let \mathbb{B} be the operator such that

$$\mathbb{B}(f)(\cdot) := \int B(\cdot, s) f(s) ds.$$

Then from Lemma 3, it holds that

$$\|\mathbb{B}\|_{\mathcal{H} \rightarrow \mathcal{H}} \leq \mu_1 \|B\|_{\mathcal{H}, \text{op}} \leq \|B\|_{\mathcal{H}, \text{op}}, \quad (30)$$

where the last inequality follows from Remark 1. Denote

$$\mathbb{A}_d(f)(\cdot) := \int A_d^*(\cdot, s) f(s) ds.$$

Then

$$\mathbb{B} = \sum_{d=1}^D z^d \mathbb{A}_d.$$

Therefore the above equality and (30) imply that

$$\left\| \sum_{d=1}^D z^d \mathbb{A}_d \right\|_{\mathcal{H} \rightarrow \mathcal{H}} \leq \left\| \sum_{d=1}^D z^d A_d^* \right\|_{\mathcal{H}, \text{op}}.$$

By assumption, $\sup_{|z| \leq 1, z \in \mathbb{C}} \left\| \sum_{d=1}^D z^d A_d^* \right\|_{\mathcal{H}, \text{op}} \leq \gamma_A < 1$. Therefore by Theorem 3, there exists a unique collection of operators $\{\mathbb{B}_i\}_{i=1}^\infty$ such that

$$X_t = \sum_{i=0}^\infty \mathbb{B}_i(\epsilon_{t-i})$$

and that

$$\sum_{i=0}^\infty \|\mathbb{B}_i\|_{\mathcal{H} \rightarrow \mathcal{H}} \leq \frac{1}{1 - \gamma_A}.$$

Therefore with probability 1,

$$\|X_t\|_{\mathcal{H}} \leq \sum_{i=0}^\infty \|B_i\|_{\mathcal{H} \rightarrow \mathcal{H}} \|\epsilon_{t-i}\|_{\mathcal{H}} \leq \frac{C_\epsilon}{1 - \gamma_A}.$$

□

The following definition is used throughout the proof in the Appendix.

Definition 4. For any bounded bivariate function $B(r, s) : [0, 1] \times [0, 1] \rightarrow \mathbb{R}$, define

$$\text{Col}(B) := \{u \in \mathcal{L}^2 : u(\cdot) = \int B(\cdot, s)w(s)ds \text{ for some } w \in \mathcal{L}^2\},$$

$$\text{Row}(B) := \{u \in \mathcal{L}^2 : u(\cdot) = \int B(s, \cdot)w(s)ds \text{ for some } w \in \mathcal{L}^2\}.$$

Lemma 5. Under the conditions in Proposition 1, it holds that

$$E \left(\int \sum_{d=1}^D v_d(s) X_{t-d}(s) ds \right)^2 \geq \frac{\kappa_\epsilon}{(1 - \gamma_A)^2} \sum_{d=1}^D \|v_d\|_{\mathcal{L}^2}^2 \text{ for all } \{v_d\}_{d=1}^D \subset \mathcal{H}.$$

Proof. Let S be a subspace of \mathcal{L}^2 such that

$$S \supset \text{span}\{\text{Col}(A_d^*) \cup \text{Row}(A_d^*)\}_{d=1}^D.$$

Observe that Theorem 2 together with $\text{rank}(A_d^*) < \infty$ directly implies that the dimensions of $\text{Col}(A_d^*)$ and $\text{Row}(A_d^*)$ are finite. Let $\{w_i\}_{i=1}^N$ be the orthonormal sub-basis in \mathcal{L}^2 of S .

Step 1. Let $\{a_d\}_{d=1}^D$ be a collection of matrices in $\mathbb{R}^{N \times N}$ such that

$$a_d(i, j) = \iint A_d^*(r, s) w_i(r) w_j(s) dr ds.$$

Since S contains $\text{Col}(A_d^*) \cup \text{Row}(A_d^*)$, it holds that

$$A_d^*(r, s) = \sum_{i,j=1}^N a_d(i, j) w_i(r) w_j(s)$$

In addition for $i = 1, \dots, N$, let

$$y_t(i) = \int X_t(s) w_i(s) ds \text{ and } \varepsilon_t(i) = \int \epsilon_t(s) w_i(s) ds.$$

Since

$$X_t(\cdot) = \sum_{d=1}^D \int A_d^*(\cdot, s) X_{t-d}(s) ds + \epsilon_t(\cdot),$$

it holds that for all $1 \leq i \leq N$,

$$\langle X_t(\cdot), w_i(\cdot) \rangle_{\mathcal{L}^2} = \left\langle \sum_{d=1}^D \int A_d^*(\cdot, s) X_{t-d}(s) ds, w_i(\cdot) \right\rangle_{\mathcal{L}^2} + \langle \epsilon_t(\cdot), w_i(\cdot) \rangle_{\mathcal{L}^2} \quad (31)$$

Therefore

$$y_t(i) = \left(\sum_{j=1}^N a_d(i, j) y_{t-d}(j) \right) + \varepsilon_t(i).$$

Then it holds that

$$y_t = \sum_{d=1}^D a_d y_{t-d} + \varepsilon_t$$

and thus $\{y_t\}_{t=1}^T$ is a VAR(D) process in \mathbb{R}^N .

Step 2. By Lemma 1,

$$\left\| \sum_{d=1}^D z^d A_d^* \right\|_{\mathcal{L}^2, \text{op}} \leq \left\| \sum_{d=1}^D z^d A_d^* \right\|_{\mathcal{H}, \text{op}}.$$

Therefore

$$\sup_{|z| \leq 1} \left\| \sum_{d=1}^D z^d A_d^* \right\|_{\mathcal{L}^2, \text{op}} \leq \sup_{|z| \leq 1} \left\| \sum_{d=1}^D z^d A_d^* \right\|_{\mathcal{H}, \text{op}} \leq \gamma_A.$$

Let $\alpha \in \mathbb{R}^N$ be such that $\|\alpha\|_2 = 1$. Denote $\alpha = [\alpha_1, \dots, \alpha_N]$ and suppose that $u = \sum_{i=1}^N \alpha_i w_i$, where $\{w_i\}_{i=1}^N$ is sub-basis in \mathcal{L}^2 of S . So $\|u\|_{\mathcal{L}^2} = 1$. Then by the definition of $\{w_i\}_{i=1}^N$, it holds that

$$\left\| \left(\sum_{d=1}^D z^d a_d \right) \alpha \right\|_2^2 = \left\| \left(\sum_{d=1}^D z^d A_d^* \right) u \right\|_{\mathcal{L}^2}^2 \leq \left\| \sum_{d=1}^D z^d A_d^* \right\|_{\mathcal{L}^2, \text{op}}^2 \|u\|_{\mathcal{L}^2}^2 = \left\| \sum_{d=1}^D z^d A_d^* \right\|_{\mathcal{L}^2, \text{op}}^2.$$

The above display implies that

$$\left\| \sum_{d=1}^D z^d a_d \right\|_{\text{op}} \leq \left\| \sum_{d=1}^D z^d A_d^* \right\|_{\mathcal{L}^2, \text{op}}$$

and so

$$\sup_{|z| \leq 1} \left\| \sum_{d=1}^D z^d a_d \right\|_{\text{op}} < \gamma_A < 1. \quad (32)$$

Step 3. By Lemma 6, it holds that for any $\{\beta_d\}_{d=1}^D \subset \mathbb{R}^N$,

$$E \left(\sum_{d=1}^D y_{t-d}^\top \beta_d \right)^2 \geq \frac{\kappa_\varepsilon}{(1-\gamma)^2} \sum_{d=1}^D \|\beta_d\|_2^2 \quad (33)$$

where

$$\gamma := \sup_{|z| \leq 1} \left\| \sum_{d=1}^D z^d a_d \right\|_{\text{op}} \quad \text{and} \quad \kappa_\varepsilon := \inf_{\beta \in \mathbb{R}^N, \|\beta\|_2=1} E(\varepsilon_t^\top \beta)^2.$$

Then (33) implies that for any $\{u_d\}_{d=1}^D \subset S$,

$$E \left(\int \sum_{d=1}^D u_d(s) X_{t-d}(s) ds \right)^2 \geq \frac{\kappa_\varepsilon}{(1-\gamma)^2} \sum_{d=1}^D \|u_d\|_{\mathcal{L}^2}^2. \quad (34)$$

Note that

$$\kappa_\varepsilon \geq \inf_{v \in \mathcal{L}^2, \|v\|_{\mathcal{L}^2}=1} E(\langle \varepsilon_t, v \rangle_{\mathcal{L}^2})^2 \geq \kappa_\varepsilon$$

and that (32) gives that $\gamma \leq \gamma_A$. So

$$E \left(\int \sum_{d=1}^D u_d(s) X_{t-d}(s) ds \right)^2 \geq \frac{\kappa_\epsilon}{(1 - \gamma_A)^2} \sum_{d=1}^D \|u_d\|_{\mathcal{L}^2}^2. \quad (35)$$

Step 4. Let

$$S = \text{span}\{\text{Col}(A_d^*) \cup \text{Row}(A_d^*)\}_{d=1}^D \cup \{v_d\}_{d=1}^D.$$

Then the desired results follows immediate from (34). \square

Lemma 6. *Let $\{y_t\}_{t=-\infty}^\infty \subset \mathbb{R}^N$ be a VAR(D) process such that*

$$y_t = \sum_{d=1}^D a_d y_{t-d} + \varepsilon_t$$

where $\{a_d\}_{d=1}^D \subset \mathbb{R}^{N \times N}$ and $\{\varepsilon_t\}_{t=-\infty}^\infty$ are i.i.d. sub-Gaussian random variables. Suppose in addition that there exist two constants $0 < \gamma < 1$ and $\kappa_\varepsilon > 0$ where

$$\gamma := \sup_{|z| \leq 1} \left\| \sum_{d=1}^D z^d a_d \right\|_{op} < 1 \quad \text{and} \quad \kappa_\varepsilon := \inf_{\beta \in \mathbb{R}^N, \|\beta\|_2=1} E(\varepsilon_t^\top \beta)^2.$$

Then $\{y_t\}_{t=-\infty}^\infty$ is stationary and invertible and it holds that for any $\{\beta_d\}_{d=1}^D \subset \mathbb{R}^N$

$$E \left(\sum_{d=1}^D y_{t-d}^\top \beta_d \right)^2 \geq \frac{\kappa_\varepsilon}{(1 - \gamma)^2} \sum_{d=1}^D \|\beta_d\|_2^2. \quad (36)$$

Proof. Let $\{Y_t\}_{t=-\infty}^\infty \subset \mathbb{R}^{ND}$ be defined as

$$Y_t = [y_t^\top, y_{t-1}^\top, \dots, y_{t-D+1}^\top]^\top.$$

Consider

$$B = \begin{bmatrix} a_1 & a_2 & \dots & a_{D-1} & a_D \\ I_N & 0 & \dots & 0 & 0 \\ 0 & I_N & \dots & 0 & 0 \\ \vdots & \vdots & \ddots & \vdots & \vdots \\ 0 & 0 & \dots & I_N & 0 \end{bmatrix} \in \mathbb{R}^{ND \times ND}. \quad (37)$$

It is well known (see for example [Basu and Michailidis \(2015\)](#) and reference therein) that under the conditions on γ and κ_ε , $\{Y_t\}_{t=-\infty}^\infty$ is a stationary and invertible VAR(1) process

such that for any $w \in \mathbb{R}^{ND}$, it holds that

$$E(Y_t^\top w) \geq \frac{\kappa_\varepsilon}{(1-\gamma)^2} \|w\|_2^2.$$

This directly implies the desired result in (36). □

C Results Related to Sobolev Spaces

C.1 Bounds for γ_n

Let $\{s_i\}_{i=1}^n$ be a collection of uniform random variables sampled from $[0, 1]$ and $\{\sigma_i\}_{i=1}^n$ is a collection of Rademacher random variables. The following theorem is Theorem 2.1 in [Bartlett et al. \(2005\)](#), which is used for bounding γ_n .

Theorem 4. *Suppose \mathcal{F} is a class of function that map $[0, 1]$ into $[-b, b]$. Then for any $\delta > 0$, it holds that with probability $1 - \exp(-c_{\mathcal{R}}\delta)$,*

$$\sup_{f \in \mathcal{F}_\alpha} \left(\int f(s) ds - \frac{1}{n} \sum_{i=1}^n f(s_i) \right) \leq C_{\mathcal{R}} \left(E(\mathcal{R}_n \mathcal{F}_\alpha) + \alpha \sqrt{\frac{\delta}{n}} + b \frac{\delta}{n} \right)$$

where $c_{\mathcal{R}}, C_{\mathcal{R}}$ are absolute constants, $\mathcal{F}_\alpha = \{f \in \mathcal{F} : \|f\|_{\mathcal{L}^2} \leq \alpha\}$, and

$$\mathcal{R}_n \mathcal{F}_\alpha := \sup_{f \in \mathcal{F}_\alpha} \mathcal{R}_n f \quad \text{and} \quad \mathcal{R}_n f = \frac{1}{n} \sum_{i=1}^n \sigma_i f(s_i).$$

To use Theorem 4 for bounding γ_n , we define

$$\zeta_n := \inf \left\{ \zeta \geq \sqrt{\frac{\log(n)}{n}} : E \sup_{\|f\|_{\mathcal{H}} \leq b, \|f\|_{\mathcal{L}^2} \leq \delta} \mathcal{R}_n f \leq \zeta \delta + b \zeta^2 \text{ for all } \delta \in (0, 1] \right\}.$$

Lemma 7 provides the probability bound for γ'_n using ζ_n .

Lemma 7. *Suppose b is any bounded constant. Then it holds that*

$$P \left(\left| \int f(s) ds - \frac{1}{n} \sum_{i=1}^n f(s_i) \right| \leq C_\zeta (\zeta_n \|f\|_{\mathcal{L}^2} + (b+1)\zeta_n^2) \text{ for all } f \text{ such that } \|f\|_{\mathcal{H}} \leq b \right) \geq 1 - 1/n^4.$$

Proof. It suffices to show that

$$P \left(\left| \int f(s) ds - \frac{1}{n} \sum_{i=1}^n f(s_i) \right| \leq C_\zeta (\zeta_n \|f\|_{\mathcal{L}^2} + (b+1)\zeta_n^2) \text{ for all } f \text{ that } \|f\|_{\mathcal{H}} \leq b, \|f\|_{\mathcal{L}^2} \leq 1 \right) \geq 1 - 1/n^4.$$

Let $\delta = C_\delta \log(n)$ such that $\exp(-c_{\mathcal{R}}\delta) \leq n^{-5}$, where $c_{\mathcal{R}}$ is defined as in Theorem 4. Let $J \in \mathbb{Z}^+$ be such that

$$2^{-J} \leq \zeta_n \leq 2^{-J+1}.$$

So $J \leq \log(n)$. For any $1 \leq j \leq J$, it holds that with probability at least $1 - \exp(-c_{\mathcal{R}}\delta) \geq 1 - n^{-5}$, for all f such that $\|f\|_{\mathcal{H}} \leq b$, $2^{-j} \leq \|f\|_{\mathcal{L}^2} \leq 2^{-j+1}$

$$\begin{aligned} \left| \int f(s)ds - \frac{1}{n} \sum_{i=1}^n f(s_i) \right| &\leq C_{\mathcal{R}} \left(E \sup_{\|f\|_{\mathcal{H}} \leq b, \|f\|_{\mathcal{L}^2} \leq 2^{-j+1}} \mathcal{R}_n f + 2^{-j+1} \sqrt{\frac{\delta}{n}} + b \frac{\delta}{n} \right) \\ &\leq C_{\mathcal{R}} \left(\zeta_n 2^{-j+1} + b \zeta_n^2 + 2^{-j+1} \sqrt{\frac{\delta}{n}} + b \frac{\delta}{n} \right) \\ &\leq C_{\mathcal{R}} (2\zeta_n \|f\|_{\mathcal{L}^2} + b \zeta_n^2 + 2C_\delta \zeta_n \|f\|_{\mathcal{L}^2} + b C_\delta^2 \zeta_n^2), \end{aligned}$$

where the first inequality follows from Theorem 4, the second inequality follows from definition of ζ_n and the last inequality follows from $\|f\|_{\mathcal{L}^2} \geq 2^{-j}$ and the fact that $C_\delta^2 \zeta_n^2 \geq \delta/n$. Therefore with probability at least $1 - Jn^{-5} \geq 1 - \log(n)n^{-5}$

$$\sup_{f \in \mathcal{H}, \|f\|_{\mathcal{H}} \leq b, \|f\|_{\mathcal{L}^2} \geq 2^{-J}} \left| \int f(s)ds - \frac{1}{n} \sum_{i=1}^n f(s_i) \right| \leq C'_1 (\zeta_n \|f\|_{\mathcal{L}^2} + b \zeta_n^2).$$

In addition, by Theorem 4 with probability at least $1 - n^{-5}$,

$$\sup_{f \in \mathcal{H}, \|f\|_{\mathcal{H}} \leq b, \|f\|_{\mathcal{L}^2} \leq 2^{-J}} \left| \int f(s)ds - \frac{1}{n} \sum_{i=1}^n f(s_i) \right| \leq C_{\mathcal{R}} (\zeta_n 2^{-J} + b \zeta_n^2) \leq C_{\mathcal{R}}(1+b)\zeta_n^2,$$

where the last inequality follows from the choice that $2^{-J} \leq \zeta_n$. Therefore it suffices to choose

$$C_\zeta = \max\{4C_{\mathcal{R}}(1+C_\delta), 4C_{\mathcal{R}}C_\delta^2\}.$$

□

Lemma 8 provides the probability bound for γ_n'' using ζ_n .

Lemma 8. *Suppose b is any bounded constant. Then it holds that*

$$\begin{aligned} P(\|f\|_{\mathcal{L}^2}^2 \leq 2\|f\|_n^2 + C'_\zeta b^2 \zeta_n^2 \text{ for all } f \text{ such that } \|f\|_{\mathcal{H}} \leq b) &\geq 1 - 1/n^4; \\ P(\|f\|_n^2 \leq 2\|f\|_{\mathcal{L}^2}^2 + C'_\zeta b^2 \zeta_n^2 \text{ for all } f \text{ such that } \|f\|_{\mathcal{H}} \leq b) &\geq 1 - 1/n^4, \end{aligned}$$

where $\|f\|_n^2 = \frac{1}{n} \sum_{i=1}^n f^2(s_i)$

Proof. Step 1. It suffices to show that

$$P(\|f\|_{\mathcal{L}^2}^2 \leq 2\|f\|_n^2 + C'_\zeta b^2 \zeta_n^2 \text{ for all } f \text{ such that } \|f\|_{\mathcal{H}} \leq b, \|f\|_{\mathcal{L}^2} \leq 1).$$

This is because for any $g \in \mathcal{H}$ such that $\|g\|_{\mathcal{L}^2} > 1$ and that $\|g\|_{\mathcal{H}} \leq b$, one can apply the above probability bounds to the function $h := \frac{g}{\|g\|_{\mathcal{L}^2}}$ and observe that $\|h\|_{\mathcal{L}^2} \leq 1$, $\|h\|_{\mathcal{H}} \leq \frac{b}{\|g\|_{\mathcal{L}^2}}$.

Step 2. Observe that the function $\phi(x) = x^2/b$ is a contraction on the interval $[-b, b]$. Therefore

$$E(\mathcal{R}_n(\phi \circ \mathcal{F})) \leq E(\mathcal{R}_n \mathcal{F}).$$

The same calculations in the proof of Lemma 7 shows that

$$P\left(\left|\int f^2(s)ds - \frac{1}{n} \sum_{i=1}^n f^2(s_i)\right| \leq C(b\zeta_n \|f\|_{\mathcal{L}^2} + b^2 \zeta_n^2) \text{ for all } f \text{ that } \|f\|_{\mathcal{L}^2} \leq 1, \|f\|_{\mathcal{H}} \leq b\right) \geq 1 - 1/n^4,$$

where C only depends on $C_{\mathcal{R}}$ and $c_{\mathcal{R}}$. Since

$$b\zeta_n \|f\|_{\mathcal{L}^2} + b^2 \zeta_n^2 \leq \frac{1}{2} \|f\|_{\mathcal{L}^2}^2 + 3b^2 \zeta_n^2,$$

The desired result follows immediately. \square

Based on Lemma 7 and Lemma 8, we provide a probability bound for γ_n in Corollary 2.

Corollary 2. Suppose that $\mathcal{H} = W^{\alpha,2}$ and that $\{s_i\}_{i=1}^n$ is a collection of uniform random variables sampled from $[0, 1]$. Let γ'_n and γ''_n be defined as in (16) and (17) respectively. Then with probability at least $1 - 1/n^4$, it holds that

$$\max\{\gamma'_n, \gamma''_n\} \leq C_{\alpha} n^{-\alpha/(2\alpha+1)},$$

where C_{α} is some constant independent of n .

Proof. Suppose $\mathcal{H} = W^{\alpha,2}$. Then from Mendelson (2002), it holds that $\zeta_n \leq C_{\alpha} n^{-\alpha/(2\alpha+1)}$. The desired results follow directly from Lemma 7 and Lemma 8. \square

C.2 Bounds for δ_n

Lemma 9 and Lemma 10 are used for proving Lemma 11, which provides the probability bound for δ'_T .

Lemma 9. Suppose $\mathcal{H} = W^{\alpha,2}$ and $0 < \beta \leq 1$ is any constant. Under the conditions in Proposition 1, it holds that

$$P\left(\left|\frac{1}{T} \sum_{t=1}^T \left(\sum_{d=1}^D \int v_d(r) X_{t-d}(r) dr\right)^2 - E\left(\sum_{d=1}^D \int v_d(r) X_{t-d}(r) dr\right)^2\right| \leq C_w \beta T^{\frac{-\alpha}{2\alpha+1}}\right. \\ \left. \text{for all } \sup_{1 \leq d \leq D} \|v_d\|_{\mathcal{H}} \leq 1 \text{ such that } \sum_{d=1}^D \|v_d\|_{\mathcal{L}^2}^2 \leq \beta^2\right) \geq 1 - 2T \exp\left(-c_w T^{\frac{1}{2\alpha+1}}\right),$$

where c_w and C_w are two absolute constants independent of T .

Proof. Let S be a subspace of \mathcal{L}^2 such that

$$S \supset \text{span}\{\text{Col}(A_d^*) \cup \text{Row}(A_d^*)\}_{d=1}^D$$

and let $\{w_i\}_{i=1}^N$ be the orthonormal sub-basis in \mathcal{L}^2 of S .

Step 1. Let $\{a_d\}_{d=1}^D \subset \mathbb{R}^{N \times N}$, $\{y_t\} \subset \mathbb{R}^N$ and $\{\varepsilon_t\} \subset \mathbb{R}^N$ be defined as in Lemma 5. Then it holds that

$$y_t = \sum_{d=1}^D a_d y_{t-d} + \varepsilon_t$$

and thus $\{y_t\}_{t=1}^T$ is a VAR(D) process in \mathbb{R}^N . Observe that (32) implies that

$$\det \left(I_N - \sum_{d=1}^D z^d a_d \right) \neq 0$$

for all $z \in \mathbb{C}$ such that $|z| \leq 1$. Thus from **Step I** of the proof of Proposition 8 in Wong et al. (2017), it holds that for any fixed $\{w_d\}_{d=1}^D \subset \mathbb{R}^N$,

$$P \left(\left| \frac{1}{T} \sum_{t=1}^T \left(\sum_{d=1}^D y_{t-d}^\top w_d \right)^2 - E \left(\sum_{d=1}^D y_{t-d}^\top w_d \right)^2 \right| \geq \eta \sum_{d=1}^D \|w_d\|_2^2 \right) \leq 2T \exp(-c_\varepsilon T \eta^2), \quad (38)$$

where c_ε depends on C_ε and γ_A only.

Step 2. Let $\{v_d\}_{d=1}^D \subset \mathcal{H}$ be any deterministic functions such that $\sup_{1 \leq d \leq D} \|v_d\|_{\mathcal{H}} \leq 1$. Suppose $S \supset \text{span}\{\text{Col}(A_d^*) \cup \text{Row}(A_d^*)\}_{d=1}^D \cup \{v_d\}_{d=1}^D$. Then (38) implies that if $\sum_{d=1}^D \|v_d\|_{\mathcal{L}^2}^2 \leq \beta^2$

$$\begin{aligned} & P \left(\left| \frac{1}{T} \sum_{t=1}^T \left(\sum_{d=1}^D \int v_d(r) X_{t-d}(r) dr \right)^2 - E \left(\sum_{d=1}^D \int v_d(r) X_{t-d}(r) dr \right)^2 \right| \geq \gamma \beta^2 \right) \\ & \leq 2T \exp(-c_\varepsilon T \gamma^2) \end{aligned}$$

Step 3. Let $\{u_j\}_{j=1}^{\mathcal{N}}$ be chosen as in Lemma 10 with $\mathcal{N} \leq \exp\left(\frac{C_{\mathcal{N}}}{\delta^{\frac{1}{\alpha}}}\right)$. Observe that

$$\begin{aligned}
& P \left(\sup_{\{w_d\}_{d=1}^D \subset \{u_j\}_{j=1}^{\mathcal{N}}} \left| \frac{1}{T} \sum_{t=1}^T \left(\sum_{d=1}^D \int w_d(r) X_{t-d}(r) dr \right)^2 - E \left(\sum_{d=1}^D \int w_d(r) X_{t-d}(r) dr \right)^2 \right| \geq 4\gamma D\beta^2 \right) \\
& \leq \mathcal{N}^D \sup_{\{w_d\}_{d=1}^D \subset \{u_j\}_{j=1}^{\mathcal{N}}} P \left(\left| \frac{1}{T} \sum_{t=1}^T \left(\sum_{d=1}^D \int w_d(r) X_{t-d}(r) dr \right)^2 - E \left(\sum_{d=1}^D \int w_d(r) X_{t-d}(r) dr \right)^2 \right| \geq 4\gamma D\beta^2 \right) \\
& \leq 2T \exp \left(\frac{C_{\mathcal{N}} D}{\delta^{\frac{1}{\alpha}}} - c_{\varepsilon} T \gamma^2 \right),
\end{aligned}$$

where the last inequality follows because $\sum_{d=1}^D \|w_d\|_{\mathcal{L}^2}^2 \leq 4D\beta^2$ and **Step 2**. For any fixed $\{v_d\}_{d=1}^D$ such that $\sup_{1 \leq d \leq D} \|v_d\|_{\mathcal{H}} \leq 1$ and $\sum_{d=1}^D \|v_d\|_{\mathcal{L}^2}^2 \leq \beta^2$, by the choice of $\{u_j\}_{j=1}^{\mathcal{N}}$, one can assume without loss of generality that for any $1 \leq d \leq D$,

$$\|v_d - u_d\|_{\mathcal{L}^2} \leq \delta \wedge \beta.$$

Therefore

$$\begin{aligned}
& \left| E \left(\sum_{d=1}^D \int u_d(r) X_{t-d}(r) dr \right)^2 - E \left(\sum_{d=1}^D \int v_d(r) X_{t-d}(r) dr \right)^2 \right| \\
& \leq \sum_{1 \leq d, e \leq D} \left| \iint (v_d(r) - u_d(r)) E(X_{t-d}(r) X_{t-e}(s)) v_e(s) dr ds \right| \\
& + \sum_{1 \leq d, e \leq D} \left| \iint u_d(r) E(X_{t-d}(r) X_{t-e}(s)) (v_e(s) - u_e(s)) dr ds \right| \\
& \leq \sum_{1 \leq d, e \leq D} \|v_d - u_d\|_{\mathcal{L}^2} E(\|X_{t-d}\|_{\infty} \|X_{t-e}\|_{\infty}) \|v_e\|_{\mathcal{L}^2} \\
& + \sum_{1 \leq d, e \leq D} \|u_d\|_{\mathcal{L}^2} E(\|X_{t-d}\|_{\infty} \|X_{t-e}\|_{\infty}) \|v_e - u_e\|_{\mathcal{L}^2} \\
& \leq 2C_X^2 D^2 (\delta \wedge \beta) \beta \leq 2C_X^2 D^2 \delta \beta.
\end{aligned}$$

Similarly,

$$\left| \frac{1}{T} \sum_{t=1}^T \left(\sum_{d=1}^D \int v_d(r) X_{t-d}(r) dr \right)^2 - \frac{1}{T} \sum_{t=1}^T \left(\sum_{d=1}^D \int w_d(r) X_{t-d}(r) dr \right)^2 \right| \leq 2C_X^2 D^2 \delta \beta.$$

So by standard covering argument

$$P\left(\left|\frac{1}{T}\sum_{t=1}^T\left(\sum_{d=1}^D\int v_d(r)X_{t-d}(r)dr\right)^2 - E\left(\sum_{d=1}^D\int v_d(r)X_{t-d}(r)dr\right)^2\right|\geq 4\gamma D\beta^2 + 4C_X^2 D^2\delta\beta\right. \\ \left.\text{for all } \sup_{1\leq d\leq D}\|v_d\|_{\mathcal{H}}\leq 1 \text{ such that } \sum_{d=1}^D\|v_d\|_{\mathcal{L}^2}^2\leq\beta^2\right)\leq 2T\exp\left(-c_{\varepsilon}\gamma^2T + \frac{C_{\mathcal{N}}D}{\delta^{\frac{1}{\alpha}}}\right).$$

The desired result follows by picking

$$\gamma = \delta = CT^{\frac{-\alpha}{2\alpha+1}}$$

for sufficiently large C depending on D, C_X, c_{ε} and $C_{\mathcal{N}}$. \square

Lemma 10. *For any fixed $\beta > 0$ and $\delta > 0$, there exists a collection of functions $\{u_j\}_{j=1}^{\mathcal{N}} \subset B_{W^{\alpha,2}}(0,1) \cap B_{\mathcal{L}^2}(0,2\beta)$ with $\mathcal{N} \leq \exp\left(\frac{C_{\mathcal{N}}}{\delta^{\frac{1}{\alpha}}}\right)$ such that for any $v \in B_{W^{\alpha,2}}(0,1) \cap B_{\mathcal{L}^2}(0,\beta)$, it holds that*

$$\min_{1\leq j\leq \mathcal{N}}\|v - u_j\|_{\mathcal{L}^2} \leq \delta \wedge \beta.$$

Proof. Let $\{u_j\}_{j=1}^{\mathcal{N}} \subset B_{W^{\alpha,2}}(0,1)$ be a \mathcal{L}^2 cover of $B_{W^{\alpha,2}}(0,1)$. This means that for any $v \in B_{W^{\alpha,2}}(0,1)$, it holds that

$$\min_{1\leq j\leq \mathcal{N}}\|v - u_j\|_{\mathcal{L}^2} \leq \delta$$

Then by the classical result (see, e.g., [Nickl and Pötscher \(2007\)](#) and reference therein), there exists a constant $C_{\mathcal{N}}$ independent of δ such that $\{u_j\}_{j=1}^{\mathcal{N}}$ can be picked so that $\mathcal{N} \leq \exp\left(\frac{C_{\mathcal{N}}}{\delta^{\frac{1}{\alpha}}}\right)$. Without loss of generality assume that $0 \in \{u_j\}_{j=1}^{\mathcal{N}}$.

Case 1. Suppose $\delta < \beta$. Then any u_j with $\|v - u_j\|_{\mathcal{L}^2} \leq \delta$ must satisfy $\|u_j\|_{\mathcal{L}^2} \leq 2\beta$. So it suffices to take the covering set to be $\{u_j\}_{j=1}^{\mathcal{N}} \cap B_{\mathcal{L}^2}(0,2\beta)$.

Case 2. Suppose $\delta \geq \beta$. Since $0 \in \{u_j\}_{j=1}^{\mathcal{N}}$,

$$\min_{1\leq j\leq \mathcal{N}}\|v - u_j\|_{\mathcal{L}^2} \leq \|v - 0\|_{\mathcal{L}^2} \leq \beta.$$

\square

Lemma 11 provides the probability bound for δ'_T . Note that the definition of δ'_T in (19) does not have the additional condition $\sum_{d=1}^D\|v_d\|_{\mathcal{L}^2}^2 \leq 1$ which used in Lemma 11. However, since $\|v_d\|_{\mathcal{H}} \leq 1$ implies that $\|v_d\|_{\mathcal{L}^2} \leq 1$. Therefore $\sup_{1\leq d\leq D}\|v_d\|_{\mathcal{H}} \leq 1$ implies that $\sum_{d=1}^D\|v_d\|_{\mathcal{L}^2}^2 \leq D$. This inequality together with a simple rescaling argument (such as that

in the proof of Lemma 8) can straightforwardly show that Lemma 11 implies that

$$P\left(\left|\frac{1}{T}\sum_{t=1}^T\left(\sum_{d=1}^D\int v_d(r)X_{t-d}(r)dr\right)^2 - E\left(\sum_{d=1}^D\int v_d(r)X_{t-d}(r)dr\right)^2\right| \leq C'_w\sqrt{DT}^{\frac{-\alpha}{2\alpha+1}}\sqrt{\sum_{d=1}^D\|v_d\|_{\mathcal{L}^2}^2}\right. \\ \left.\text{for all } \{v_d\}_{d=1}^D \text{ such that } \sup_{1\leq d\leq D}\|v_d\|_{\mathcal{H}}\leq 1\right) \geq 1 - 2T^2\exp\left(-c'_wT^{\frac{1}{2\alpha+1}}\right).$$

Lemma 11. Suppose $\mathcal{H} = W^{\alpha,2}$. Under the conditions in Proposition 1, it holds that

$$P\left(\left|\frac{1}{T}\sum_{t=1}^T\left(\sum_{d=1}^D\int v_d(r)X_{t-d}(r)dr\right)^2 - E\left(\sum_{d=1}^D\int v_d(r)X_{t-d}(r)dr\right)^2\right| \leq C'_wT^{\frac{-\alpha}{2\alpha+1}}\sqrt{\sum_{d=1}^D\|v_d\|_{\mathcal{L}^2}^2}\right. \\ \left.\text{for all } \{v_d\}_{d=1}^D \text{ such that } \sup_{1\leq d\leq D}\|v_d\|_{\mathcal{H}}\leq 1 \text{ and that } \sum_{d=1}^D\|v_d\|_{\mathcal{L}^2}^2\leq 1\right) \geq 1 - 2T^2\exp\left(-c'_wT^{\frac{1}{2\alpha+1}}\right).$$

Proof. Let $J \in \mathbb{Z}^+$ be such that $2^{-J} \leq T^{\frac{-2\alpha}{2\alpha+1}} \leq 2^{-J+1}$. So $J \leq \log(T)$. For any $1 \leq j \leq J$, it holds that with probability at least $1 - 2T\exp\left(-c_wT^{\frac{1}{2\alpha+1}}\right)$, for all $\{v_d\}_{d=1}^D$ such that $\sup_{1\leq d\leq D}\|v_d\|_{\mathcal{H}}\leq 1$ and $2^{-j} \leq \sum_{d=1}^D\|v_d\|_{\mathcal{L}^2}^2 \leq 2^{-j+1}$,

$$\left|\frac{1}{T}\sum_{t=1}^T\left(\sum_{d=1}^D\int v_d(r)X_{t-d}(r)dr\right)^2 - E\left(\sum_{d=1}^D\int v_d(r)X_{t-d}(r)dr\right)^2\right| \\ \leq C_wT^{\frac{-\alpha}{2\alpha+1}}\sqrt{2^{-j+1}} \leq C_wT^{\frac{-\alpha}{2\alpha+1}}\sqrt{2\sum_{d=1}^D\|v_d\|_{\mathcal{L}^2}^2}$$

where the first inequality follows from Lemma 9. So by union bound, with probability at least $1 - 2JT\exp(-c_wT^{\frac{1}{2\alpha+1}})$, for all $\sum_{d=1}^D\|v_d\|_{\mathcal{L}^2}^2 \geq 2^{-J}$,

$$\left|\frac{1}{T}\sum_{t=1}^T\left(\sum_{d=1}^D\int v_d(r)X_{t-d}(r)dr\right)^2 - E\left(\sum_{d=1}^D\int v_d(r)X_{t-d}(r)dr\right)^2\right| \leq \sqrt{2}C_wT^{\frac{-\alpha}{2\alpha+1}}\sqrt{\sum_{d=1}^D\|v_d\|_{\mathcal{L}^2}^2}. \quad (39)$$

In addition, observe that if $\sum_{d=1}^D \|v_d\|_{\mathcal{L}^2}^2 \leq 2^{-J} \leq T^{\frac{-2\alpha}{2\alpha+1}}$,

$$\begin{aligned}
\frac{1}{T} \sum_{t=1}^T \left(\sum_{d=1}^D \int v_d(r) X_{t-d}(r) dr \right)^2 &= \frac{1}{T} \sum_{t=1}^T \sum_{d,e=1}^D \int v_d(r) X_{t-d}(r) dr \int v_e(r) X_{t-e}(r) dr \\
&\leq \frac{1}{T} \sum_{t=1}^T \sum_{d,e=1}^D \|v_d\|_{\mathcal{L}^2} \|v_e\|_{\mathcal{L}^2} C_X^2 \\
&= C_X^2 \left(\sum_{d=1}^D \|v_d\|_{\mathcal{L}^2} \right)^2 \\
&\leq D C_X^2 \sum_{d=1}^D \|v_d\|_{\mathcal{L}^2}^2 \\
&\leq D C_X^2 T^{\frac{-\alpha}{2\alpha+1}} \sqrt{\sum_{d=1}^D \|v_d\|_{\mathcal{L}^2}^2}.
\end{aligned}$$

Similarly, if $\sum_{d=1}^D \|v_d\|_{\mathcal{L}^2}^2 \leq 2^{-J} \leq T^{\frac{-2\alpha}{2\alpha+1}}$,

$$\left| E \left(\sum_{d=1}^D \int v_d(r) X_{t-d}(r) dr \right) \right|^2 \leq D C_X^2 T^{\frac{-\alpha}{2\alpha+1}} \sqrt{\sum_{d=1}^D \|v_d\|_{\mathcal{L}^2}^2}.$$

Therefore if $\sum_{d=1}^D \|v_d\|_{\mathcal{L}^2}^2 \leq 2^{-J} \leq T^{\frac{-2\alpha}{2\alpha+1}}$,

$$\left| \frac{1}{T} \sum_{t=1}^T \left(\sum_{d=1}^D \int v_d(r) X_{t-d}(r) dr \right)^2 - E \left(\sum_{d=1}^D \int v_d(r) X_{t-d}(r) dr \right)^2 \right| \leq 2 D C_X^2 T^{\frac{-\alpha}{2\alpha+1}} \sqrt{\sum_{d=1}^D \|v_d\|_{\mathcal{L}^2}^2}. \quad (40)$$

The desired result follows from (39) and (40). \square

Lemma 12 provides the probability bound for δ_T'' .

Lemma 12. Suppose $\mathcal{H} = W^{\alpha,2}$ and Assumption 3 holds. Let $\{s_i\}_{i=1}^n$ being a collection of uniform random variables sampled from $[0, 1]$ independent of $\{\epsilon_t\}_{t=1}^T$. Under the conditions in Proposition 1, it holds that

$$P \left(\sup_{1 \leq d \leq D, r \in [0,1], s \in [0,1]} \left| \frac{1}{T} \sum_{t=1}^T X_{t-d}(r) \epsilon_t(s) \right| \geq 3 C_X C_\epsilon \sqrt{\frac{\log(T)}{T}} \right) \leq 1/T^3.$$

Proof. Step 1. Let $r, s \in [0, 1]$ be given. Let $y_\tau = \sum_{t=1}^\tau X_{t-d}(r)\epsilon_t(s)$. One has

$$|y_\tau - y_{\tau-1}| \leq |X_{\tau-d}(r)\epsilon_\tau(s)| \leq C_X C_\epsilon.$$

Let \mathcal{F}_τ be the sigma algebra generated by $\{\epsilon_t\}_{t=1}^\tau$. Then

$$E(y_{\tau+1}|\mathcal{F}_\tau) = y_\tau.$$

Therefore, by Azuma Hoeffding inequality, it holds that

$$P\left(\left|\frac{1}{T}\sum_{t=1}^T X_{t-d}(r)\epsilon_t(s)\right| \geq \delta\right) \leq 2\exp\left(-\frac{T^2\delta^2}{2C_X^2 C_\epsilon^2}\right). \quad (41)$$

Step 2. Let $\mathcal{G} := \{r_m\}_{m=1}^M$ be a equally spaced grid on $[0, 1]$. Observe that for any $s \in [0, 1]$, there exist m such that $|r_m - s| \leq 1/M$. Therefore for any $f \in W^{\alpha,2}$ with $\alpha \geq 1$,

$$|f(r_m) - f(s)| \leq \|f'\|_{\mathcal{L}^2}|r_m - s| \leq \|f\|_{\mathcal{H}}|r_m - s| \leq \|f\|_{\mathcal{H}}/M.$$

Therefore given any $r, s \in [0, 1]$, there exists $r_m, r_{m'}$ such that

$$|X_{t-d}(r) - X_{t-d}(r_m)| \leq C_X/M \text{ and } |\epsilon_t(s) - \epsilon_t(r_{m'})| \leq C_\epsilon/M$$

and therefore it holds that

$$\begin{aligned} & |X_{t-d}(r)\epsilon_t(s) - X_{t-d}(r_m)\epsilon_t(r_{m'})| \\ & \leq |X_{t-d}(r)\epsilon_t(s) - X_{t-d}(r_m)\epsilon_t(s)| + |X_{t-d}(r_m)\epsilon_t(s) - X_{t-d}(r_m)\epsilon_t(r_{m'})| \\ & \leq \|X_{t-d}\|_\infty C_\epsilon/M + \|\epsilon_t\|_\infty C_X/M \\ & \leq 2C_X C_\epsilon/M. \end{aligned} \quad (42)$$

So

$$\begin{aligned} & P\left(\sup_{r,s \in [0,1]} \left|\frac{1}{T}\sum_{t=1}^T X_{t-d}(r)\epsilon_t(s)\right| \geq \delta + 2C_X C_\epsilon/M\right) \\ & \leq P\left(\sup_{r_m, r_{m'} \in \mathcal{G}} \left|\frac{1}{T}\sum_{t=1}^T X_{t-d}(r_m)\epsilon_t(r_{m'})\right| \geq \delta\right) \\ & \leq M^2 2\exp\left(-\frac{T^2\delta^2}{2C_X^2 C_\epsilon^2}\right). \end{aligned}$$

where the first inequality follows from (42) and the second inequality follows from (41) and

union bound. So by union bound again,

$$P \left(\sup_{1 \leq d \leq D, r \in [0,1], s \in [0,1]} \left| \frac{1}{T} \sum_{t=1}^T X_{t-d}(r) \epsilon_t(s) \right| \geq \delta + 2C_X C_\epsilon / M \right) \leq DM^2 2 \exp \left(-\frac{T^2 \delta^2}{2C_X^2 C_\epsilon^2} \right).$$

The desired result follows by taking $\delta = C_X C_\epsilon \sqrt{\frac{\log(T)}{T}}$ and $M = \sqrt{T}$. \square

The probability bound for δ'_T in Lemma 11 and for δ''_T in Lemma 12 imply a probability bound on δ_T , summarized in the following corollary.

Corollary 3. *Suppose $\mathcal{H} = W^{\alpha,2}$ and Assumption 3 holds. Let δ'_n and δ''_n be defined as in (19) and (20) respectively. Under the conditions in Proposition 1, there exists constants c'_w, C'_w such that*

$$P \left(\delta'_T \geq C'_w T^{\frac{-\alpha}{2\alpha+1}} \right) \leq 2T^2 \exp \left(-c'_w T^{\frac{1}{2\alpha+1}} \right) \quad \text{and} \quad P \left(\delta''_T \geq 3C_X C_\epsilon \sqrt{\frac{\log(T)}{T}} \right) \leq T^{-3}.$$

D Proof of Proposition 2

Proof of Proposition 2. Let $S_1, S_2 \subset \mathcal{H}$. Denote

$$A|_{S_1 \times S_2}[f, g] = A[\mathcal{P}_{S_1} f, \mathcal{P}_{S_2} g].$$

Let $S = \text{span}\{\mathbb{K}(s_i, \cdot)\}_{i=1}^n$ and that S^\perp is the orthogonal complement of S in \mathcal{H} . Then

$$A = A|_{S \times S} + A|_{S \times S^\perp} + A|_{S^\perp \times S} + A|_{S^\perp \times S^\perp}.$$

From Lemma 13, $A|_{S \times S}$ can be written as

$$A|_{S \times S}[f, g] = \sum_{1 \leq i, j \leq n} a_{ij} \langle \mathbb{K}(s_i, \cdot), f \rangle_{\mathcal{H}} \langle \mathbb{K}(s_j, \cdot), g \rangle_{\mathcal{H}}.$$

Step 1. In this step, it is shown that $\{A(s_i, s_j)\}_{i,j=1}^n$ only depend on $A|_{S \times S}$. Observe that

$$A|_{S \times S^\perp}(x_i, x_j) = A|_{S \times S^\perp}[\mathbb{K}(s_i, \cdot), \mathbb{K}(s_j, \cdot)] = A[\mathcal{P}_S \mathbb{K}(s_i, \cdot), \mathcal{P}_{S^\perp} \mathbb{K}(s_j, \cdot)] = 0.$$

Similarly $A|_{S^\perp \times S}[\mathbb{K}(s_i, \cdot), \mathbb{K}(s_j, \cdot)] = 0$ and $A|_{S^\perp \times S^\perp}[\mathbb{K}(s_i, \cdot), \mathbb{K}(s_j, \cdot)] = 0$ for all $1 \leq i, j \leq n$.

Step 2. Let $\{\widehat{B}_d\}_{d=1}^D$ be a solution to (13) and let $\widehat{A}_d = \widehat{B}_d|_{S \times S}$. Then by **Step 1** it

holds that $\widehat{A}_d(s_i, s_j) = \widehat{B}_d(s_i, s_j)$ for all $1 \leq i, j \leq n$ and all $1 \leq d \leq D$. Therefore

$$\begin{aligned} & \sum_{t=1}^T \sum_{i=1}^n \left(X_t(s_i) - \sum_{d=1}^D \frac{1}{n} \sum_{j=1}^n \widehat{A}_d(s_i, s_j) X_{t-d}(s_j) \right)^2 \\ &= \sum_{t=1}^T \sum_{i=1}^n \left(X_t(s_i) - \sum_{d=1}^D \frac{1}{n} \sum_{j=1}^n \widehat{B}_d(s_i, s_j) X_{t-d}(s_j) \right)^2. \end{aligned}$$

From Lemma 14 it holds that $\|\widehat{B}_d\|_{\mathcal{H},*} \geq \|\widehat{A}_d\|_{\mathcal{H},*}$. As a result, $\{\widehat{A}_d\}_{d=1}^D$ is also a solution to (13). So by Lemma 13,

$$\langle \widehat{A}_d[f], g \rangle_{\mathcal{H}} = \sum_{1 \leq i, j \leq n} \widehat{a}_{d,ij} \langle \mathbb{K}(s_i, \cdot), f \rangle_{\mathcal{H}} \langle \mathbb{K}(s_j, \cdot), g \rangle_{\mathcal{H}}$$

as desired. \square

Lemma 13. *Let $A : \mathcal{H} \rightarrow \mathcal{H}$ be any linear compact operator and let S be any subspace of \mathcal{H} spanned by $\{v_1, \dots, v_m\}$. Then there exists $\{a_{ij}\}_{i,j=1}^m$ not necessarily unique such that*

$$\langle A|_{S \times S}[f], g \rangle_{\mathcal{H}} = \sum_{i,j=1}^m a_{ij} \langle v_i, f \rangle_{\mathcal{H}} \langle v_j, g \rangle_{\mathcal{H}}.$$

Proof. Let $\{u_i\}_{i=1}^m$ be the orthonormal basis of $S \subset \mathcal{H}$. Since each u_i can be written as linear combination of $\{v_1, \dots, v_m\}$, it suffices to show that

$$\langle A|_{S \times S}[f], g \rangle_{\mathcal{H}} = \sum_{i,j=1}^m a_{ij} \langle u_i, f \rangle_{\mathcal{H}} \langle u_j, g \rangle_{\mathcal{H}}.$$

Since S is a linear subspace of \mathcal{H} , there exists $\{u_i\}_{i=m+1}^{\infty}$ such that $\{u_i\}_{i=1}^{\infty}$ is the basis of \mathcal{H} and that

$$\langle A|_{S \times S}[f], g \rangle_{\mathcal{H}} = \sum_{i,j=1}^{\infty} a_{ij} \langle u_i, f \rangle_{\mathcal{H}} \langle u_j, g \rangle_{\mathcal{H}}.$$

where $a_{ij} = \langle A[u_i], u_j \rangle_{\mathcal{H}}$. Therefore

$$\begin{aligned} \langle A|_{S \times S}[f], g \rangle_{\mathcal{H}} &= \sum_{i,j=1}^{\infty} a_{ij} \langle u_i, \mathcal{P}_S f \rangle_{\mathcal{H}} \langle u_j, \mathcal{P}_S g \rangle_{\mathcal{H}} \\ &= \sum_{i,j=1}^{\infty} a_{ij} \langle \mathcal{P}_S u_i, f \rangle_{\mathcal{H}} \langle \mathcal{P}_S u_j, g \rangle_{\mathcal{H}} \\ &= \sum_{i,j=1}^m a_{ij} \langle u_i, f \rangle_{\mathcal{H}} \langle u_j, g \rangle_{\mathcal{H}}. \end{aligned}$$

□

Lemma 14. *Let $A : \mathcal{H} \rightarrow \mathcal{H}$ be any linear compact operator and S be any finite-dimensional subspace of \mathcal{H} . Then $\|A|_{S \times S}\|_{\mathcal{H},*} \leq \|A\|_{\mathcal{H},*}$.*

Proof. Let S be of dimension K . Observe that $A^\top A$ is a self-adjoint and compact operator from $\mathcal{H} \rightarrow \mathcal{H}$. Let $\lambda_1 \geq \lambda_2 \geq \dots \geq 0$ be the eigenvalues of $A^\top A$, let $\nu_1 \geq \nu_2 \geq \dots \geq 0$ be the eigenvalues of $\mathcal{P}_S A^\top A \mathcal{P}_S$ and let $\tau_1 \geq \tau_2 \geq \dots \geq 0$ be the eigenvalues of $\mathcal{P}_S A^\top \mathcal{P}_S \mathcal{P}_S A \mathcal{P}_S$.

Observe that

$$\|A\|_{\mathcal{H},*} = \sum_{i=1}^{\infty} \sqrt{\lambda_i} \quad \text{and} \quad \|A|_{S \times S}\|_{\mathcal{H},*} = \sum_{i=1}^K \sqrt{\tau_i}.$$

Therefore it suffices to show that for all i

$$\lambda_i \geq \tau_i.$$

Since by Corollary 4, $\lambda_i \geq \nu_i$ and by Corollary 5, $\nu_i \geq \tau_i$, the desired result follows. □

Theorem 5 (Min-Max Theorem). *Let B be a compact, self-adjoint operator on \mathcal{H} with $\lambda_1 \geq \lambda_2 \geq \dots$ being the eigenvalues of B . Then*

$$\begin{aligned} \max_{T_k \subset \mathcal{H}} \min_{v \in T_k, \|v\|_{\mathcal{H}}=1} \langle B[v], v \rangle_{\mathcal{H}} &= \lambda_k \text{ and} \\ \min_{T_{k-1} \subset \mathcal{H}} \max_{v \in T_{k-1}^\perp, \|v\|_{\mathcal{H}}=1} \langle B[v], v \rangle_{\mathcal{H}} &= \lambda_k, \end{aligned}$$

where T_k denote any subspace of \mathcal{H} of dimension k .

This is a well-known results for operators.

Corollary 4. *Let B be compact self-adjoint positive definite operator on $\mathcal{H} \rightarrow \mathcal{H}$ and S be any M dimensional subspace of \mathcal{H} . Let $\lambda_1 \geq \lambda_2 \geq \dots \geq 0$ be the eigenvalues of B and $\nu_1 \geq \nu_2 \geq \dots$ be the eigenvalues of $\mathcal{P}_S B \mathcal{P}_S$. Then for all i , it holds that*

$$\lambda_i \geq \nu_i.$$

Proof. Since S is of dimension M , $\nu_{M+1} = \nu_{M+2} = \dots = 0$. Let $\{u_i\}_{i=1}^M$ denote the eigenvectors of $\mathcal{P}_S B \mathcal{P}_S$ corresponding to $\{\nu_i\}_{i=1}^M$ and let $S_k = \text{span}\{u_i\}_{i=1}^k$. Then for $k \leq m$, it holds that

$$\lambda_k \geq \min_{v \in S_k, \|v\|_{\mathcal{H}}=1} \langle B[v], v \rangle_{\mathcal{H}} = \min_{v \in S_k, \|v\|_{\mathcal{H}}=1} \langle \mathcal{P}_S B \mathcal{P}_S[v], v \rangle_{\mathcal{H}} = \nu_k,$$

where the first inequality follows from the Min-max theorem. For $k > m$,

$$\lambda_k \geq 0 = \nu_i.$$

□

Corollary 5. Let A be any compact operator and S be any M dimensional subspace of \mathcal{H} . Let $\lambda_1 \geq \lambda_2 \geq \dots$ be the eigenvalues of $\mathcal{P}_S A^\top A \mathcal{P}_S$ and $\nu_1 \geq \nu_2 \geq \dots$ be the eigenvalues of $\mathcal{P}_S A^\top \mathcal{P}_S \mathcal{P}_S A \mathcal{P}_S$. Then for all i , it holds that

$$\lambda_i \geq \nu_i.$$

Proof. Let $B = A \mathcal{P}_S$. Therefore $Bv = 0$ for any $v \in S^\perp$. So

$$\begin{aligned} \lambda_k &= \max_{T_k \subset \mathcal{H}} \min_{v \in T_k, \|v\|_{\mathcal{H}}=1} \langle B^\top B[v], v \rangle_{\mathcal{H}} = \max_{T_k \subset \mathcal{H}} \min_{v \in T_k, \|v\|_{\mathcal{H}}=1} \|Bv\|_{\mathcal{H}}^2, \\ \nu_k &= \max_{T_k \subset \mathcal{H}} \min_{v \in T_k, \|v\|_{\mathcal{H}}=1} \langle B^\top \mathcal{P}_S \mathcal{P}_S B[v], v \rangle_{\mathcal{H}} = \max_{T_k \subset \mathcal{H}} \min_{v \in T_k, \|v\|_{\mathcal{H}}=1} \|\mathcal{P}_S Bv\|_{\mathcal{H}}^2. \end{aligned}$$

For any v , it holds that $\|Bv\|_{\mathcal{H}} \geq \|\mathcal{P}_S Bv\|_{\mathcal{H}}^2$ as \mathcal{P}_S is the projection operator onto S . Therefore $\lambda_k \geq \nu_k$ as desired. \square

E Proof of Theorem 1

Remark: Equations (16), (17) and (19) are repeatedly used in the proof of Theorem 1. Note that by rescaling, (16), (17) and (19) can be applied to any function with bounded norm in \mathcal{H} . For example, consider $g \in \mathcal{H}$, $\|g\|_{\mathcal{H}} > 1$. Let $f = g/\|g\|_{\mathcal{H}}$ and apply (16) to f , we have

$$\left| \int g(s) ds - \frac{1}{n} \sum_{i=1}^n g(s_i) \right| \leq \gamma \|g\|_{\mathcal{L}^2} + \gamma^2 \|g\|_{\mathcal{H}}.$$

This rescaling calculation is applied repeatedly in the proof of Theorem 1.

Proof of Theorem 1. Note that we have $C_A > \max_{1 \leq d \leq D} \tau_d$. Observe that $\{A_d^*\}_{d=1}^D \in \mathcal{C}_\tau$ since $\|A_d^*\|_{\mathcal{H},*} \leq \tau_d$ for $d = 1, \dots, D$. Thus we have

$$\begin{aligned} & \sum_{t=1}^T \sum_{i=1}^n \frac{1}{Tn} \left(X_t(s_i) - \sum_{d=1}^D \frac{1}{n} \sum_{j=1}^n \hat{A}_d(s_i, s_j) X_{t-d}(s_j) \right)^2 \\ & \leq \sum_{t=1}^T \sum_{i=1}^n \frac{1}{Tn} \left(X_t(s_i) - \sum_{d=1}^D \frac{1}{n} \sum_{j=1}^n A_d^*(s_i, s_j) X_{t-d}(s_j) \right)^2 \end{aligned}$$

Denote $\Delta_d = A_d^* - \widehat{A}_d$. Then standard calculation gives

$$\frac{1}{Tn} \sum_{t=1}^T \sum_{i=1}^n \left(\sum_{d=1}^D \frac{1}{n} \sum_{j=1}^n \Delta_d(s_i, s_j) X_{t-d}(s_j) \right)^2 \quad (43)$$

$$\leq \frac{2}{Tn} \sum_{t=1}^T \sum_{i=1}^n \left(\sum_{d=1}^D \frac{1}{n} \sum_{j=1}^n \Delta_d(s_i, s_j) X_{t-d}(s_j) \right) \left(X_t(s_i) - \sum_{d=1}^D \frac{1}{n} \sum_{j=1}^n A_d^*(s_i, s_j) X_{t-d}(s_j) \right) \quad (44)$$

Step 1. Observe that

$$\sup_{1 \leq i \leq n} \|\Delta_d(s_i, \cdot)\|_{\mathcal{H}} \leq \sup_{r \in [0,1]} \left(\|A_d^*(r, \cdot)\|_{\mathcal{H}} + \|\widehat{A}_d(r, \cdot)\|_{\mathcal{H}} \right) \leq \|\widehat{A}_d\|_{\mathcal{H},*} + \|A_d^*\|_{\mathcal{H},*} \leq 2C_A, \quad (45)$$

where the second to last inequality follows from Lemma 2. Therefore for any fixed t and i ,

$$\begin{aligned} & \left(\sum_{d=1}^D \frac{1}{n} \sum_{j=1}^n \Delta_d(s_i, s_j) X_{t-d}(s_j) \right)^2 \\ & \geq \frac{1}{2} \left(\sum_{d=1}^D \int \Delta_d(s_i, r) X_{t-d}(r) dr \right)^2 - 2 \left(\sum_{d=1}^D \int \Delta_d(s_i, r) X_{t-d}(r) dr - \frac{1}{n} \sum_{j=1}^n \Delta_d(s_i, s_j) X_{t-d}(s_j) \right)^2 \\ & \geq \frac{1}{2} \left(\sum_{d=1}^D \int \Delta_d(s_i, r) X_{t-d}(r) dr \right)^2 - \left(\gamma_n \sum_{d=1}^D \|\Delta_d(s_i, \cdot)\|_{\mathcal{L}^2} + 2C_A C_X \gamma_n^2 \right)^2 \\ & \geq \frac{1}{2} \left(\sum_{d=1}^D \int \Delta_d(s_i, r) X_{t-d}(r) dr \right)^2 - 2\gamma_n^2 \left(\sum_{d=1}^D \|\Delta_d(s_i, \cdot)\|_{\mathcal{L}^2} \right)^2 - 8C_A^2 C_X^2 \gamma_n^4 \\ & \geq \frac{1}{2} \left(\sum_{d=1}^D \int \Delta_d(s_i, r) X_{t-d}(r) dr \right)^2 - 2\gamma_n^2 D \sum_{d=1}^D \|\Delta_d(s_i, \cdot)\|_{\mathcal{L}^2}^2 - 8C_A^2 C_X^2 \gamma_n^2 \end{aligned} \quad (46)$$

where the second inequality follows from (16) and the fact that

$$\sup_{1 \leq d \leq D, 1 \leq i \leq n} \|\Delta_d(s_i, \cdot) X_{t-d}(\cdot)\|_{\mathcal{H}} \leq \sup_{1 \leq i \leq n} \|\Delta_d(s_i, \cdot)\|_{\mathcal{H}} \|X_{t-d}\|_{\mathcal{H}} \leq 2C_A C_X,$$

and $\gamma_n^4 \leq \gamma_n^2$ is used in the last inequality. In addition,

$$\begin{aligned}
& \frac{1}{T} \sum_{t=1}^T \left(\sum_{d=1}^D \int \Delta_d(s_i, r) X_{t-d}(r) dr \right)^2 \\
& \geq E \left(\sum_{d=1}^D \int \Delta_d(s_i, r) X_{t-d}(r) dr \right)^2 - \delta_T C_A \sqrt{\sum_{d=1}^D \|\Delta_d(s_i, \cdot)\|_{\mathcal{L}^2}^2} \\
& \geq \kappa_X \sum_{d=1}^D \|\Delta_d(s_i, \cdot)\|_{\mathcal{L}^2}^2 - \frac{2\delta_T^2 C_A^2}{\kappa_X} - \frac{\kappa_X}{2} \sum_{d=1}^D \|\Delta_d(s_i, \cdot)\|_{\mathcal{L}^2}^2 \\
& = \frac{\kappa_X}{2} \sum_{d=1}^D \|\Delta_d(s_i, \cdot)\|_{\mathcal{L}^2}^2 - \frac{2\delta_T^2 C_A^2}{\kappa_X}, \tag{47}
\end{aligned}$$

where the first inequality follows from (19), the second inequality follows from Assumption 3. Therefore

$$\begin{aligned}
(43) &= \frac{1}{Tn} \sum_{t=1}^T \sum_{i=1}^n \left(\sum_{d=1}^D \frac{1}{n} \sum_{j=1}^n \Delta_d(s_i, s_j) X_{t-d}(s_j) \right)^2 \\
&\geq \frac{1}{Tn} \sum_{t=1}^T \sum_{i=1}^n \frac{1}{2} \left(\sum_{d=1}^D \int \Delta_d(s_i, r) X_{t-d}(r) dr \right)^2 - \frac{2\gamma_n^2 D}{n} \sum_{i=1}^n \sum_{d=1}^D \|\Delta_d(s_i, \cdot)\|_{\mathcal{L}^2}^2 - 8C_A^2 C_X^2 \gamma_n^2 \\
&\geq \frac{\kappa_X}{4n} \sum_{i=1}^n \sum_{d=1}^D \|\Delta_d(s_i, \cdot)\|_{\mathcal{L}^2}^2 - \frac{2\delta_T^2 C_A^2}{\kappa_X} - \frac{2\gamma_n^2 D}{n} \sum_{i=1}^n \sum_{d=1}^D \|\Delta_d(s_i, \cdot)\|_{\mathcal{L}^2}^2 - 8C_A^2 C_X^2 \gamma_n^2 \\
&\geq \frac{\kappa_X}{8n} \sum_{i=1}^n \sum_{d=1}^D \|\Delta_d(s_i, \cdot)\|_{\mathcal{L}^2}^2 - \frac{2\delta_T^2 C_A^2}{\kappa_X} - 8C_A^2 C_X^2 \gamma_n^2 \tag{48}
\end{aligned}$$

where the first inequality follows from (46), the second inequality follows from (47), and the last inequality follows from the assumption that $\kappa_X \geq 64\gamma_n^2 D$

Step 2. Observe that

$$\begin{aligned}
& \frac{1}{2} \cdot (44) \\
&= \frac{1}{Tn} \sum_{t=1}^T \sum_{i=1}^n \sum_{d=1}^D \left(\frac{1}{n} \sum_{j=1}^n \Delta_d(s_i, s_j) X_{t-d}(s_j) \right) \epsilon_t(s_i) \\
&+ \frac{1}{Tn} \sum_{t=1}^T \sum_{i=1}^n \sum_{d=1}^D \left(\frac{1}{n} \sum_{j=1}^n \Delta_d(s_i, s_j) X_{t-d}(s_j) \right) \sum_{d=1}^D \left(\int A_d^*(s_i, s) X_{t-d}(s) ds - \frac{1}{n} \sum_{j=1}^n A_d^*(s_i, s_j) X_{t-d}(s_j) \right) \\
&\leq \sum_{d=1}^D \frac{1}{n^2} \sum_{i,j=1}^n |\Delta_d(s_i, s_j)| \sup_{1 \leq d \leq D, 1 \leq i,j \leq n} \left| \frac{1}{T} \sum_{t=1}^T X_{t-d}(s_j) \epsilon_t(s_i) \right| \\
&+ C_X \sum_{d=1}^D \frac{1}{n^2} \sum_{i,j=1}^n |\Delta_d(s_i, s_j)| D \sup_{1 \leq t \leq T, 1 \leq i \leq n, 1 \leq d \leq D} \left| \int A_d^*(s_i, s) X_{t-d}(s) ds - \frac{1}{n} \sum_{j=1}^n A_d^*(s_i, s_j) X_{t-d}(s_j) \right|
\end{aligned}$$

From (20), it holds that

$$\sup_{1 \leq d \leq D, 1 \leq i,j \leq n} \left| \frac{1}{T} \sum_{t=1}^T X_{t-d}(s_j) \epsilon_t(s_i) \right| \leq \delta'_T \leq \delta_T.$$

In addition, since for any $1 \leq i \leq n$

$$\|A_d^*(s_i, \cdot) X_{t-d}(\cdot)\|_{\mathcal{L}^2} \leq \|A_d^*(s_i, \cdot) X_{t-d}(\cdot)\|_{\mathcal{H}} \leq \sup_{r \in [0,1]} \|A_d^*(r, \cdot)\|_{\mathcal{H}} \|X_{t+1-d}\|_{\mathcal{H}} \leq C_A C_X,$$

(16) implies that

$$\sup_{1 \leq t \leq T, 1 \leq i \leq n, 1 \leq d \leq D} \left| \int A_d^*(s_i, s) X_{t-d}(s) ds - \frac{1}{n} \sum_{j=1}^n A_d^*(s_i, s_j) X_{t-d}(s_j) \right| \leq C_A C_X (\gamma_n + \gamma_n^2) \leq 2C_A C_X \gamma_n.$$

Therefore

$$\begin{aligned}
\frac{1}{2} \cdot (44) &\leq \sum_{d=1}^D \frac{1}{n^2} \sum_{i,j=1}^n |\Delta_d(s_i, s_j)| (\delta_T + 2DC_A C_X \gamma_n) \leq \sum_{d=1}^D \sqrt{\frac{1}{n^2} \sum_{i,j=1}^n \Delta_d^2(s_i, s_j)} (\delta_T + 2DC_A C_X \gamma_n) \\
&\leq \frac{\kappa_X}{64} \sum_{d=1}^D \frac{1}{n^2} \sum_{i,j=1}^n \Delta_d^2(s_i, s_j) + \frac{64}{\kappa_X} (\delta_T^2 + DC_A C_X \gamma_n^2) \\
&\leq \frac{\kappa_X}{32} \sum_{d=1}^D \frac{1}{n} \sum_{i=1}^n \|\Delta_d(s_i, \cdot)\|_{\mathcal{L}^2}^2 + \frac{\kappa_X DC_A}{16} \gamma_n^2 + \frac{64}{\kappa_X} (\delta_T^2 + DC_A C_X \gamma_n^2), \tag{49}
\end{aligned}$$

where the second inequality follows from $\frac{1}{n^2} \sum_{i,j=1}^n |\Delta_d(s_i, s_j)| \leq \sqrt{\frac{1}{n^2} \sum_{i,j=1}^n \Delta_d^2(s_i, s_j)}$, the third inequality follows from Hölder's inequality and the last inequality follows from (17) and the fact that

$$\|\Delta_d(s_i, \cdot)\|_{\mathcal{H}} \leq \|\Delta_d\|_{\mathcal{H},*} \leq 2C_A.$$

Step 3. Combining (48) and (49), one has

$$\begin{aligned} & \frac{\kappa_X}{8} \sum_{d=1}^D \frac{1}{n} \sum_{i=1}^n \|\Delta_d(s_i, \cdot)\|_{\mathcal{L}^2}^2 - \frac{2\delta_T^2 C_A^2}{\kappa_X} - 8C_A^2 C_X^2 \gamma_n^2 \\ & \leq \frac{\kappa_X}{32} \sum_{d=1}^D \frac{1}{n} \sum_{i=1}^n \|\Delta_d(s_i, \cdot)\|_{\mathcal{L}^2}^2 + \left(\frac{\kappa_X D C_A}{16} + D C_A C_X\right) \gamma_n^2 + \frac{64}{\kappa_X} \delta_T^2, \end{aligned}$$

which implies that

$$\frac{\kappa_X}{16} \sum_{d=1}^D \frac{1}{n} \sum_{i=1}^n \|\Delta_d(s_i, \cdot)\|_{\mathcal{L}^2}^2 \leq C'_1 (\gamma_n^2 + \delta_T^2). \quad (50)$$

for some C'_1 only depending on κ_X, D, C_A, C_X . Since

$$\left\| \int \Delta_d(\cdot, r)^2 dr \right\|_{\mathcal{H}} \leq \int \sup_{r \in [0,1]} \|\Delta_d(\cdot, r)\|_{\mathcal{H}}^2 dr \leq \|\Delta_d\|_{\mathcal{H},\text{op}}^2 \leq 4C_A^2,$$

(17) implies that

$$\frac{1}{n} \sum_{i=1}^n \|\Delta_d(s_i, \cdot)\|_{\mathcal{L}^2}^2 \geq \frac{1}{2} \|\Delta_d\|_{\mathcal{L}^2}^2 - C_A^2 \gamma_n^2.$$

Therefore (50) and the above display give

$$\frac{\kappa_X}{32} \|\Delta_d\|_{\mathcal{L}^2}^2 \leq \frac{\kappa_X}{16} \sum_{d=1}^D \frac{1}{n} \sum_{i=1}^n \|\Delta_d(s_i, \cdot)\|_{\mathcal{L}^2}^2 + \gamma_n^2 \leq C'_1 (\gamma_n^2 + \delta_T^2).$$

The above equation directly implies the desired result. \square

Proof of Corollary 1. Suppose $\mathcal{H} = W^{\alpha,2}$. From Corollary 2 it holds that with probability at least $1 - 1/n^4$,

$$\max\{\gamma'_n, \gamma''_n\} \leq C_\alpha n^{-\alpha/(2\alpha+1)}.$$

where C_α is some constant independent of n . From Corollary 3, it holds that

$$P\left(\delta'_T \geq C'_w T^{\frac{-\alpha}{2\alpha+1}}\right) \leq 2T^2 \exp\left(-c'_w T^{\frac{1}{2\alpha+1}}\right) \quad \text{and} \quad P\left(\delta''_T \geq 3C_X C_\epsilon \sqrt{\frac{\log(T)}{T}}\right) \leq T^{-3}.$$

The result immediately follows from Theorem 1. □

E.1 Proof of Proposition 3

Proof of Proposition 3. Define

$$\tilde{X}_{T+1}(r) := \sum_{d=1}^D \int \hat{A}_d(r, s) X_{T+1-d}(s) ds.$$

Step 1. Since

$$\begin{aligned} & \left\| \int \hat{A}_d(\cdot, s) X_{t+1-d}(s) ds - \int A_d^*(\cdot, s) X_{t+1-d}(s) ds \right\|_{\mathcal{L}^2} \\ &= \left\| \int (\hat{A}_d(\cdot, s) - A_d^*(\cdot, s)) X_{t+1-d}(s) ds \right\|_{\mathcal{L}^2} \\ &\leq \int \left\| \hat{A}_d(\cdot, s) - A_d^*(\cdot, s) \right\|_{\mathcal{L}^2} X_{t+1-d}(s) ds \\ &\leq \left\| \hat{A}_d - A_d^* \right\|_{\mathcal{L}^2} \|X_{t+1-d}\|_{\mathcal{L}^2}, \end{aligned}$$

and therefore

$$\begin{aligned} \|E(X_{T+1} | \{X_t\}_{t=1}^T) - \tilde{X}_{T+1}\|_{\mathcal{L}^2} &= \left\| \sum_{d=1}^D \int \hat{A}_d(\cdot, s) X_{t+1-d}(s) ds - \sum_{d=1}^D \int A_d^*(\cdot, s) X_{t+1-d}(s) ds \right\|_{\mathcal{L}^2} \\ &\leq D \sum_{d=1}^D \left\| \int (\hat{A}_d(\cdot, s) - A_d^*(\cdot, s)) X_{t+1-d}(s) ds \right\|_{\mathcal{L}^2} \\ &\leq D \sum_{d=1}^D \left\| \hat{A}_d - A_d^* \right\|_{\mathcal{L}^2} \|X_{t+1-d}\|_{\mathcal{L}^2} \\ &\leq C'_1 D C_X \left(n^{\frac{-\alpha}{2\alpha+1}} + T^{\frac{-\alpha}{2\alpha+1}} \right), \end{aligned}$$

where the last inequality follows from Corollary 1.

Step 2. Observe that for any $r \in [0, 1]$, and any $t \in [1, \dots, T]$,

$$\|\hat{A}_d(r, \cdot) X_t(\cdot)\|_{\mathcal{H}} \leq C_A C_X,$$

therefore by (16), it holds that for all $r \in [0, 1]$,

$$\begin{aligned} & \left| \frac{1}{n} \sum_{j=1}^n \hat{A}_d(r, s_j) X_{T+1-d}(s_j) - \int \hat{A}_d(r, s) X_{T+1-d}(s) ds \right| \\ & \leq \|\hat{A}_d(r, \cdot) X_t(\cdot)\|_{\mathcal{L}^2} \gamma_n + \|\hat{A}_d(r, \cdot) X_t(\cdot)\|_{\mathcal{H}} \gamma_n^2 \\ & \leq 2C_A C_X \gamma_n. \end{aligned}$$

Let $\hat{X}_{T+1}(r) = \sum_{d=1}^D \frac{1}{n} \sum_{j=1}^n \hat{A}_d(r, s_j) X_{T+1-d}(s_j)$. Therefore

$$\begin{aligned} & \|\hat{X}_{T+1} - \tilde{X}_{T+1}\|_{\mathcal{L}^2} \leq \|\hat{X}_{T+1} - \tilde{X}_{T+1}\|_{\infty} \\ & = \sup_{r \in [0, 1]} \left| \frac{1}{n} \sum_{j=1}^n \hat{A}_d(r, s_j) X_{T+1-d}(s_j) - \int \hat{A}_d(r, s) X_{T+1-d}(s) ds \right| \\ & \leq 2C_A C_X \gamma_n \leq 2C_A C_X C_{\alpha} n^{\frac{-\alpha}{2\alpha+1}}, \end{aligned}$$

where the last inequality follows from Corollary 2. The desired result follows from the inequality that

$$\|E(X_{T+1} | \{X_t\}_{t=1}^T) - \hat{X}_{T+1}\|_{\mathcal{L}^2} \leq \|E(X_{T+1} | \{X_t\}_{t=1}^T) - \tilde{X}_{T+1}\|_{\mathcal{L}^2} + \|\hat{X}_{T+1} - \tilde{X}_{T+1}\|_{\mathcal{L}^2}$$

The proof for $\frac{1}{n} \sum_{j=1}^n \left(E(X_{T+1}(s_j) | \{X_t\}_{t=1}^T) - \hat{X}_{T+1}(s_j) \right)^2 \leq C_1'' \left(n^{\frac{-2\alpha}{2\alpha+1}} + T^{\frac{-2\alpha}{2\alpha+1}} \right)$ follows the same argument and thus is omitted. \square

F Accelerated gradient method for nuclear norm penalization

We use the accelerated gradient method (AGM, Algorithm 2 in Ji and Ye (2009)) to solve the trace norm minimization problem in (25), i.e.

$$\arg \min_W g(W) + \|W\|_* = \arg \min_W \|X - \mathcal{K}WZ\|_F^2 + \|W\|_*.$$

To implement AGM, we first calculate the gradient $\nabla g(W)$ for a given W . We have $g(W) = \|X - \mathcal{K}WZ\|_F^2 = \left\| X - \sum_{d=1}^D \mathcal{K}_d W_d Z_d \right\|_F^2$. By matrix calculus, for the component-wise gradient, we have $\nabla g(W_d) = -2\mathcal{K}_d^\top (X - \sum_{d'=1}^D \mathcal{K}_{d'} W_{d'} Z_{d'}) Z_d^\top$ for $d = 1, \dots, D$. Due to

the block diagonal structure of W , the gradient is $\nabla g(W) = \begin{bmatrix} \nabla g(W_1) & & \\ & \ddots & \\ & & \nabla g(W_D) \end{bmatrix}$.

Denote $W_{(k)} = \begin{bmatrix} W_{(k)1} & & \\ & \ddots & \\ & & W_{(k)D} \end{bmatrix}$ to be the value of W at step k of AGM. To update $W_{(k)}$ using AGM, two quantities to be calculated are equations (8) and (9) in [Ji and Ye \(2009\)](#).

Equation (8) in [Ji and Ye \(2009\)](#) can be written as

$$\begin{aligned} Q_{t_k}(W, W_{(k-1)}) &:= P_{t_k}(W, W_{(k-1)}) + \|W\|_* \\ &= g(W_{(k-1)}) + \langle W - W_{(k-1)}, \nabla g(W_{(k-1)}) \rangle + \frac{t_k}{2} \|W - W_{(k-1)}\|_F^2 + \|W\|_* \\ &= \left\| X - \sum_{d=1}^D \mathcal{K}_d W_{(k-1)d} Z_d \right\|_F^2 + \sum_{d=1}^D \left(\langle W_d - W_{(k-1)d}, \nabla g(W_{(k-1)d}) \rangle + \frac{t_k}{2} \|W_d - W_{(k-1)d}\|_F^2 + \|W_d\|_* \right), \end{aligned}$$

where $\langle A, B \rangle = \text{tr}(A^\top B)$ denotes the matrix inner product. Thus, equation (8) in [Ji and Ye \(2009\)](#) can be calculated component-wisely for W_1, \dots, W_D .

Equation (9) in [Ji and Ye \(2009\)](#) can be written as

$$\begin{aligned} &\frac{t_k}{2} \left\| W - \left(W_{(k-1)} - \frac{1}{t_k} \nabla g(W_{(k-1)}) \right) \right\|_F^2 + \|W\|_* \\ &= \sum_{d=1}^D \left(\frac{t_k}{2} \left\| W_d - \left(W_{(k-1)d} - \frac{1}{t_k} \nabla g(W_{(k-1)d}) \right) \right\|_F^2 + \|W_d\|_* \right). \end{aligned}$$

Thus the minimization of equation (9) in [Ji and Ye \(2009\)](#) can be performed on W_1, \dots, W_D separately using singular value decomposition as in Theorem 3.1 of [Ji and Ye \(2009\)](#).

G Additional simulation results

Figures [6](#) and [7](#) give the boxplot of PE by Bosq, ANH and RKHS for FAR(1) under signal strength $\kappa = 0.2$ and 0.8 respectively. Figure [8](#) give the boxplot of PE by ANH and RKHS for FAR with autoregressive order selection under signal strength $(\kappa_1, \kappa_2) = (0, 0.5)$.

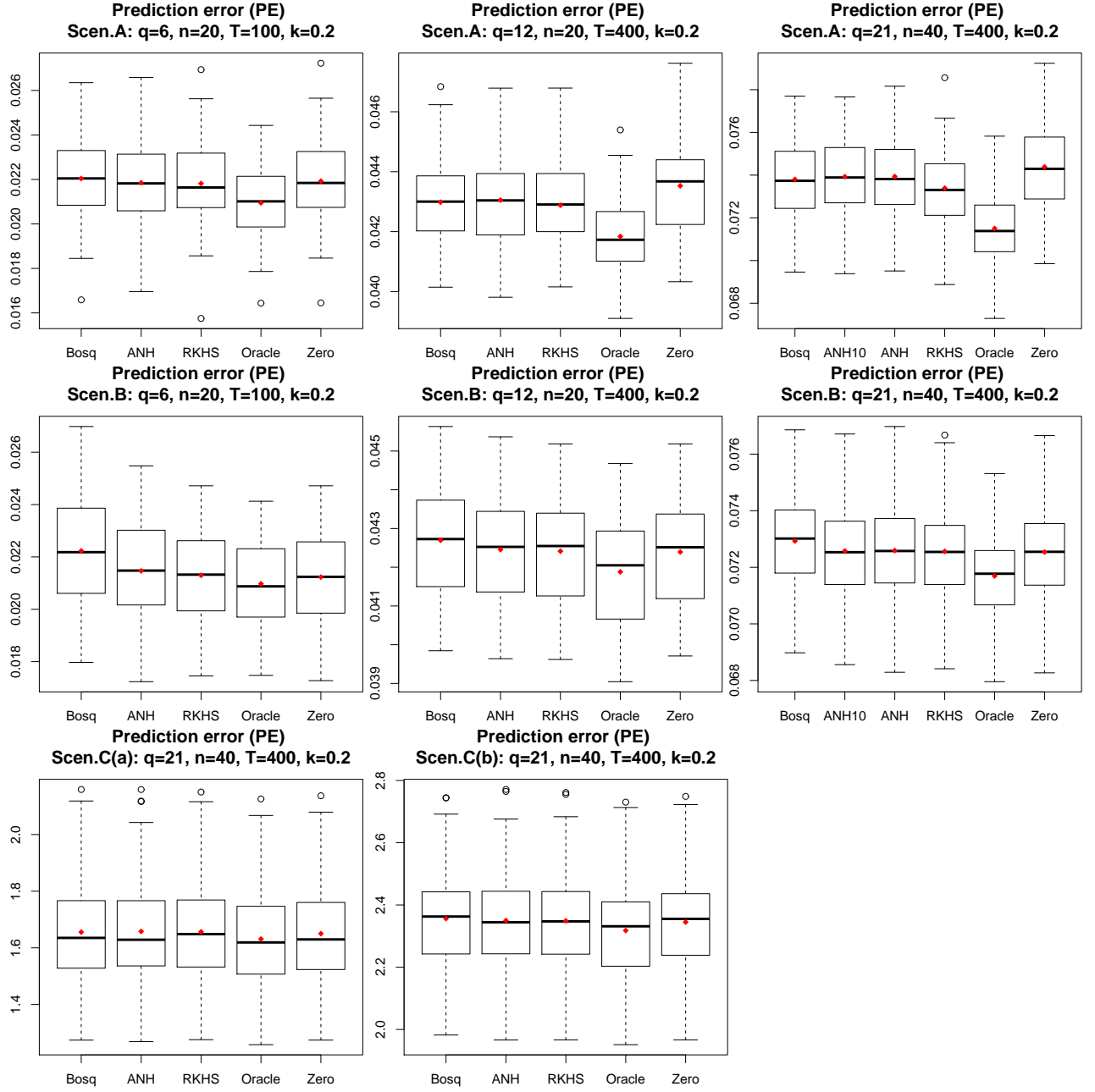


Figure 6: Boxplot of prediction error (PE) for FAR(1) across 100 experiments with signal strength $\kappa = 0.2$. ANH10 stands for ANH based on 10 cubic B-splines under $q = 21$.

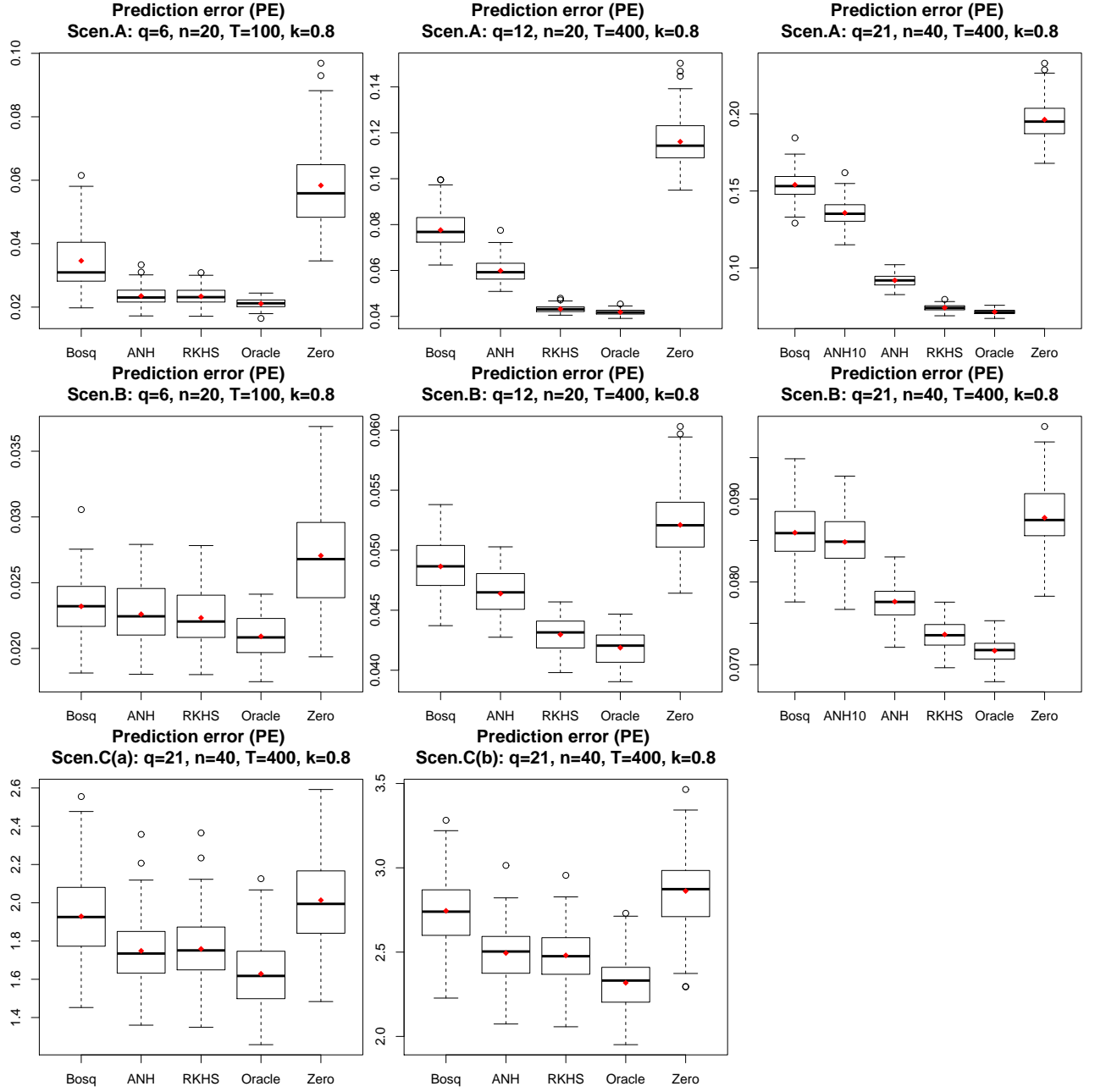


Figure 7: Boxplot of prediction error (PE) for FAR(1) across 100 experiments with signal strength $\kappa = 0.8$. ANH10 stands for ANH based on 10 cubic B-splines under $q = 21$.

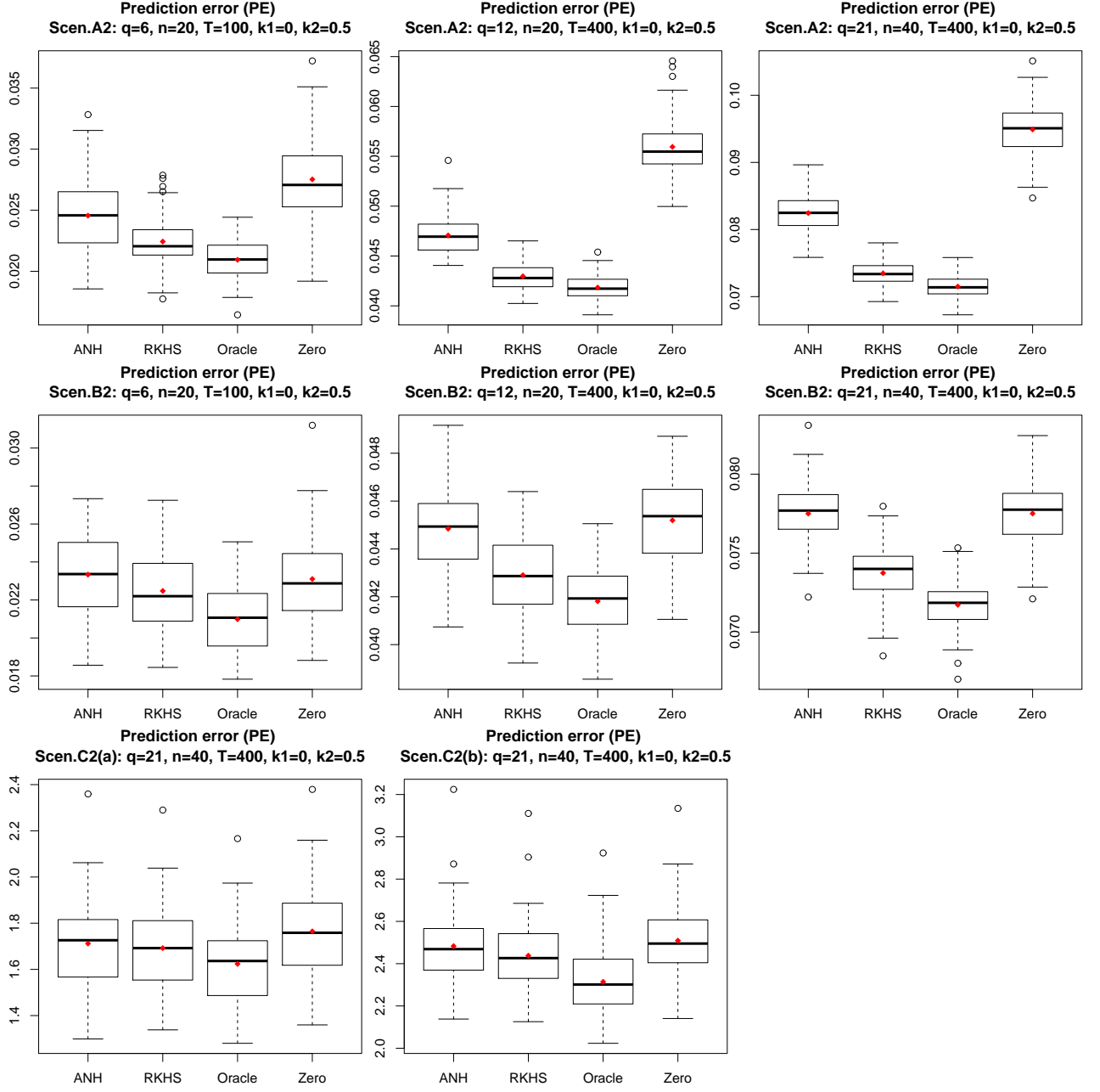


Figure 8: Boxplot of prediction error (PE) for FAR with autoregressive order selection across 100 experiments with signal strength $\kappa_1 = 0, \kappa_2 = 0.5$.